Exploring the Regulation of Fasting Blood Glucose by G6PC2

By

Karin Janae Bosma

Dissertation

Submitted to the Faculty of the

Graduate School of Vanderbilt University

in partial fulfillment of the requirements

for the degree of

DOCTOR OF PHILOSOPHY

in

Molecular Physiology and Biophysics

May 8, 2020

Nashville, Tennessee

Approved:

David A. Jacobson, PhD

Maureen A. Gannon, PhD

Jamey D. Young, PhD

Dale S. Edgerton, PhD

ACKNOWLEDGMENTS

First, I need to thank members of the O'Brien lab, past and present, for their support and their contributions to this work. Thank you to Kristen Syring and Kayla Boortz for teaching me the ways of the lab, and for their help and encouragement during the early years of graduate school. I cannot adequately thank Ken Oeser for all his help with countless RNA preparations, genotyping reactions, and plasmid preps, among other experiments. He has taught me new crossword clue answers, patiently answered questions about plants, animals, and geography, and provided plenty of ideas for places to explore outside the lab. I believe I can safely say I will never work with anyone quite like Ken again, and I'm thankful to have had the chance to do so.

I also need to thank our collaborators and cores at Vanderbilt that contributed to this work. I am grateful for the excellent work performed by the Hormone Assay and Analytical Services Core, the Islet Procurement and Analysis Core, and the Translational Pathology Shared Resource. I have been incredibly fortunate to have the expertise and guidance of a large number of collaborators in completing this work: Dr. Owen McGuinness, Dr. Alvin Powers, Dr. Jamey Young, Dr. Lea Davis, Dr. Anna Means, Dr. Wen-hong Li, Mohsin Rahim, Kritika Singh, Slavina Goleva, Greg Poffenberger, and Anastasia Coldren.

I am immensely grateful to the members of my thesis committee: Dr. David Jacobson, Dr. Maureen Gannon, Dr. Jamey Young, and Dr. Dale Edgerton. Their critiques, guidance, and support over the last few years has been invaluable. I greatly appreciate how they have pushed me to think harder about my data and carefully about my words, and I am a better scientist and thinker for it.

Thank you also to the Molecular Physiology and Biophysics students, staff, and faculty. Being part of this department has made graduate school far more enjoyable, and I will miss the relay races, happy hours, holiday parties, and coffee hours. A special thank you goes to Karen

Gieg, whose readiness to help, cheerful smile, and depth of knowledge made planning events, scheduling meetings, filling out paperwork, and similar tasks so much easier.

Of course, none of this work would have been possible without my mentor, Dr. Richard O'Brien. I cannot express how thankful I am for the numerous hours he invested in me and my project. Thank you for answering my endless questions without much obvious annoyance, for the hours spent editing my presentations and my writing, for being unceasingly optimistic even in the face of rejected papers and conflicting data, and for challenging me while also being supportive and encouraging. I am a better writer, speaker, and scientist because of his teaching and guidance.

Finally, I need to express my immense gratitude to my family and friends for their support over the past five years. I don't have the space to list them by name, but thank you to all my friends both here in Nashville and elsewhere; while they frequently didn't know what I was talking about or what exactly I was doing in graduate school, they never failed to be people I could celebrate with in good times and lean on in bad times, and who could provide relief from the stress and pressure of graduate school. Special thanks to Cherie, Susan, and Maria; graduate school wouldn't have been the same without your friendship and support.

I am incredibly grateful to my family. My family helped me celebrate achievements, provided comfort during harder times, and have always pushed me to pursue my goals and to do my best in whatever I chose to do. To my parents, Ben and Mary, and my siblings, Craig, Anna, Melanie, and Bryan, and my nieces and nephews, thank you for your love and support over these past several years in particular. I cannot begin to express what it has meant to me to know that you were all supporting me in this process, and I know I could not have done this without you. Thank you for always being there for me, and for your confidence in me, even when I doubted myself.

ACKNOWLEDGMENT OF SUPPORT

Funding for this research has been provided to Dr. O'Brien through the National Institutes of Health (grant DK92589). I have been supported by the Molecular Endocrinology Training Grant (NIH 5T32 DK07563). Research from collaborating laboratories was supported by the following grants: O.P.M., DK043748 and DK078188; A.C.P., UC4 DK104211, DK106755, DK89572, and by grants from the JDRF and the Department of Veterans Affairs (BX000666); W.H.L. JDRF grant 1-SRA-2018-675-S-B; L.K.D., R56MH120736; J.D.Y DK106348. The Vanderbilt Islet Procurement and Analysis Core and the Vanderbilt Hormone Assay & Analytical Services Core were supported by NIH grant P60 DK20593 (to the Vanderbilt Diabetes Research Training Center). Human pancreatic islets were provided by the NIDDK-funded Integrated Islet Distribution Program at the City of Hope (NIH Grant # 2UC4 DK098085). The Vanderbilt Translational Pathology Shared Resource was supported by NCI/NIH Cancer Center Support Grant 2P30 CA068485-14 and the Vanderbilt Mouse Metabolic Phenotyping Center Grant 5U24DK059637-13.

TABLE OF CONTENTS

Page

ABBREVIATIONS

AA	Amino acid
AMPK	Adenosine monophosphate-activated protein kinase
APC	Antigen presenting cells
ATF4	Activating transcription factor 4
ATF6	Activating transcription factor 6
ATP	Adenosine triphosphate
BCS	Beta cell-specific
CAM	Cardiovascular-associated mortality
cAMP	Cyclic adenosine monophosphate
CAT	Catalase
ChIP	Chromatin immunoprecipitation
CHOP	C/EBP homologous protein
CICR	Calcium induced calcium release
DAG	Diacylglycerol
DCCT	Diabetes Control and Complications Trial
DM	Diabetes mellitus
DNL	De novo lipogenesis
DPP4	Dipeptidyl peptidase 4
EA	European American
EHR	Electronic health record
ER	Endoplasmic reticulum

ERAD	ER associated degradation
ES	Embryonic stem cell
FBG	Fasting blood glucose
FPI	Fasting plasma insulin
G6P	Glucose-6-phosphate
G6PC1	Glucose-6-phosphatase catalytic subunit 1
G6PC2	Glucose-6-phosphatase catalytic subunit 2
G6PC3	Glucose-6-phosphatase catalytic subunit 3
GAD65	Glutamic acid decarboxylase
GCK	Glucokinase
GIP	Glucose-independent insulinotropic peptide
GLP1	Glucagon-like peptide 1
GLP1R	Glucagon-like peptide 1 receptor
GPx	Glutathione peroxidase
GSD1a	Glycogen storage disease type 1a
GSD1b	Glycogen storage disease type 1b
GSIS	Glucose-stimulated insulin secretion
GWAS	Genome-wide association study
HAAF	Hypoglycemia-associated autonomic failure
HbA1c	Hemoglobin A1c (glycated hemoglobin)
HGP	Hepatic glucose production
HLA	Human leukocyte antigen
IDDM	Insulin-dependent diabetes mellitus

IGRP	Islet-specific glucose-6-phosphatase catalytic subunit related protein
IHTG	Intrahepatic triglyceride content
IPGTT	Intraperitoneal glucose tolerance test
IRE1	Inositol-requiring enzyme 1
IRS1	Insulin receptor substrate 1
IRS2	Insulin receptor substrate 2
ITT	Insulin tolerance test
JNK	c-Jun N-terminal kinase
K_{ATP}	ATP-sensitive potassium channel
KO	Knockout
KOMP	Knockout Mouse Project
LabWAS	Laboratory-wide association study
LPL	Lipoprotein lipase
MAF	Minor allele frequency
MAG	Monoacylglycerol
MAPK	Mitogen-activated protein kinase
MODY	Maturity-onset diabetes of the young
mTOR	Mammalian target of rapamycin
NADPH	Nicotinamide adenine dinucleotide phosphate
NIDDM	Non-insulin-dependent diabetes mellitus
NOD	Non-obese diabetic
nPKC	Novel protein kinase C
OGTT	Oral glucose tolerance test

PERK	PRK-like ER kinase
PheWAS	Phenome-wide association study
PI3K	Phosphoinositide-3-kinase
PKA	Protein kinase A
PNDM	Permanent neonatal diabetes mellitus
PPARγ	Peroxisome proliferator-activated receptor gamma
ROS	Reactive oxygen species
RXR	Retinoid X receptor
S6K1	Ribosomal protein S6 kinase 1
SD	Synthetic Derivative
SGLT2	Sodium-glucose co-transporter 2
SNP	Single nucleotide polymorphism
SOD	Superoxide dismutase
STZ	Streptozatocin
T1D	Type 1 diabetes
T2D	Type 2 diabetes
TCA	Tricarboxylic acid
TZD	Thiazolidinedione
UGRP	Ubiquitous glucose-6-phosphatase catalytic subunit related protein
UPR	Unfolded protein response
VAT	Visceral adipose tissue
WT	Wild type
ZnT8	Zinc transporter 8

LIST OF FIGURES

LIST OF TABLES

CHAPTER 1

Introduction

Diabetes Mellitus

Diabetes mellitus (DM) is a chronic disease primarily characterized by hyperglycemia stemming from the inability of the beta cell to produce or secrete sufficient quantities of insulin. According to the International Diabetes Federation, approximately 463 million adults ages 20-79, or 1 in every 11 adults, has diagnosed diabetes, with that number predicted to increase to over 700 million adults by 2045 [10]. Several tests can be used to diagnose diabetes in the clinic: a fasting plasma glucose level greater than or equal to 126 mg/dL, a plasma glucose level greater than or equal to 200 mg/dL two hours after an oral glucose bolus, or a glycated hemoglobin (HbA1c) greater than or equal to 6.5% [11]. Complications of DM include blindness, kidney failure, cardiovascular disease, and limb amputation, and it is estimated that in 2019 DM and its associated complications will result in 4.2 million deaths and over $750 billion in healthcare costs [10]. Because of the increasing prevalence of and costs associated with DM, there is a pressing need for new treatments and new methods of prevention. However, DM is a heterogeneous group of disorders, which differ primarily in the reason for insufficient levels of insulin to maintain glycemic control. Two major forms of DM are type 1 diabetes (T1D) and type 2 diabetes (T2D).

Type 1 Diabetes

T1D was formerly known as insulin-dependent diabetes (IDDM) or juvenile diabetes, since it was typically diagnosed in children or young adults, though it can present at any age. It is less

common than type 2 diabetes, accounting for 10% of all diabetes cases [10]. This disease is caused by autoimmune destruction of the insulin-producing beta cells within the pancreatic islet and therefore the loss of the ability to make insulin. Patients typically experience excessive thirst, excessive hunger, and excessive urination, which are all symptoms of chronic hyperglycemia [12]. Treatment is primarily focused on insulin replacement, achieved through close monitoring of glucose levels using blood glucose meters or continuous glucose monitors and administration of exogenous insulin or insulin analogues, either through injections or insulin pumps [13]. There are also ongoing efforts to combine continuous glucose monitoring and insulin pumps with a computer algorithm to create a closed-loop system, also termed an "artificial pancreas" [12]. Large-scale trials such as the Diabetes Control and Complications Trial (DCCT) [14] and subsequent analyses of data from those trials have shown that tight glycemic control via intensive treatment of hyperglycemia is associated with a decreased risk for long-term complications, including nephropathy, neuropathy, and retinopathy [15-17].

However, intensive treatment to prevent these chronic complications can increase the incidence of severe hypoglycemia. Hypoglycemia, clinically defined as a plasma glucose level ≤70 mg/dL, is the cause of death for 2-4% of individuals with T1D, and patients experience an estimated two episodes of hypoglycemia per week [18]. It most commonly occurs due to insulin excess, lack of food intake, or exercise, and, if not treated quickly, will lead to seizures, coma, and death [19]. Counterregulatory responses in patients with T1D become impaired over time, and therefore they cannot raise glucose levels on their own. Additionally, there is an attenuation of the neural symptom response, meaning that patients do not experience symptoms such as shaking, hunger, anxiety, or sweating that are indicative of a low blood glucose level, a condition known as hypoglycemia-associated autonomic failure (HAAF) [20]. The lack of appropriate

counterregulatory glucagon response from alpha cells in type 1 diabetics has been established for nearly 50 years [21-23]. One possible explanation for this impaired secretion, in addition to loss of inhibition from beta cells, is altered expression of nuclear regulators and alpha-cell enriched factors, including *MAFB*, *ARX*, and *PTGER3*, among others. Brissova et al showed these molecular changes were accompanied by functional defects in alpha cells, though the cause of these changes is still unclear [24].

It is thought that T1D develops from a combination of environmental factors and genetic susceptibility. The nature and contribution of external factors to disease development is not well understood, but may include viral infections, components of the gut microbiome, Vitamin D, or a lack of exposure to microorganisms early in life that affects immune system development (known as the "hygiene hypothesis") [25]. One or more of these factors, or indeed some as yet unidentified factor, triggers the process of autoimmunity. Autoantibodies to beta cell antigens can be detected prior to the onset of symptoms, with the risk of developing the disease increasing with an increasing spectrum of autoantibodies. More than 90% of newly-diagnosed patients have autoantibodies and T-cells reactive to insulin, glutamic acid decarboxylase (GAD65), insulinoma-associated antigen 2, and zinc transporter 8 (ZnT8) [12, 26]. Additionally, populations of T-cells, but not autoantibodies, were identified in mice and subsequently in humans against islet-specific glucose-6-phosphatase catalytic subunit related protein, or IGRP (also known as glucose-6-phosphatase catalytic subunit 2, or G6PC2) [27-30]. It is generally thought that antigen-presenting cells (APCs) present these autoantigens to autoreactive T-cells, including cytotoxic $CD8^+$ T-cells, which then destroy the beta cells [31]. Until roughly 90% of the beta cells are destroyed, patients remain asymptomatic, though inflammation and beta cell stress and destruction are ongoing. Studies have begun to investigate modulation of these $CD8^+$ T-cells as a method of preventing

disease development. A recent trial using a monoclonal antibody, telizumab, to alter $CD8^+$ T-cell function found that treatment delayed the progression to clinical T1D in high-risk patients by approximately 2 years, demonstrating that immune system modulation may be a viable preventative measure for T1D [32].

Given the important role of autoimmunity in the pathogenesis of T1D, it is perhaps unsurprising that much of the genetic susceptibility for T1D is associated with the immune system. The human leukocyte antigen (HLA) loci, which maps to chromosome 6, has the strongest genetic association with the development of T1D, potentially accounting for half of the genetic susceptibility for T1D [33]. The HLA complex is important in the regulation of the immune system, and is thought to play a part in the development of other autoimmune diseases as well. Genetic changes in other loci have also been associated with T1D, though their effects are far more modest than those in the HLA locus. To date, over 60 loci have been associated with T1D susceptibility in genetic studies [34]. These include other genes that are involved in the immune system or beta cell function, including *insulin* (*INS*)*, cytotoxic T-lymphocyte-related protein 4* (*CTLA4*)*, protein tyrosine phosphatase 22* (*PTPN22*)*, interleukin 2 receptor alpha* (*IL2RA*)*,* and *C-type lectin domain family member 16* (*CLEC16A*), among others [35, 36].

There are multiple mouse models that can be used to mimic the pathogenesis of T1D. The most commonly used spontaneous or autoimmune model is the non-obese diabetic (NOD) mouse. These mice exhibit a susceptibility to autoimmune diabetes due to a combination of genetic variants and environmental conditions, and will develop insulitis due to lymphocyte infiltration as early as 3-4 weeks of age [37]. This leads to beta cell destruction, though, similar to humans, clinical symptoms are not exhibited until roughly 90% of beta cells are lost, usually around 10-14 weeks of age. The NOD mouse model has been useful in elucidating the autoimmune mechanisms

in T1D. While multiple targets of autoimmunity were identified in islets, questions remained about which might be a primary target for autoimmunity and therefore essential for the development of T1D. A key study in NOD mice demonstrated the necessity of autoimmunity to insulin for the development of the disease [38]. Transgenic NOD mice were generated that expressed a mutant form of insulin to which T-cells do not react, and these mice were crossed with NOD mice where both insulin genes were knocked out, producing NOD mice that only expressed this mutant insulin. In female double-knockout transgenic mice, there was no evidence of autoantibodies to insulin or insulitis, and none of the mice developed diabetes, demonstrating the necessity of autoimmunity to insulin for T1D to develop [38]. Subsequent studies in humanized NOD mice determined that IGRP is another important autoantigen in T1D [39, 40]. However, work from the O'Brien lab determined that deletion of IGRP from NOD mice did not halt or even slow the progression of T1D, indicating that, at least in mice, T-cell recognition of IGRP is a secondary, downstream event in T1D progression and is not necessary for the development of the disease [41].

Another commonly used model of insulin-deficient diabetes is the Akita mouse, which has a mutation in the *insulin 2* gene. This mutation prevents correct processing of proinsulin, leading to protein misfolding and endoplasmic reticulum (ER) stress which is toxic to the beta cell. These mice develop diabetes by 3-4 weeks of age, and must receive insulin treatment to survive [42]. In addition to genetic and autoimmune models, there are chemical methods of inducing diabetes that mimic some aspects of T1D. Treatment of mice with streptozatocin (STZ) or alloxan, which are cytotoxic glucose analogs, will lead to selective beta cell death with precise dosing. Unlike T1D in humans and NOD mice, there is no autoimmune component to the development of diabetes in Akita or STZ-treated mice, but these models provide a relatively simple and inexpensive way to induce insulin-deficient diabetes and examine the effects of beta cell loss on metabolism [37].

Type 2 Diabetes

T2D was previously known as non-insulin dependent DM (NIDDM), and is the most common form of DM, accounting for 90% of cases. Lifestyle factors play a primary role in the risk of developing T2D, with obesity, physical inactivity, high-fat diet, and smoking all increasing the chance of developing the disease. Obesity alone is thought to contribute to 55% of T2D cases [43]. T2D is characterized by hyperglycemia that results from insulin resistance and insufficient functional beta cell mass. Insulin resistance is a metabolic abnormality in which the ability of insulin to suppress lipolysis and glucose production and stimulate glucose uptake is blunted. This increases demand on the beta cells to produce insulin. T2D develops when this demand for increased insulin secretion cannot be met due to insufficient beta cell mass and/or impaired beta cell function. The mechanisms behind beta cell failure and insulin resistance will be discussed further in **Mechanisms of Insulin Resistance** and **Mechanisms of Beta Cell Failure**.

There is also a genetic component to T2D; concordance among monozygotic twins is nearly 100%, and individuals with a family history of T2D have a 25% chance of developing the disease themselves [43]. Genetic studies have identified hundreds of loci that are linked to altered risk for T2D [44]. Rare or low-frequency variants that have major effects on protein function appear to make only modest contributions to T2D risk, but have played an important role in understanding the disease [45]. It is estimated that 1-4% of all cases of diabetes are monogenic forms of diabetes, where a change in a single gene leads to development of the disease [46]. Rare, typically *de novo* mutations in genes essential to beta cell function, such as *glucokinase (GCK)*, *ATP-binding cassette transporter sub-family C member 8 (ABCC8)*, *potassium inwardly rectifying channel sub-family J member 11 (KCNJ11)*, or *INS* have been shown to cause neonatal forms of diabetes [47]. The most common form of monogenic diabetes is maturity-onset diabetes of the

young, or MODY [48]. There are currently 14 separate subtypes of MODY, which represent distinct genetic mutations [49]. Inheritance of these mutations is typically autosomal dominant, and both presentation and treatment of the disease varies depending on the mutation [46]. The four most common subtypes account for 80-90% of MODY cases, and are caused by mutations in *HNF4A*, *GCK*, *HNF1A*, and *HNF1B* [48, 49]. These genes are known to be important to beta cell development and/or function, but because they are also expressed in other cell types, it is unclear if the etiology of MODY is specific to their effects in the beta cell.

Recently, genome wide association studies (GWAS) have been used to elucidate genes involved in complex human traits and/or diseases. This methodology is used to find associations between SNPs throughout the human genome and altered risk for a particular disease or condition; it is an unbiased approach and allows for the identification of genes with more modest impacts on disease risk [50]. Single nucleotide polymorphisms (SNPs) linked to T2D risk have been identified in genes such as *GCK*, *TCF7L2*, *FTO*, *HNF1B*, *KCNJ11*, *WFS1*, *HHEX*, *PPARG*, and *SLC30A8*, among many others (reviewed in [51]). The mechanism behind the association between T2D and some of these loci is clear, with signals in *GCK*, *WFS1*, and *SLC30A8*, for example, being linked to changes in islet function, but many of these loci still need to be investigated to determine how they contribute to T2D risk.

Pancreas Structure and Function

The pancreas is composed of both exocrine and endocrine tissue. Exocrine tissue makes up 98-99% of the pancreas, and is composed of mini structures called acini. Within these acini, cells produce digestive enzymes, including proteases such as trypsin and carboxypeptidase, amylases, and lipases, which are then secreted into a system of ducts that lead to the small intestine [52].

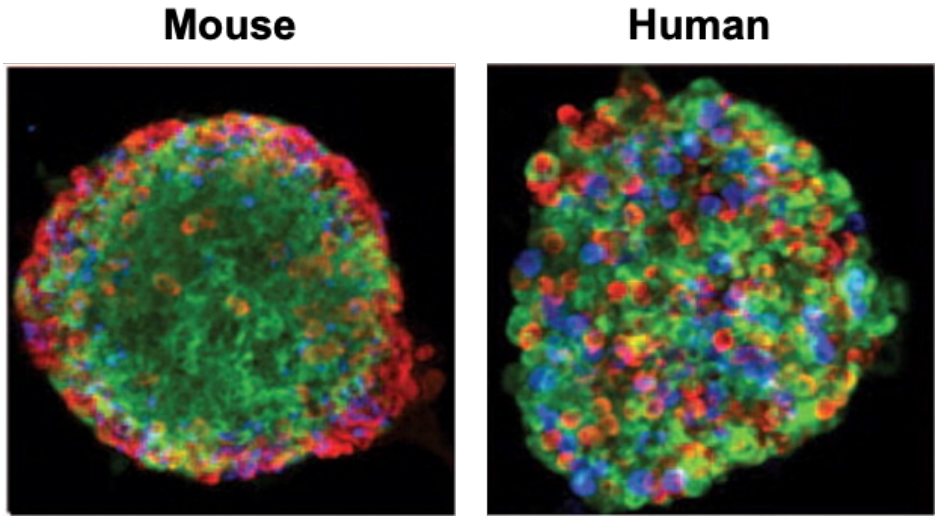

Figure 1.1. Architecture of the islet of Langerhans. Representative combined confocal images of a mouse (left) and human (right) islet of Langerhans, illustrating pancreatic islet cell composition and distribution. Beta cells, green; alpha cells, red; delta cells, blue. Adapted from [8].

Endocrine tissue comprises the remaining 1-2% of the pancreas, and is organized into structures called islets of Langerhans (Figure 1.1). Within the islets, there are five distinct cell types, each of which secrete a specific hormone in response to secretogogues in the blood. Beta cells are the most numerous cell type in the islet, comprising approximately 70% of the cells within the mouse islet and 50% of the cells within the human islet [53]. Beta cells synthesize and release insulin under high glucose conditions, thus stimulating uptake of glucose from the blood into tissues and suppressing hepatic glucose production. Alpha cells make up roughly 20% of mouse islet cells and 40% of human islet cells [53], and secrete glucagon under low glucose conditions, which stimulates hepatic glucose production to raise blood glucose levels. Less than 10% of mouse or human islet cells are delta cells, which produce somatostatin; this hormone acts through a paracrine mechanism to suppress both insulin and glucagon secretion [54]. PP cells, also known as gamma cells, make up less than 5% of mouse or human islet cells, and secrete pancreatic polypeptide in response to low glucose or high protein levels, which then acts to reduce appetite and food intake [52]. Finally, less than 1% of islet cells are epsilon cells [52]. These cells secrete ghrelin, which acts on the hypothalamus to induce a state of hunger and thereby increase food intake. Together, these endocrine cell types and their secreted hormones act to maintain glucose homeostasis. The function of the insulin-producing beta cell will be the focus of this dissertation.

Glucose-Stimulated Insulin Secretion (GSIS)

Insulin release from the beta cell can be triggered by glucose (Figure 1.2). As glucose levels in the blood rise, as occurs after a meal, glucose enters the beta cell through a glucose transporter (GLUT2 in rodents, GLUT1 in humans) [55]. In the cytoplasm, glucose is converted to glucose-6-phosphate (G6P) through the action of the enzyme glucokinase (GCK) [56]. G6P is next

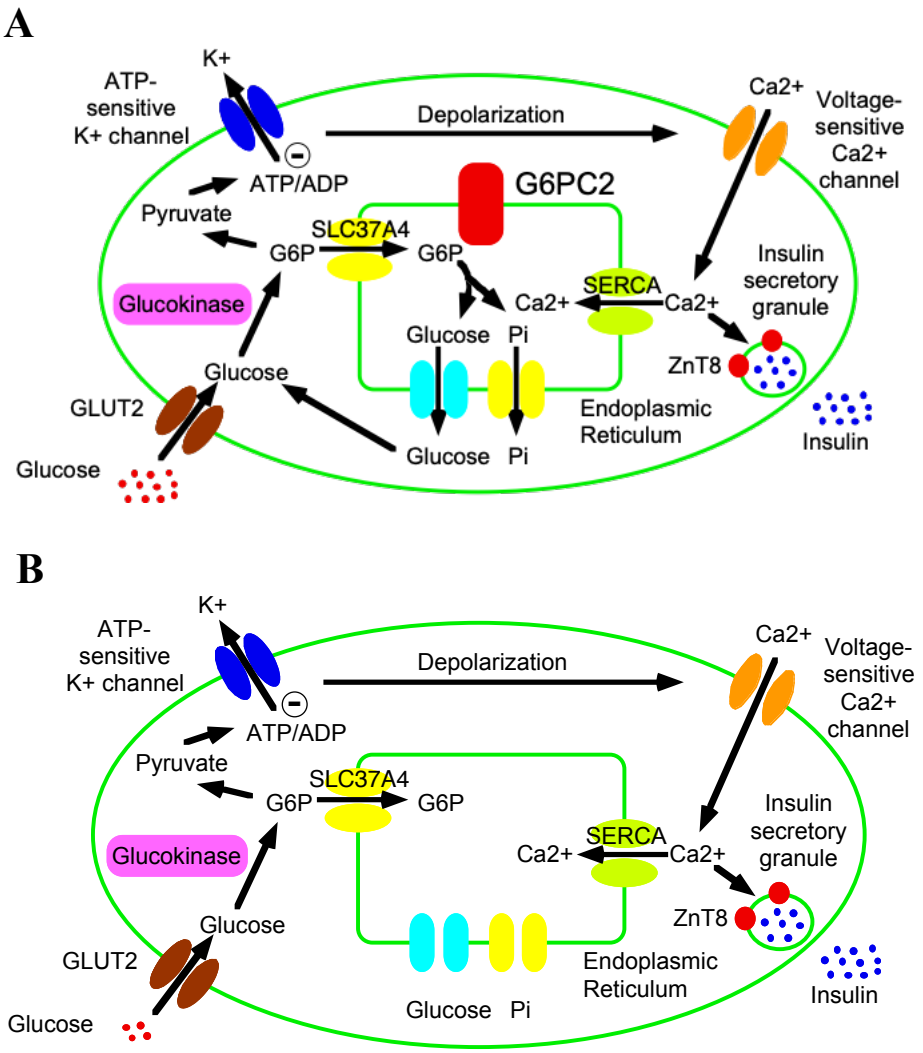

Figure 1.2. Model for the regulation of glucose-stimulated insulin secretion (GSIS) by G6PC2. **A**: Glucose enters the beta cell through GLUT2 (GLUT1 in humans) and is converted to glucose-6-phosphate (G6P) by glucokinase. G6P continues to be metabolized through glycolysis, producing ATP. A rise in intracellular ATP is sensed by the ATP-sensitive potassium channel, which responds by closing. This results in depolarization of the membrane and opening of voltage-sensitive calcium channels, which allows an influx of calcium to stimulate insulin secretion. G6PC2 opposes the action of glucokinase by hydrolyzing G6P, creating a futile substrate cycle. **B**: When G6PC2 is absent, a lower level of fasting blood glucose is needed to achieve the same level of insulin secretion.

metabolized through glycolysis, producing pyruvate which can enter the mitochondrion and be metabolized through the tricarboxylic acid (TCA) cycle, producing adenosine triphosphate (ATP). This increase in ATP or the ATP:adenosine-diphosphate (ADP) ratio is sensed by ATP-sensitive potassium channels (K_{ATP}) present in the plasma membrane, which respond by closing [57]. Closure of these channels leads to depolarization of the plasma membrane. This depolarization in turn triggers the opening of voltage-gated calcium channels, which allows calcium to flow into the cell [58]. This influx of extracellular calcium stimulates further calcium release from intracellular stores in the ER, a process known as calcium-induced calcium release (CICR). Increasing cytoplasmic calcium levels leads to fusion of insulin-containing secretory vesicles with the plasma membrane, releasing insulin into the bloodstream [59].

While regulating K_{ATP} channels is important for the triggering pathway of GSIS, there appears to be a role for a K_{ATP}-independent pathway that amplifies GSIS. Evidence for this amplifying pathway came from observations of patients with mutations in SUR1, a regulatory component of the K_{ATP} channel. Loss of SUR1 function results in loss of trafficking of the K_{ATP} complex to the plasma membrane, leading to constant depolarization of the plasma membrane and persistently elevated calcium levels that causes hyperinsulinism [57]. However, patients with these mutations can still increase insulin secretion in response to a glucose bolus [60]. This initial finding was later supported by evidence from isolated islets from K_{ATP} channel knockout mice showing rapid insulin secretion in response to glucose [61]. The mechanisms and modulators that underlie this amplifying pathway have not yet been fully elucidated, though studies have suggested roles for nicotinamide adenine dinucleotide phosphate (NADPH), malonyl-CoA, monoacylglycerol (MAG), and cyclic adenosine monophosphate (cAMP), among others (reviewed in [62] and [63]).

The presence of an islet-specific glucose-6-phosphatase provides an alternate fate for G6P in addition to being metabolized by mitochondria. G6PC2 can hydrolyze G6P to release glucose and free phosphate, creating a futile substrate cycle with GCK. This cycling would be predicted to shift the dose-response curve for GSIS and reduce fasting blood glucose (FBG); this will be discussed further in the section on **G6PC2 Function *In Vivo***.

Insulin Signaling

In a metabolically-healthy individual, insulin is released by the beta cell into the portal vein, and initially encounters the liver. Roughly 50% of this insulin is cleared by the liver, and the remainder is circulated to periphery, where it encounters insulin-sensitive and/or metabolically important tissues such as the brain, adipose tissue, and skeletal muscle [64]. Insulin binds to the alpha subunit of its receptor, inducing a conformational change that allows the beta subunits to be auto-phosphorylated on multiple tyrosine residues. This in turn allows for the recruitment of scaffolding proteins and substrates, which can then be phosphorylated to perpetuate the insulin signaling cascade. The two major insulin-stimulated pathways activate phosphoinositide-3-kinase (PI3K) and mitogen-activated protein kinase (MAPK). The former is important for mediating insulin's metabolic effects, including stimulation of glucose uptake by skeletal muscle and adipose and suppression of hepatic glucose production (HGP), while the latter pathway is primarily responsible for the mitogenic effects of insulin [65].

In the liver, insulin signaling promotes protein synthesis, glycogen synthesis, de novo lipogenesis (DNL), and suppresses gluconeogenesis. In both skeletal muscle and adipose, glucose transport through GLUT4 is increased, and lipolysis is decreased in adipose tissue through the action of insulin [65]. The overall effect of insulin is to decrease plasma glucose levels by

stimulating its uptake into tissues for storage and future use. However, in some cases, a normal plasma insulin level is insufficient to stimulate this glucose-lowering response, due to the presence of insulin resistance. The beta cell must compensate by increasing insulin secretion. This hypersecretion of insulin may also drive an increase in insulin resistance, since tissues such as the heart and skeletal muscle protect themselves from nutrient-induced toxicity by decreasing the response to insulin signaling (reviewed in [66]). Eventually, the pancreatic beta cells are unable to secrete sufficient insulin due to loss of function or mass, resulting in hyperglycemia and T2D. The mechanisms behind both insulin resistance and beta cell failure are important to understand when developing treatments to prevent or treat T2D, and these will be covered in **Mechanisms of Insulin Resistance** and **Mechanisms of Beta Cell Failure**.

Mechanisms of Insulin Resistance

There have been multiple mechanisms proposed for the development of insulin resistance. First, it is thought that in obesity, the storage capacity of the adipocyte is saturated, resulting in the distribution of this excess lipid to other tissues, including liver and muscle [67]. Indeed, studies have demonstrated that in humans, intrahepatic triglyceride content (IHTG) is a better indicator of hepatic insulin resistance than visceral adipose tissue (VAT) volume, and that removal of VAT without changes in IHTG does not improve metabolic function [68, 69]. Lipid accumulation in both liver and muscle can activate stress-induced protein kinases, including novel protein kinase C (nPKCs) and c-Jun N-terminal kinases (JNKs) [65]. These kinases can phosphorylate serine residues on the insulin receptor and/or insulin receptor substrate 1 and 2 (IRS1 and IRS2), and thus interfere with insulin signaling.

Activation of nPKCs has been observed in insulin-resistant liver and skeletal muscle in both mice and humans. In rats that had insulin resistance induced by chronic glucose infusion, levels of membrane-associated PKCε increased, indicative of sustained activation [70]. Additionally, PKCε translocation to the membrane was increased in muscle biopsies from obese humans with or without T2D [71]. PKCε also appears to be activated in liver biopsies from obese, non-diabetic humans [72] and in the livers of rats fed a high-fat diet for only 3 days, a model in which hepatic insulin resistance can be studied in the absence of peripheral insulin resistance [73]. Further study demonstrated a critical role for PKCε in hepatic insulin resistance [74]. Treatment of rats on the same short-term high fat diet paradigm with an antisense oligonucleotide for PKCε did not develop insulin resistance; this same study also showed that PKCε interacts with the insulin receptor and affects its activity *in vivo* [74]. PKCs can be activated by diacylglycerol (DAG), which may accumulate in a state of nutritional excess such as obesity. Increased levels of DAG and other bioactive lipids such as ceramide can be detected in liver and muscle in the context of obesity and diabetes; this may be due to shunting of excess lipid into biosynthetic pathways for these molecules. Alternatively, an increase in the rates of fatty acid oxidation without a concomitant increase in TCA cycle flux leads to accumulation of mitochondrial-derived lipid byproducts, which may play a role particularly in muscle insulin resistance [75].

JNKs are activated by the ER stress pathway known as the unfolded protein response (UPR), which can be triggered in response to the nutrient excess present in obesity, or by the accumulation of misfolded proteins within the ER. Three canonical pathways compose the UPR, which work to reduce protein synthesis & enhance protein folding or degradation to reduce stress within the ER; these pathways may also initiate cell death if the stress cannot be mitigated [76]. Each canonical pathway is activated by one of three transmembrane sensors: inositol-requiring

enzyme 1 (IRE1), PKR-like ER kinase (PERK), and activating transcription factor 6 (ATF6). Under normal conditions, these sensors are bound by the chaperone BiP/GRP78, but this interaction is disrupted by the accumulation of misfolded proteins, activating the UPR [65]. IRE1 oligomerizes and auto-phosphorylates, activating its endoribonuclease activity and allowing it to splice XBP1, which in turn acts to regulate genes involved in ER-associated degradation (ERAD) and protein folding. Similarly, PERK dimerizes and autophosphorylates to become an active kinase, and activates eIF2α. eIF2α decreases mRNA translation initiation overall, but preferentially upregulates selected mRNAs important to the UPR, such as activating transcription factor 4 (ATF4), which regulates genes involved in ER homeostasis [77]. Finally, ATF6 moves to the Golgi, where it is processed, and then translocates to the nucleus, where it functions as a transcription factor for genes involved in protein processing, folding, and degradation [78]. JNK can be activated through the IRE1 or PERK pathways, and phosphorylates IRS1 and IRS2 on serine residues, thus impairing insulin signaling and contributing to insulin resistance [79]. Markers of ER stress have been identified in liver and adipose tissue from obese humans, and this stress was alleviated after weight loss surgery alongside improvements in insulin sensitivity [80]. Additionally, treatment with chemical chaperones reduced active JNK and IRS1 serine phosphorylation in the liver and adipose tissue of obese mice, and improved whole-body insulin sensitivity [81]. These studies and others indicate that reducing ER stress in metabolically important tissues may be a viable treatment for reducing insulin resistance and improving glucose homeostasis.

There are many other pathways that may play a role in insulin resistance. Peptide hormones are released from adipocytes, including leptin and adiponectin, which act to decrease triglyceride synthesis and enhance insulin action in other tissues such as the liver and skeletal muscle, and

alterations in levels of these hormones are associated with insulin resistance [82]. High levels of some circulating amino acids present in obese individuals [83] can activate hVps34 (a class 3 PI3K), which activates mammalian target of rapamycin (mTOR) and ribosomal protein S6 kinase 1 (S6K1). S6KI can phosphorylate IRS1 and thus inhibit insulin signaling [84].

Overnutrition can activate NF-κB in adipose, liver, and muscle, which stimulates the release of pro-inflammatory cytokines. These in turn can signal to inhibit insulin signaling, and promote a state of inflammation and insulin resistance, though this can be partly mitigated with large doses of salicylates [85]. One mechanism for the effects of NF-κB signaling on inflammation and insulin resistance is through its effects on macrophages [86] While macrophages typically reside in lean adipose tissue, in the setting of obesity they increase in number, and exhibit a pro-inflammatory phenotype [87, 88]. Increasing numbers of activated inflammatory macrophages can secrete chemokines that in turn recruit and activate more macrophages, setting up a feed-forward mechanism that propagates an inflammatory state and can inhibit insulin signaling in other tissues by activating the JNK pathway, among others [89]. NF-κB signaling can promote the survival of these pro-inflammatory macrophages and thus contribute to inflammation [86], though this is not likely to be the sole mechanism regulating macrophage number and activation [90]. Overall, insulin resistance likely results from the combined effect of negative impacts on insulin signaling in multiple tissues through multiple pathways.

Mechanisms of Beta Cell Failure

While obesity can lead to a state of insulin resistance, only a subset of obese individuals will develop T2D. This progression occurs due to failure of the beta cell to produce sufficient insulin to maintain glycemic control. This failure is thought to arise from a combination of

insufficient beta cell mass and a decline in beta cell function. Beta cell mass is determined by the beta cell number and size. Hypertrophy, proliferation, and neogenesis can increase beta cell mass, while decreases in beta cell mass can occur through de-differentiation, altered identity, apoptosis, and atrophy [91]. Beta cell mass increases from embryogenesis to adulthood, and in normal circumstances is altered in accordance with an organism's requirement for insulin. For example, in settings of obesity or pregnancy, beta cell mass increases to compensate for the increased demand for insulin, and the factors that govern this expansion remain an important area of study (reviewed in [91]), as well as the mechanisms by which beta cell mass is lost (reviewed in [92] and [93]).

In addition to compensations in mass, there is also a compensatory increase in insulin synthesis and secretion from beta cells in the face of insulin resistance. However, chronic nutrient excess and the increased demand for insulin can cause lipotoxicity and excitotoxicity, causing stress on the beta cell, negatively impacting beta cell function and decreasing its sensitivity to glucose [94]. This leads to an increase in blood glucose levels that is below the criteria for diagnosing diabetes, known as impaired glucose tolerance. This chronic hyperglycemia can eventually lead to glucotoxicity, which causes further stress on the beta cell, leading to significant dysfunction and/or death. The exact mechanism by which this occurs is unclear, but is likely the result of a number of factors. First, the increased glycolytic flux leads to the increased generation of reactive oxygen species (ROS), which induces oxidative stress and impairs insulin secretion [95]. Hyperglycemia can also induce ER stress due to an increased demand for insulin synthesis and processing. Prolonged activation of the UPR (described in **Mechanisms of Insulin Resistance**) can upregulate C/EBP-homologous protein (CHOP), which plays a role in initiating apoptosis. This can be seen in the Akita mouse model and in humans with mutations in the *insulin*

gene, where insulin misfolding leads to activation of the UPR and eventually beta cell death and diabetes [96, 97]. In humans, inactivating mutations in *WFS1* lead to increased ER stress via disruptions in calcium homeostasis, leading to beta cell death and diabetes as part of Wolfram syndrome [98]. Overall, much like insulin resistance, it is likely a combination of pathways and factors contribute to the failure of beta cells that leads to T2D.

Treatments for T2D

Because the prevalence of diabetes is increasing worldwide, and 90% of diabetes cases are T2D, there is a great interest in treatments for T2D. Diet and exercise are encouraged as initial treatments and can be effective in treating and preventing the disease, but frequently these interventions are not sufficient, and patients must rely on various drugs to control their diabetes. Current drugs include metformin, sulfonylureas, thiazolidinediones (TZDs), sodium-glucose co-transporter 2 (SGLT2) inhibitors, and drugs that target the incretin signaling pathway.

Metformin is a member of the biguanide family, and is recommended as a first-line oral therapy for T2D. It is a potent anti-hyperglycemic, lowering blood glucose levels without overt hypoglycemia [99]. The exact mechanism of metformin action is still an area of study, but there are several potential effects that could all act to lower blood glucose. First, metformin can improve insulin sensitivity, possibly through increasing insulin receptor expression and its tyrosine kinase activity. Second, recent studies have suggested that metformin treatment can increase glucagon-like peptide 1 (GLP-1) levels and islet GLP-1 receptor expression, leading to an increase in insulin secretion [100]. Another action of metformin is to decrease HGP through inhibition of complex 1 of the mitochondrial respiratory chain and subsequent activation of adenosine monophosphate-activated protein kinase (AMPK), which suppresses hepatic glucose production [99]. Finally, *in*

vivo studies in humans suggest that metformin may not suppress hepatic glucose production, but instead acts to suppress lipolysis and improve glucose clearance [101, 102]. Despite its initial efficacy, studies have shown that as many as 42% of patients experience failure to lower their HbA1c on metformin within two years of drug initiation [103].

Sulfonylureas have been used for over 50 years in treating T2D [104]. They have two major mechanisms of action: stimulating the beta cell to secrete insulin, and decreasing hepatic insulin clearance [105], though some effects on insulin sensitivity and insulin receptor activity have also been reported [106]. Sulfonylureas bind to the SUR1 receptor on the beta cell, thus inhibiting the ATP-sensitive potassium channel and depolarizing the membrane. This depolarization results in an influx of calcium and a release of insulin. This mechanism of action is predominantly glucose-independent, and therefore hypoglycemia is a significant risk of sulfonylurea therapy [104]. Beta cells must still be intact and functional for treatment to be effective. However, chronic sulfonylurea administration may eventually lead to beta cell failure due to hyperexcitability, and patients frequently begin to rely on insulin to lower their blood glucose [107].

Thiazolidinediones (TZDs) exert their effect on blood glucose by improving insulin sensitivity in adipose tissue, muscle, and liver. They are direct, high-affinity ligands for peroxisome proliferator-activated receptor gamma (PPARγ), which forms a heterodimer with retinoid X receptor (RXR). Binding of TZD to this heterodimer results in a conformational change that displaces co-repressor complexes, allowing PPARγ-RXR to bind to co-activator complexes and increase expression of target genes. The primary target genes for PPARγ-RXR are those involved in energy balance and lipid metabolism, and include such genes as those for *lipoprotein lipase (LPL), GCK*, and *GLUT4* [108]. Because PPARγ is most highly expressed in adipose tissue, the improvement in insulin sensitivity by TZDs is primarily attributed to its activity in that tissue,

and the effects in muscle and liver may be secondary, and attributable to endocrine signaling from adipose tissue. Recent studies have also suggested that TZDs may have positive effects on beta cells that also contribute to improvements in glycemia, including increasing insulin storage capacity, protecting against oxidative stress, and preserving beta cell mass [109]. However, two TZDs, troglitazone and rosiglitazone, have been documented to cause an increased risk of liver toxicity and cardiovascular events, respectively, and this, along with other significant side effects, has limited the current use of TZDs in T2D treatment [110].

Sodium-glucose co-transporter 2 (SGLT2) inhibitors, one of the newest approved classes of T2D drugs, act to lower blood glucose by acting on the kidney rather than the pancreas or liver. SGLT2 is located primarily in the renal proximal tubule where it acts to reabsorb ~90% of glucose that is filtered at the glomerulus [111]. These inhibitors prevent this glucose reabsorption, thus increasing the amount of glucose excreted in urine and lowering both FBG and HbA1c. Treatment with SGLT2 inhibitors has additional beneficial effects, including weight loss, decreased blood pressure, and protection from cardiovascular effects [112]. However, these drugs are also associated with a number of potentially serious side effects, including genitourinary infections, Fournier gangrene, hypoglycemia (mainly when used in combination with insulin or sulfonylureas), ketoacidosis, bone fractures, and lower limb amputations [112].

Finally, there is a category of T2D therapeutics that targets the incretin pathway. Incretins are peptide hormones released by enteroendocrine cells in the small intestine after ingestion of a meal that act to enhance insulin secretion, and may account for as much as 50% of the postprandial insulin secretory response. This incretin response is impaired in patients with T2D and this impairment may contribute to decreases in insulin secretion and hyperglycemia [113]. Two incretin hormones are glucose-independent insulinotropic peptide (GIP) and glucagon-like peptide

1 (GLP-1). Exogenous administration of GLP-1 was shown to increase insulin secretion and normalize blood glucose in patients with T2D, whereas GIP administration did not [114], making GLP-1 an attractive basis for drug development. GLP-1 receptors are expressed in multiple tissues, including pancreatic islets, heart, lungs, and nervous system. Binding of GLP-1 or an agonist to its receptor increases cAMP production which activates protein kinase A (PKA), which in the beta cell leads to increased calcium levels and insulin secretion [115]. It is unclear if endogenous GLP-1 acts directly on the beta cell or if it instead exerts effects on a central neural locus. In mice, beta cell-specific knockdown of the GLP-1 receptor (GLP1R) did not affect oral glucose tolerance [116]. Activation of GLP1R in the brain of mice improved oral glucose tolerance [117], indicating a role for GLP1R in the brain. However, loss of GLP1R in three separate brain regions had no effect on glucose tolerance [118]. Further study is necessary to clarify the sites of action of GLP-1 and their relative contributions to its effects on blood glucose regulation.

Several GLP-1 receptor agonists have been developed as treatments for T2D, and have beneficial effects including decreasing HbA1c, weight loss, increasing satiety, decreasing gastric emptying, and suppressing glucagon secretion [113]. Another target within this incretin pathway is dipeptidyl peptidase 4 (DPP-4), an endogenous enzyme that degrades incretins rapidly within the blood. Inhibition of this enzyme decreases the rate of GLP-1 degradation, keeping the concentration of endogenous GLP-1 high enough to maintain a therapeutic effect. However, recent reports have indicated that GLP-1 receptor agonists and DPP-4 inhibitors may be associated with an increased risk for acute pancreatitis, though this is still the subject of debate [115, 119].

The Glucose-6-Phosphatase Catalytic Subunit Gene Family

The glucose-6-phosphatase catalytic subunit gene family is composed of 3 members: G6PC1 (also known as G6PC, G6Pase, or G6Pase-α), G6PC2 (also known as IGRP), and G6PC3 (also known as UGRP or G6Pase-β). They primarily differ in their pattern of tissue expression and activity, as well as their roles in human phenotypes or diseases. Table 1.1 summarizes the key features of the G6PC gene family. All 3 family members encode proteins of similar length with nine transmembrane domains that reside in the ER membrane, and have similar predicted topology [120]. G6PC1 is primarily expressed in the liver and kidney, G6PC2 is highly expressed in islet beta cells, and G6PC3 is expressed ubiquitously. The gene for *G6PC2* is located on chromosome 2, whereas the *G6PC1* and *G6PC3* genes are located on chromosome 17.

G6PC1

The liver plays an important role in the maintenance of whole-body glucose homeostasis. In a post-prandial state, glucose is taken up by the liver and converted to G6P, which can be metabolized through glycolysis or the pentose phosphate pathway, or stored as glycogen. When glucose is not immediately available, such as during a fast or in a pre-prandial state, the liver must produce glucose by either breaking down its glycogen stores through glycogenolysis or producing glucose from gluconeogenic precursors such as amino acids, glycerol, and lactate. Because both glycogenolysis and gluconeogenesis result in the production of G6P, which could reenter metabolic pathways, it was postulated that there must be an enzyme that could dephosphorylate G6P to release glucose and phosphate and thus allow for glucose to be released from the liver for use by other tissues [121]. Isolation and identification of this enzyme proved difficult due to its localization in the ER membrane, but Chou and colleagues were able to successfully identify the

Gene	G6PC1 (G6Pase)	G6PC2 (IGRP)	G6PC3 (UGRP)
Tissue	Liver	Islet Beta Cells	Ubiquitous
Size	357 AA	355 AA	346 AA
% Ident.	100	50	36
Chromosome	17q21	2	17q21
Location	ER	ER	ER
# TM	9	9	9
Substrate	G6P	G6P	G6P
Vmax (nmol/mg/min)	666.7 [4]	32 [6]	108.7 [4]
Km (mM)	2.5	0.45	2.5
Effect of Altered Function in Humans	Glycogen Storage Disease 1a	Reduced FBG	Neutropenia

Table 1.1. The Glucose-6-Phosphatase Catalytic Subunit Gene Family

gene for this enzyme by studying a mouse model with radiation-induced chromosomal deletions [122]; this strain develops severe hypoglycemia that is lethal shortly after birth as a result of decreased G6Pase activity [123]. They screened a murine liver cDNA library with probes from both wild type and albino mutant mice, and isolated the cDNA encoding the murine glucose-phosphatase catalytic subunit G6pc1 [122], and used this to identity human G6PC1 [124]. G6pc1 was later found to be expressed in the liver, kidneys, and small intestine [125]. Further characterization established that G6PC1 is a one part of a multi-component enzyme system, comprised of a G6P transporter (encoded by the *SLC37A4* gene), a glucose transporter, and a catalytic subunit (G6PC1, G6PC2, or G6PC3). G6P enters the ER lumen through SLC37A4, where it is then hydrolyzed by the catalytic subunit to glucose and free phosphate (Figure 1.3) [120].

Due to its role in the liver in glucose homeostasis, and the fact that it is the most active of the G6PC isoforms, it is perhaps not surprising that mutations in *G6PC1* are linked to disease states. Loss of function mutations in *G6PC1* cause glycogen storage disease type 1a (GSD1a). Without G6PC1 to hydrolyze G6P in the liver, glucose cannot be properly generated from gluconeogenesis or glycogenolysis, and patients cannot maintain proper glucose homeostasis. Patients typically present with hypoglycemia, hepatomegaly, hyperlipidemia, enlarged kidneys, lactic acidemia, and growth retardation [126]. More than 84 mutations have been identified in patients with GSD1a, many of which have been functionally characterized (reviewed in [127]). There is another form of glycogen storage disease, GSD1b, which is caused by mutations in the *SLC37A4* gene. Patients with these mutations exhibit similar impaired glucose homeostasis to those in GSD1a, but have additional complications of neutropenia and myeloid dysfunction [128], which can be explained by the loss of G6Pase activity in non-hepatic tissues. This underscores the importance of the entire G6Pase system in maintaining glucose homeostasis.

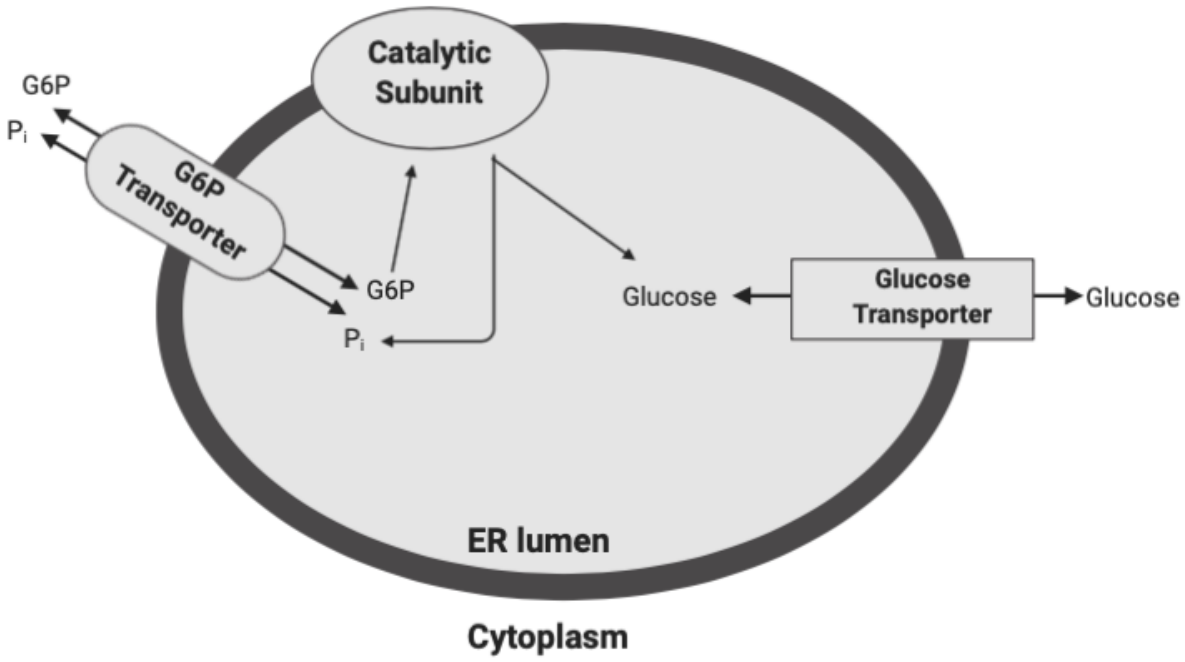

Figure 1.3. Model of the glucose-6-phosphatase multicomponent enzyme system. The glucose-6-phosphatase system is composed of a glucose-6-phosphate (G6P) transporter, a catalytic subunit, and a glucose transporter. G6P enters the ER lumen through the transporter, where the catalytic subunit acts to hydrolyze G6P to release glucose and a free phosphate.

Interestingly, increased G6PC1 expression and activity are a key feature of both T1D and T2D. Studies have found an increase of 2-3 fold in both *G6PC1* mRNA and glucose-6-phosphatase activity in the liver of rodents with diabetes [129, 130]. This is likely due to the relative (T2D) or absolute (T1D) decrease in insulin secretion, since G6PC1 activity is decreased following insulin treatment. Insulin signaling regulates *G6PC1* transcription through FOXO1 binding sites; it excludes FOXO1, a transcriptional activator, from the nucleus so it cannot bind the *G6PC1* promoter, and thus *G6PC1* expression is decreased [131]. In situations where insulin signaling is decreased, such as diabetes, *G6PC1* expression is inappropriately high, which helps to elevate blood glucose and contributes to the pathogenesis of the disease.

G6PC3

The gene for *G6PC3* was discovered with a BLAST search using human *G6PC2* as the query [132]. It was initially named the ubiquitously expressed glucose-6-phosphatase catalytic subunit-related protein, or UGRP, but was later renamed G6PC3 to reflect its relationship to the other G6PC family members. It shares 36% homology with G6PC1, and has the same predicted topology and function as G6PC1 and G6PC2 [132]. Initial studies using transient transfections to measure G6P hydrolysis by G6PC3 were unsuccessful, but later groups demonstrated its activity using adenoviral transfections of COS cells, showing it to have a similar K_m to G6PC1 but with a V_{max} approximately 6-fold lower [126, 133]. As its original name suggests, G6PC3 is expressed in multiple tissues throughout the body, with highest expression observed in skeletal muscle, intermediate expression in heart, brain, kidney, and pancreas, and very low expression in liver, lung, small intestine, and peripheral blood leukocytes [132]. *G6pc3* knockout (KO) mice were generated to determine if G6PC3 activity had physiological relevance; while G6Pase activity was

decreased in brain homogenates from KO mice, they did not have a significant metabolic phenotype [134]. However, *G6pc3* KO mice did have defective function in both neutrophils and macrophages, leading to a congenital neutropenia [135, 136]. These mouse data match human studies showing that loss of G6PC3 causes a severe congenital neutropenia, also known as Dursun Syndrome [137-139]. This may also explain why patients with GSD1b, who have mutations in *SLC37A4*, also experience neutropenia, since loss of either G6PC3 or SLC37A4 would cause the loss of the functional G6Pase complex [128].

Recent studies have begun to elucidate the mechanism by which loss of function of G6PC3 or SLC37A4 leads to neutropenia. Neutrophils from patients with mutations in either *G6PC3* or *SLC37A4* have reduced glucose utilization, which causes aberrant glycosylation and increased ER stress, leading to decreased neutrophil function and apoptosis [140]. Further work has shown that the neutropenia seen in patients with these mutations may be due to a failure to eliminate a non-canonical metabolite [141]. 1,5-anhydroglucitol (1,5AG) is a glucose analog normally present in blood, and it can be taken up and phosphorylated in cells to produce 1,5-anhydroglucitol-6-phosphate (1,5AG6P). 1,5AG6P is typically eliminated from cells after dephosphosphorylation by G6PC3 & SLC37A4, but if the activity of either G6PC3 or SLC37A4 is decreased, 1,5AG6P will accumulate in cells [141]. In neutrophils deficient in either G6PC3 or SLC37A4, 1,5AG6P inhibits the first step of glycolysis through inhibition of hexokinases [141], and this is particularly detrimental to neutrophils which rely almost entirely on glucose metabolism for energy production [142]. Interestingly, treatment with SGLT2 inhibitors decreases the concentration of 1,5AG in the blood which leads to increased neutrophil numbers, indicating that decreasing 1,5AG levels may be a viable treatment option for the neutropenia seen in patients with *G6PC3* or *SLC37A4* mutations [141].

G6PC2

G6PC2, initially named islet-specific glucose-6-phosphatase catalytic subunit-related protein, or IGRP, was cloned from a mouse insulinoma cell line, and was determined to share 50% identity with G6PC1, having similar predicted topology and conserved catalytically-important residues [143] and being localized to the ER [144]. The mouse gene was then cloned [145], and the human and rat genes were identified shortly after [146]. Expression of the gene was found to be restricted to the pancreatic islet [27, 143, 147]. These early studies were unable to demonstrate any G6P hydrolysis after overexpression of G6PC2, but one group was able to show that human G6PC2 has 20-40 fold less activity than G6PC1 when overexpressed in COS cells [6]. Historically there has been much debate as to the physiological relevance of G6Pase activity and glucose cycling in pancreatic islets [148-150]. The rate of glucose dephosphorylation was estimated to be 3-4.5% in islets from healthy mice, 15.7% in STZ-induced diabetic mice, and 40% in islets from ob/ob mice [151, 152]. This indicated that glucose cycling was present in mouse islets at variable levels. In contrast, studies in isolated rat islets suggested that the rate of cycling was too low to significantly affect GSIS [150]. However, *G6PC2* is a pseudogene in rats, and it is thought that G6PC1 mediates cycling instead, since it has been detected in rat islets [153]. Additionally, the rat islets were cultured in low glucose; therefore, since glucose is known to stimulate *G6PC1* transcription, under low glucose conditions *G6PC1* expression is likely to be low and thus the rate of cycling would be low [154, 155]. Both the mouse and rat islet studies were conducted using radioactive tracers, which lack sensitivity and rely on assumptions that may underestimate the rate of cycling by as much as 25% [156]. Recently, developments have been made in tracer studies that allow for the use of stable isotopes in place of radioactive tracers. Using this methodology, Wall et al demonstrated a rate of glucose cycling of 16% of the net glucose uptake in mouse islets

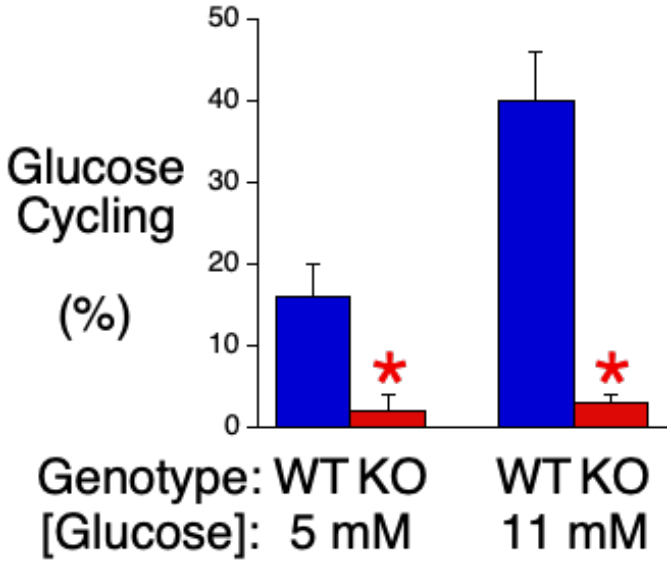

Figure 1.4. Glucose cycling is abolished in *G6pc2* KO mouse islets. The rate of glucose cycling increases in WT mouse islets with increasing glucose concentration, but is indistinguishable from background in *G6pc2* KO mouse islets. WT n = 10 incubations of 100 islets; KO n = 8 incubations of 100 islets. *p<0.05 vs. WT islets. Adapted from [7].

incubated in 5mM glucose, and this rate of cycling increased to 40% when the glucose level was increased to 11mM (Figure 1.4) [7]. Significantly, glucose cycling was abolished in islets isolated from *G6pc2* KO mice, indicating that the action of G6pc2 does contribute to glucose cycling in beta cells by opposing the action of glucokinase [7]. These data, in conjunction with the GWAS data discussed below, demonstrate the importance of G6PC2 function.

GWAS have been performed to look for genes associated with glycemic traits such as FBG and fasting insulin levels, and have identified over 50 loci associated with variations in glycemic traits, many of which are also associated with T2D risk [50]. The impetus for these GWAS studies on FBG came from the observation that variations in FBG levels have been associated with risk for the development of T2D and cardiovascular-associated mortality (CAM). Studies have shown that an increase in FBG of 9-18 mg/dL is associated with a 30% increased risk of CAM in a European population [157], while a reduction in FBG of 9 mg/dL is associated with a 25% decreased risk of CAM in an Asian population [158]. Additionally, Gerstein et al found that individuals with FBG levels between 100-125 mg/dL have a 5-fold increased risk of developing T2D than those with FBG levels below 100 mg/dL [159].

There are three genes that have the largest effect size on FBG levels that are consistently replicated across independent GWAS: *MTNR1B*, *GCK*, and *G6PC2*. *MTNR1B* encodes melatonin receptor 1b (MT2) whose ligand, melatonin, is a neurohormone that regulates circadian rhythm. MT2 is found in the retina and some areas of the brain, and it has been detected in isolated islets and sorted beta cells as well [160]. The SNP rs10830963 in the *MTNR1B* locus has been associated with variations in FBG across multiple studies [161]. It is not clear whether this SNP exerts its effects on FBG through direct mechanisms on the beta cell or through indirect mechanisms involving alterations of circadian rhythm in the brain. The G allele of this SNP has been shown to

increase expression of *MTNR1B*, which inversely correlated with GSIS from isolated islets. Additionally, incubation of 832/13 cells with melatonin inhibited GSIS [162].

An association between FBG and glucokinase was initially identified using a candidate gene approach that specifically looked for associations between SNPs in the *GCK* gene and FBG [163]. GCK is an isozyme of hexokinase expressed primarily in the liver, pancreatic islet, gut, and brain, where it catalyzes the first step in glycolysis and glycogen synthase by phosphorylating glucose to G6P [164]. It has a high K_M and, unlike other hexokinases, is not inhibited by its product G6P, allowing it to function as a glucose sensor in those tissues where it is expressed [165]. GCK also acts as a regulator of glycolytic flux, and as such can influence insulin secretion in the beta cell. Decreased GCK activity decreases glycolytic flux and insulin secretion, leading to hyperglycemia. Heterozygous loss of function mutations in *GCK* cause a form of MODY, while homozygous loss of function results in permanent neonatal diabetes mellitus (PNDM). Increasing GCK activity increases insulin secretion; rare activating mutations lead to persistent hyperinsulinemic hypoglycemia of infancy (PHHI) [164]. Finally, more recently GWAS have confirmed that a common variant, rs1799884, located in the -30 position of the *GCK* promoter, is associated with small but significant variations in FBG [166], likely because this SNP reduces *GCK* expression.

Finally, GWAS have identified a number of SNPs in *G6PC2* that are associated with variations in FBG [167-169]. One common SNP, rs560887, has a minor allele frequency of ~30% in Caucasians, and is the strongest common genetic determinant of FBG levels by effect size and significance, accounting for almost 1% of total FBG variance in humans [167, 170]. This SNP is located in intron 3 of *G6PC2*, and minigene analyses showed that the minor A allele of this SNP affects G6PC2 protein expression by reducing splicing efficiency and inclusion of exon 4, thus

reducing full-length *G6PC2* expression by approximately 10% [171]. The G/A genotype is associated with a 1 mg/dL reduction in FBG relative to the G/G genotype, and A/A is associated with a further 1mg/dL reduction relative to G/A [168]. Further discussion of *G6PC2* SNPs and functional studies on their effects can be found in Chapter 5.

Many of these studies also showed an association between these SNPs and variations in HbA1c [160, 168, 172]. A meta-analysis of 23 previous GWAS confirmed the association between SNPs in *G6PC2*, *GCK*, and *MTNR1B* with HbA1c, and also found that the allele associated with increased HbA1c was the same allele associated with elevated FBG. Subsequent conditional analyses suggested that the association between these SNPs and HbA1c was due to their effect on glycemia rather than a direct effect on HbA1c alone [173].

G6PC2 Function *In Vivo*

While the liver and, to some extent, the kidney, are the primary glucose-producing organs, the presence of G6PC isoforms and their activity in other tissues, including the pancreatic beta cell, has generated an appreciation for the contribution of G6PC isoforms in other tissues to glucose homeostasis. Indeed, the presence of glucose-6-phosphatase activity from G6PC2 in the beta cell led to the hypothesis that G6PC2 could act to modulate the sensitivity of GSIS by opposing the action of glucokinase. It was hypothesized that G6PC2 would act to form a futile substrate cycle with glucokinase, which would modulate insulin secretion. Therefore, it was predicted that in the absence of G6PC2, the dose-response curve for GSIS would be shifted to the left, resulting in a lower blood glucose concentration being needed to achieve the same level of insulin secretion and hence lowering FBG (Figure 1.5) [1].

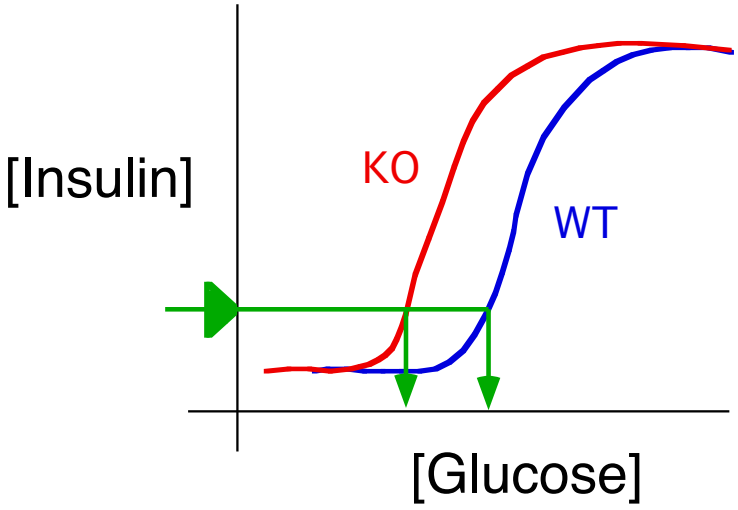

Figure 1.5. Model of the effect of *G6PC2* deletion on GSIS and FBG. Deletion of G6PC2 causes a leftward shift in the dose-response curve for GSIS, resulting in decreased FBG levels relative to WT with no significant different in FPI levels.

Consistent with this model and the glucose cycling data, previous data from the O'Brien lab further established the role of G6pc2 *in vivo* [1, 134]. Insulin secretion in islets isolated from *G6pc2* KO mice was significantly increased at submaximal glucose concentrations when compared to islets from wild-type (WT) mice, consistent with the hypothesis that deletion of *G6pc2* shifts the dose-response curve for GSIS [1]. Similar results were seen in perfused pancreata, where KO mice had increased insulin secretion at submaximal glucose concentrations. Additionally, FBG was significantly reduced in both female and male *G6pc2* WT mice bred on either a pure C57BL/6J [1] (Figure 1.6) or mixed background [147], consistent with a role for G6pc2 in the modulation of FBG. This decrease in FBG was not associated with changes in fasting plasma insulin (FPI), plasma glucagon, glucose tolerance, or insulin sensitivity [1, 147]. These data also fit with the human GWAS data that associated SNPs in *G6pc2* with variations in FBG.

Subsequent studies from the O'Brien lab sought to elucidate the physiological role of *G6pc2*. The association between elevated FBG and increased risk for the development of T2D and CAM implies that the presence of G6PC2 is detrimental to health in the modern environment of excess nutrients. In contrast, the regulation of FBG by G6PC2 must have conferred some advantage during evolution. Two studies have investigated the role of G6PC2 in the modulation of the effects of glucocorticoids, which are released during periods of stress. Using a physical restraint paradigm, which stresses the mouse and increases endogenous glucocorticoid levels, Boortz et al showed that *G6pc2* expression was induced in WT 129SvEv mice, which enhanced the difference in FBG between WT and *G6pc2* KO mice, and protected the WT mice against low blood glucose [174]. Additionally, treatment with the synthetic glucocorticoid dexamethasone induced *G6pc2* expression in both C57BL/6J and 129SvEv WT mice, which was associated with elevated FBG [175]. Glucocorticoids can induce human *G6PC2* expression through a

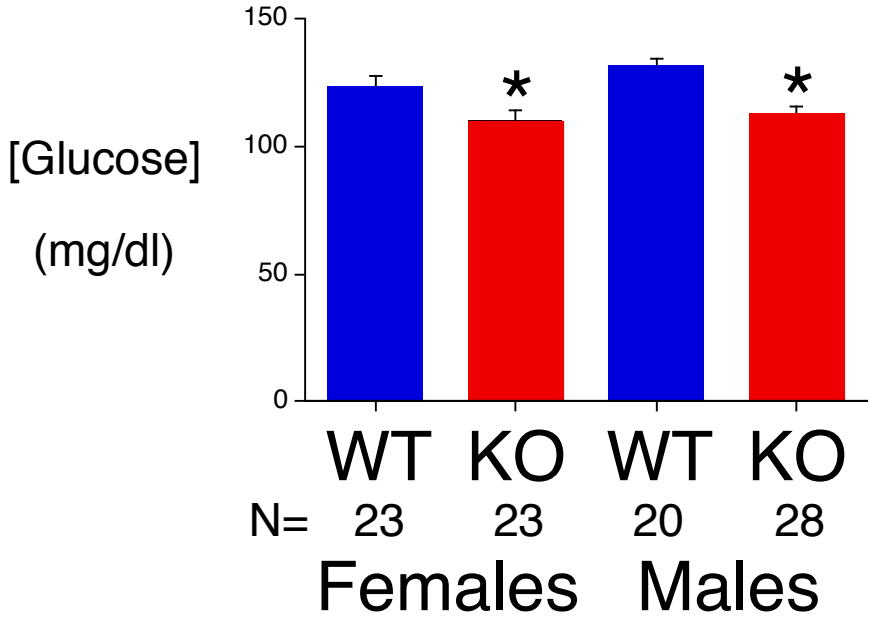

Figure 1.6. *G6pc2* KO mice have significantly reduced FBG levels relative to WT mice [1]. 17-week-old mice were fasted for 6 hours, then anesthetized prior to blood isolation from the retro-orbital venous plexus. Glucose concentrations were measured in whole blood using a glucose monitor. Results show mean ± SEM. *$p<0.05$

glucocorticoid response element in the *G6PC2* promoter, and dexamethasone was shown to induce expression of a *G6PC2* fusion gene in transient transfection and expression of the endogenous *G6PC2* gene in human islets [174, 175]. This induction of *G6PC2* expression would serve to transiently elevate blood glucose levels, making more glucose available to peripheral tissues in times of stress, which would be beneficial [176].

The O'Brien lab also observed that female C57BL/6J *G6pc2* KO mice were lighter than their WT counterparts on both chow and high-fat diets [1]. While SNPs in *G6PC2* have not been associated with variations in body weight in humans, this observation raised the questions about a potential effect of *G6PC2* on body weight. The effect of *G6pc2* deletion in mice on body weight and body composition was found to be highly dependent on variables such as gender, genetic background, and diet, suggesting that *G6pc2* deletion alone was not sufficient to affect body weight [177]. However, *G6pc2* KO mice had decreased FBG regardless of genetic background, gender, or diet, indicating that the effect of *G6pc2* deletion on FBG is largely independent of these variables [177]. This also supports GWAS data that showed an effect of *G6pc2* SNPs on FBG in multiple populations [161, 168, 169, 172]. These studies all suggest that the presence of *G6pc2* may have played a role through evolution to modulate FBG.

Summary

Overall, the data presented in this introduction clearly support a role for *G6PC2* in beta cell function and modulation of the set point for FBG. In fact, prior work from our lab and others suggests that G6PC2 would be a potential novel therapeutic target to lower FBG, and thereby decrease the risk of developing T2D and/or CAM. The broad goal of the studies described in this dissertation is to determine if G6PC2 should continue to be pursued as a novel target for lowering

FBG, as well as determine the tissues through which G6PC2 mediates its action and identify any additional beneficial or adverse effects of the inhibition of G6PC2. This dissertation will show (1) that beta cell-specific knockdown of *G6PC2* is sufficient to reduce FBG, and that its action on FBG is primarily mediated through the beta cell, (2) that loss of G6PC2 function may protect against hyperglycemia in the context of a high-fat diet, but may also lead to an increased risk of hypoglycemia in the context of a prolonged fast or a low-carbohydrate diet, and (3) that rare variants in *G6PC2* can significantly decrease protein expression, and therefore may have a larger impact than common SNPs on FBG.

CHAPTER 2

Materials and Methods

Generation of Germline and Beta Cell-Specific *G6pc2* KO Mice

The generation of germline *G6pc2* KO mice on a pure C57BL/6J genetic background has been previously described [1, 147].

The generation of adult beta cell-specific (BCS) *G6pc2* KO mice was achieved by purchasing embryonic stem (ES) cells containing a floxed *G6pc2* allele from the Knockout Mouse Project (KOMP) Repository (Project #CSD28099). In the floxed allele, FRT sites surround the LacZ and Neo components of the targeting vector, whereas LoxP sites surround *G6pc2* exon 3, which encodes the third transmembrane domain [143]. These ES cells were injected into fertilized eggs by the Vanderbilt Transgenic Mouse/ES Stem Cell Resource. Offspring in which germline transmission had been achieved were mated with 129S4/SvJaeSor-*Gt(ROSA)26Sor*$^{tm1(FLP1)Dym}$*/J* mice (JAX Stock #003946). These mice express the *FLP1* recombinase gene, which removes the LacZ and Neo components of the targeting vector in the floxed *G6pc2* allele thereby converting the allele from a non-expressive form to a conditional allele. Finally, the resulting offspring were mated with *Ins1-CreERT2* knock-in mice (JAX; Stock #026802). These knock-in mice express the *CreERT2* recombinase gene driven by the endogenous mouse *insulin1* promoter [178]. Treatment of homozygous floxed mice expressing the *Ins1-CreERT2* gene with tamoxifen (3 IP injections of tamoxifen (1 mg/kg in corn oil) on alternate days at 8 weeks of age) allowed for the removal of exon 3 from the floxed *G6pc2* allele in beta cells in adult mice thereby inactivating the gene.

PCR Genotyping of Germline and BCS *G6pc2* KO Mice

Mouse tail DNA was genotyped using PCR in conjunction with primers that distinguished between the WT and targeted alleles.

The following primers were used for genotyping WT and germline *G6pc2* KO mice:

WT Forward: 5'-TGGCACTAGGAAAGGCCTGA-3'

WT Reverse: 5'-GCTGCCATTGTTCTGCCTGT-3'

KO Forward: 5'-GCAGCGCATCGCCTTCTATC-3'

KO Reverse: 5'-TCCAAAGGCGTATTTAGCAA-3'

The following primers were used to assess the presence of the Cre gene in WT and floxed *G6pc2* mice as previously described [178]:

Forward: 5'-AAACGTTGATGCCGGTGAACG-3'

Reverse: 5'-CAGCCACCAGCTTGCATGAT-3'

The following primers were used to assess the presence of the *Ins1* gene in WT and floxed *G6pc2* mice:

Forward: 5'-GGACCCACAAGTGGAACAAC-3'

Reverse: 5'-GCAGGAAGCAGAATTCCAGA-3'

The following primers were used to assess the presence of the WT or floxed *G6pc2* allele:

WT Forward: 5'-TTGAGTTGGAAATGTTTATCTGATT-3'

WT Reverse: 5'-AAAGACTGCATTGACTTTAACAGC-3'

Floxed Forward: 5'-CATTATACGAAGTTATGGTCTGAGC-3'

Floxed Reverse: 5'-AAAGACTGCATTGACTTTAACAGC-3'

Tail DNA was isolated and purified using standard procedures [179]. The WT and targeted allele fragments were amplified using 2.8 ng genomic DNA and the Bio-Rad iQ SYBR Green

Supermix (Hercules, CA) under the following reaction conditions: 95°C for 30 sec; 58°C for 60 sec; 72°C for 60 sec for 40 cycles. Standard curve analyses were performed for each set of samples to determine the efficiencies of the PCR reactions, which were all greater than 95%.

Animal Care

The Vanderbilt University Medical Center Animal Care and Use Committee approved all protocols used. All animal housing and surgical facilities used for the mice in these studies met the American Association for the Accreditation of Laboratory Animal Care standards. Mice were maintained on a standard rodent chow diet (calorie contributions: 28% protein, 12% fat, 60% carbohydrate (14% disaccharides); LabDiet 5001; PMI Nutrition International), with food and water were provided *ad libitum*. Where specified, mice were placed on a high fat diet (calorie contributions: 15% protein, 59% fat, 26% carbohydrate (42% disaccharides); Mouse Diet F3282; BioServ) at 33 weeks of age (unless otherwise specified) and maintained on the diet for 12 weeks (unless otherwise specified). Where specified, mice were placed on a ketogenic diet (calorie contributions: 4.6% protein, 93.4% fat, 1.8% carbohydrate (78% disaccharides); Mouse Diet F3666; BioServ) at 8 weeks of age and maintained on the diet for 8 weeks.

Phenotypic Analysis of Fasted Mice

Mice were fasted for 5 hours and then weighed. After an additional hour of fasting, mice were anesthetized using isoflurane and blood samples were isolated from the retro-orbital venous plexus. Glucose concentrations were measured in whole blood using a glucose monitor (Accu-Check Advantage; Roche, Indianapolis, USA). EDTA (5 μl; 0.5 M) was then added to blood samples prior to isolation of plasma by centrifugation. Aprotinin (5 μl, Sigma Aldrich) was added

to the plasma to prevent proteolysis of glucagon. Insulin samples were assayed using RIA [180] by the Vanderbilt Hormone Assay and Analytical Services Core. Plasma ketones were measured using the Ketone Body Assay kit (Sigma Aldrich, St. Louis, MO). Plasma glucagon was assayed using a highly specific and sensitive immunoassay (Mercodia; Kit #10-1271-01) by the Vanderbilt Hormone Assay and Analytical Services Core. Plasma ketones were measured using the Ketone Body Assay Kit (Sigma Aldrich; Kit #MAK134), according to the manufacturer's instructions. Plasma cholesterol was assayed using a cholesterol reagent kit (Raichem; Kit #80035), according to the manufacturer's instructions. Amino acid levels were assayed by HPLC by the Vanderbilt Hormone Assay and Analytical Services Core.

Intraperitoneal Glucose Tolerance Tests (IPGTTs)

IPGTTs were performed on 6 hour fasted conscious mice. Briefly, mice were fasted for 5 hours before being weighed, then allowed to recover for 1 hour before injection with 2g/kg body weight dose of glucose in sterile PBS. Glucose levels were measured in tail vein samples prior to glucose injection and thereafter at 15, 30, 60, 90, and 120 minutes using a Freestyle glucose meter (Abbott).

Insulin Tolerance Tests (ITTs)

ITTs were performed on 5 hour fasted conscious mice. Briefly, mice were fasted for 4 hours before being weighed, then allowed to recover for 1 hour before injection with 0.75U/kg body weight dose of insulin in sterile PBS. Glucose levels were measured in tail vein samples prior to glucose injection and thereafter at 7.5, 15, 22.5, 30, 37.5, 45, and 60 minutes using a Freestyle glucose meter (Abbott).

Analysis of Blood Glucose Levels after Intraperitoneal Glucose Bolus

Glucose-stimulated increases in plasma insulin *in vivo* during IPGTT were measured in 6 hour fasted mice. Mice were fasted for 5 hours before being weighed, then allowed to recover for 1 hour. Mice were then anesthetized using isoflurane, and basal blood samples were isolated from the retro-orbital venous plexus. Mice were allowed to recover for 15 mins before a 2g/kg dose of glucose was injected IP. After 15 mins mice were once again anesthetized using isoflurane and blood samples again isolated from the retro-orbital venous plexus. Glucose concentrations were measured in whole blood using an Accu-Check Advantage glucose meter (Roche, Indianapolis, IN). EDTA (5 μl; 0.5 M) was added to blood samples prior to isolation of plasma by centrifugation. Plasma samples collected from the retro-orbital plexus were assayed for insulin using RIA by the Vanderbilt Hormone Assay and Analytical Services Core.

Mouse and Human Islet Isolation

Mouse islets were isolated by the Vanderbilt Islet Procurement and Analysis Core as previously described [181]. Human islets were obtained by A.C.P. through the NIDDK-funded Integrated Islet Distribution Program (https://iidp.coh.org/) and handled and assessed as previously described [3]. Human islets designated as 'Group 1' [3] based on islet perifusion analyses were used for these studies.

Analysis of Gene Expression

Tissue RNA was isolated using the ToTALLY RNA kit whereas islet RNA was isolated using the RNAqueous kit (Ambion, Carlsbad, CA). The Turbo DNA-free DNAse Treatment Kit (Ambion, Carlsbad, CA) was then used to remove trace genomic DNA followed by cDNA

generation using the iScript DNA Synthesis Kit (Bio-Rad, Hercules, CA). Gene expression was then quantitated by PCR using the dUTP-containing FastStart SYBR Green Master Mix in conjunction with Uracil-DNA-Glycosylase (Roche, Nutley, NJ). Fold induction of gene expression was calculated using the 2(-ΔΔC(T)) method [182].

The following mouse primer pairs were used for the analysis of gene expression:

G6pc1 Forward	5'-ACCAAGGGAGGAAGGATGGA-3'
G6pc1 Reverse	5'-CTGCCACCCAGAGGAGATTG-3'
G6pc2 Forward	5'- GAGACCCGGTGACAAGAAGA-3'
G6pc2 Reverse	5'- GCCACTTGGAAAGCAGACTAA-3'
G6pc2 BCS 5'UTR Forward	5'-AGTTCCACCTGCTTCATGCT-3'
G6pc2 BCS Exon 3 Reverse	5'-ATGACATACCAGACGCACGA-3'
G6pc3 Forward	5'-TGTGGCTCTGGGTCACCTTT-3'
G6pc3 Reverse	5'-TGGAGTACCCGGATTCATGC-3'
Slc37a4 Forward	5'-GCCAGTAAGGCTGCAGTTGG-3'
Slc37a4 Reverse	5'-TCTGGCTGGCTTACCCTTCA-3'
Ppia Forward	5'-GGCCGATGACGAGCCC-3'
Ppia Reverse	5'-TGTCTTTGGAACTTTGTCTGCAA-3'
Slc2a2 Forward	5'-TCATTGCTGGACGAAGTGTATC-3'
Slc2a2 Reverse	5'-ACATTGGAACCAGTCCTGAAA-3'
Ins2 Forward	5'-CACCCAGGCTTTTGTCAAGC-3'
Ins2 Reverse	5'-CCAGTGCCAAGGTCTGAAGG-3'
Gck Forward	5'-CTTCAAGGAGCGGTTTCACG-3'
Gck Reverse	5'-GCATTTGTGGGGTGTGGAGT-3'

Prss1 (Trypsinogen) Forward:	5’-TCTGTGGAGGTTCCCTCATC-3’
Prss1 (Trypsinogen) Reverse:	5’-GTTGGGGTGCTTGATGATCT-3’
Ctrb1 (Chymotrypsinogen) Forward:	5’-AGGGCTCCGATGAAGAGAAT-3’
Ctrb1 (Chymotrypsinogen) Reverse:	5’-TCAGAGAACTGGGCAGGAGT-3’
Amy2a2 (Amylase) Forward:	5’-GTGAATGTTGGCAGTGATGG-3’
Amy2a2 (Amylase) Reverse:	5’-GGGCTCAGAAGACAAAGCAC-3’
Cpa1 (Carboxypeptidase A1) Forward:	5’-GGGACCCTCGTCAGTGTTTA-3’
Cpa1 (Carboxypeptidase A1) Reverse:	5’-GTGCCCCACAAAGTTCTCAT-3’
Slc30a8 Forward	5’-TTGCATCTGGGTGCTGACTG-3’
Slc30a8 Reverse	5’-GCTCGGACACTGGCATTAGC-3’
Gys2 Forward	5’-CCACACTGCTTGGGCGTTAT-3’
Gys2 Reverse	5’-AGCATGTGCTCTGCCTCGAT-3’
InsR Forward	5’-GCTCTGTCCGCATCGAGAAG-3’
InsR Reverse	5’-CGTTCCACAAACTGCCCATT-3’

Hematoxylin and Eosin Analysis of Tissue Morphology

Mice were euthanized at 8 months of age and the pancreata were formalin-fixed. Pancreata were then paraffin-embedded and sections cut at a depth of 5 μm, dewaxed and stained in hematoxylin and eosin by the Vanderbilt Translational Pathology Shared Resource.

Immunofluorescence of Pancreatic Cryo-Sections

Freshly dissected mouse pancreata were fixed in 4% PFA at 4°C for 1 hour, washed three times with PBS, and immersed in PBS containing 30% sucrose overnight at 4°C. The fixed

pancreata were briefly dried over a paper towel and immersed in the optimal cutting temperature compound for at least 2 hours before freezing over an acetone/dry ice bath. The frozen tissue blocks were stored at -80 ^{0}C until sectioning. Cryo-sections (10 μm) were cut on a cryostat (Leica, Buffalo Grove, IL) at -20°C and mounted on SuperFrost Plus glass slides (Fisher Scientific, Hampton, NH).

For immunostaining, pancreatic cryo-sections were rehydrated in PBS for 10 min, permeabilized with 0.3% Triton X-100 for 30 min, and washed three times with PBST (0.1% Triton X-100 in PBS). After blocking with 10% donkey serum in PBST for 1 hour, primary antibody diluted in 10% donkey serum in PBST was added and incubated at 4°C overnight. Slides were then washed three times with PBS before addition of secondary antibodies in 10% donkey serum in PBST and incubation at room temperature for 1 hour. Slides were then washed three times with PBST. After staining with DAPI (300 nM for 5 min) and rinsing with PBS, slides were covered with Fluoromount-G and sealed with a coverslip. Antibodies used were as follows: For insulin: primary antibody (guinea pig, Dako A0564, 1:500), secondary antibody (donkey anti-guinea pig IgG conjugated with AF488, Jackson ImmunoResearch 706-545-148, 1:200). For G6pc2: primary antibody (rabbit, a generous gift from Howard Davidson, University of Colorado, 1:50), secondary antibody (donkey anti-rabbit IgG conjugated with Cy3, Jackson ImmunoResearch 715-165-151, 1:200). Labeled slides were imaged on an inverted confocal microscope (Zeiss LSM780) under the same setting. Intensity of G6pc2 immunofluorescence was quantified with ImageJ software after background subtraction.

Electronic Health Record (EHR)-Based Analyses of Human Research Subjects

EHR-based analyses were conducted using data on human subjects in the Vanderbilt University Medical Center (VUMC) BioVU DNA databank. Genotyping data in BioVU is linked to the Synthetic Derivative (SD), a de-identified version of the VUMC EHR repository. Detailed descriptions of program operations, ethical considerations, and continuing oversight and patient engagement have been published [183, 184]. The methods used to perform phenome-wide association studies (PheWAS) have been previously published [185, 186]. The methods used to perform laboratory value-wide association studies (LabWAS) are described in the GitHub repository [https://bitbucket.org/juliasealock/labwas/src/master/].

The BioVU sample was restricted to a homogenous European American (EA) population (N = 50,115) and an African American (AfAm) population (N = 9,640), based on global genetic ancestry estimated from principal components. The PheWAS package in R was used to perform 1,212 logistic regressions to determine whether any Phecodes (hierarchical clustering of International Classification of Disease (ICD) codes) were significantly associated with our SNPs of interest after adjusting for sex, age (defined for each individual as median age across their medical record) and the top four principal components of ancestry [185, 186]. For each phenotype, we required a minimum number of 100 cases for inclusion in the PheWAS. We used the LabWAS package to perform 453 linear regressions to determine whether any laboratory values were associated with SNP genotype. The SNPs tested were common in both EA and AfAm populations.

Measurement of Glucose Cycling

Glucose cycling was analyzed as previously described [7]. Briefly, aliquots of ~100 islets were incubated for 24 or 72 hours at 28°C in RPMI-1640 medium containing 5 mM or 11 mM

glucose in a volume of 175 μl. Islets were incubated in either naturally labeled glucose or [1,2,3,4,5,6,6-$^{2}H_{7}$]glucose (D7-glucose) (98% isotopic purity per site; Cambridge Isotope Laboratories, Inc., Andover, MA). Following the 24 or 72 hour incubation, islets were resuspended by pipetting and pelleted by centrifugation. The supernatant was retained for GC-MS analysis of glucose concentration and mass isotopomer distribution, with glucose concentration determined through comparison to a standard curve. Glucose cycling and glucose uptake rates were calculated as described previously [7].

Measurement of Glycolysis

Glycolysis was analyzed as previously described [187-189]. Briefly, aliquots of ~100 WT and germline *G6pc2* KO islets were incubated for 2 hours at 37°C in Krebs bicarbonate buffer containing 5.6 mM glucose spiked with 1 μl D-[5-^{3}H]glucose (Perkin Elmer, Waltham, MA; 10Ci/mmol; 1 mCi/ml) in a volume of 100 μl. Following the incubation, islets were pelleted by centrifugation. The supernatant was retained for analysis of $^{3}H_{2}O$ generation whereas DNA content of the cell pellet was measured using the Hoechst reagent (Sigma, St. Louis, MO) as described [187].

Measurement of Hepatic Glycogen Content

Hepatic glycogen content was assessed as previously described [134, 190]. Briefly, frozen liver was extracted with boiling 5M KOH, and the glycogen was precipitated with 2 vol. of 95% (vol/vol) ethanol before being re-precipitated with ethanol, and dissolved in water. Glycogen was then hydrolyzed using amyloglucosidase, and the resulting glucose was analyzed using UV-methods with hexokinase and glucose-6-phosphate dehydrogenase.

Cell Culture

Rat islet-derived 832/13 cells, a generous gift from Dr. Chris Newgard, were passaged as sub-confluent cultures in RPMI medium supplemented with 10% (vol/vol) fetal bovine serum, 0.05 mM β-mercaptoethanol, 100 U/ml penicillin, and 100 μg/ml streptomycin.

Human G6PC2 and Human G6PC1 Expression Vector Construction

The construction of plasmids encoding human G6PC2 (accession number NM_021176), human G6PC1 (accession number NM_000151), mouse G6PC2 (accession number NM_021331), and mouse G6PC1 (accession number NM_008061) in the pcDNA3.1D v5-His-TOPO vector with a C-terminal V5-His Tag has been previously described [132, 191]. Our human WT *G6PC2* plasmid contains a leucine at amino acid 219 [146]. Alternate alleles of the SNP rs492594 switch a valine for a leucine at AA 219.

The pJPA5-Mod expression vector was generated by the addition to pJPA5 of a polylinker containing the following restriction endonuclease recognition sites: EcoRI, HindIII, BglII, BamHI, EcoRV, XhoI, and PmeI. WT human G6PC2 with a C-terminal V5-His tag and WT human G6PC1 with a C-terminal V5-His tag were isolated as HindIII-PmeI fragments from the pcDNA3.1D v5-His-TOPO vector, and then ligated into the HindIII-PmeI-digested pJPA5-Mod vector.

Site Directed Mutagenesis and Plasmid Preparation

Non-synonymous variants were generated in human *G6PC2* in the pJPA5 vector using the Quikchange II Site-Directed Mutagenesis kit (Agilent) or by ligating HindIII-PmeI fragments of variants previously generated in human G6PC2 in the pcDNA3.1D v5-His-TOPO vector [2] into the HindIII-PmeI-digested pJPA5-Mod vector. Sanger sequencing was used to verify all

mutations. Four independent preps were made for each mutant described. All mutant plasmid constructs were purified by centrifugation through cesium chloride gradients [192].

SNP Databases

Human *G6PC2* SNPs were identified using the UCSC Genome Browser (https://genome.ucsc.edu/), HumSAVR (http://omictools.com/humsavar-tool) or dbSNP (http://www.ncbi.nlm.nih.gov/SNP/) databases.

Western Blotting

Plasmids encoding either WT or variant mouse G6PC1, human G6PC1, mouse G6PC2, or human G6PC2 in the pcDNA3.1D v5-His-TOPO vector, or human G6PC1 or human G6PC2 in the pJPA5 vector (3μg) were transiently transfected in semi-confluent 832/13 cells in 3.5 cm diameter dishes using lipofectamine reagent (Invitrogen) as previously described [193]. Following transfection, cells were incubated in serum-containing media for 18-20 hours. Cells were then harvested using 50 mM Tris, pH 8.0, 150 mM NaCl, 5.8 mM PMSF, and 1% NP-40. Protein samples were quantified using the Pierce BCA Protein Assay Kit (Thermo Fisher Scientific) according to manufacturer's instructions. 20 μg of cell extract was electrophoresed on 10% SDS-polyacrylamide gels and the proteins transferred to PVDF membrane (PerkinElmer). Protein expression was determined by immunoblotting with a conjugated mouse monoclonal anti-V5-horseradish peroxidase (HRP) antibody (1:5000, Invitrogen #46-0708). A primary anti-beta actin monoclonal antibody (1:10,000, Sigma Aldrich #A2228) with an anti-mouse IgG HRP secondary antibody (1:10,000, Promega #W4021) was used to determine beta actin expression as a loading control. HRP activity was assayed using the Pierce ECL reagent (Thermo Fisher Scientific).

Protein expression data were normalized by scanning both V5 and actin signals on Western blots; the ratio of V5:actin expression obtained with the human G6PC2 variants was expressed as a percentage relative to the ratio obtained with WT. The expected sizes of human G6PC2, mouse G6pc2, human G6PC1 and mouse G6pc1 with V5 His tags are 45.60, 45.71, 45.54 and 45.51 kDa, respectively. As previously observed, both the human G6PC1 [132] and mouse G6pc1 [191] expression plasmids generate doublets, possibly though the use of alternate methionine start codons (Figure 5.2)

Fusion Gene Assays

The *in situ* assay used to assess G6PC1 and G6PC2 enzyme activity has been previously described [2]. Briefly, semi-confluent 832/13 cells in 3.5 cm diameter dishes were co-transfected with 2μg of a plasmid encoding an glucose-responsive promoter-luciferase fusion gene, 0.5μg of SV40-Renilla luciferase (Promega), and the indicated amount of either empty vector, WT G6PC1 or G6PC2 driven by the indicated expression vector, or variant G6PC1 or G6PC2 driven by the indicated expression vector, using lipofectamine reagent (Invitrogen) as previously described [193]. Following transfection, cells were incubated for 18-20 hours in serum-free medium supplemented with 2mM or 30mM glucose. Cells were then harvested using Passive Lysis Buffer (Promega). Firefly & Renilla luciferase activity were assayed using the Dual Luciferase Assay kit (Promega). To correct for variations in transfection efficiency, the results were calculated as the ratio of firefly:Renilla luciferase activity, and were expressed relative to the ratio obtained with empty vector at 30mM glucose or relative to the ratio obtained with a catalytically-dead variant, as indicated.

For the ATF6-luciferase fusion gene assay, semi-confluent 832/13 cells in 3.5 cm diameter dishes were co-transfected with 2μg of a plasmid encoding an ATF6-luciferase fusion gene [194], 0.5μg of SV40-Renilla luciferase (Promega), and the indicated amount of either empty pJPA5 vector or the pJPA5 vector encoding either WT human G6PC2 or variant G6PC2, using lipofectamine reagent (Invitrogen) as previously described [193]. Following transfection, cells were incubated for 18-20 hours in serum-containing medium. Cells were then harvested using Passive Lysis Buffer (Promega). Firefly & Renilla luciferase activity were assayed using the Dual Luciferase Assay kit (Promega). To correct for variations in transfection efficiency, the results were calculated as the ratio of firefly:Renilla luciferase activity, and were expressed relative to the ratio obtained with empty vector.

Statistical Analyses

Mouse data were analyzed either using a Student's t-test, two sample assuming equal variance or a one-way ANOVA, assuming normal distribution and equal variance, as indicated. *Post hoc* analyses were performed using the Bonferroni correction for multiple comparisons. EHR associations were analyzed with logistic and linear regressions using the PheWAS package in R and the LabWAS package in R. PheWAS and LabWAS results were deemed significant if the p-value of the association passed a Bonferroni multiple testing correction to account for 1,212 logistic and 453 linear regressions that were performed, respectively. Fusion gene assays and Western blots were analyzed using the Student's t-test: two sample assuming equal variance. The level of significance was as indicated.

CHAPTER 3

Pancreatic Islet Beta Cell-Specific Deletion of *G6pc2* Reduces Fasting Blood Glucose

Introduction

The role of *G6PC2* in beta cell function and the modulation of FBG has been extensively covered in the introduction of this dissertation. The beta cell glucose sensor, glucokinase, which catalyzes the formation of G6P from glucose, was thought to be the key factor that determines the rate of beta cell glycolytic flux [164, 165]. This glycolytic rate determines the sensitivity of GSIS to glucose and hence the influence of beta cells on FBG [164, 165]. However, in isolated germline *G6pc2* KO islets, glucose-6-phosphatase activity [1] and glucose cycling (Figure 1.4) [7] are abolished. This results in a leftward shift in the dose response curve for GSIS [1] such that under fasting conditions, insulin levels are the same in WT and germline *G6pc2* KO mice but FBG is reduced in KO mice (Figure 1.6) [1, 147]. These data challenge the existing dogma and suggest a new paradigm in which a glucokinase/G6PC2 futile cycle, rather than glucokinase alone, determines the rate of beta cell glycolytic flux and hence the sensitivity of GSIS to glucose (Figure 1.5).

Based on Northern blotting and immunohistochemistry, *G6PC2* was thought to be only expressed in pancreatic islets in mice [143] and humans [146]. However, human RNA-Seq data, available through the GTEx database, suggest very low expression of *G6PC2* in other tissues, including liver, skeletal muscle, and hypothalamus, raising the possibility that G6PC2 is functionally important in non-islet tissues.

The experiments described in this chapter provide further support for this new model by showing that glucose cycling also exists in human islets and that germline deletion of *G6pc2* enhances glycolysis in mouse islets. In addition, gene expression analyses, electronic health record-derived phenotype analyses, and studies in a novel mouse model in which *G6pc2* is specifically deleted in beta cells all suggest that G6PC2 is not active in non-islet tissues, and instead imply that an islet-specific action of G6PC2 is sufficient to mediate the effect of G6PC2 on FBG.

Results

G6pc Isoforms Exhibit Tissue-Specific Expression in Male Mice

While published data strongly suggest that G6PC2 is active in islets, a major unanswered question is whether it is also active in other tissues. The observation from GTEx data that *G6PC2* is expressed at low levels in multiple tissues raise this possibility, though it is important to note that there is currently no evidence for detectable G6PC2 protein expression outside of islets. Whether G6PC2 is functionally active in these tissues is likely to depend in part on its expression relative to other *G6PC* isoforms. We therefore used real time PCR to compare the tissue specific expression of mouse *G6pc1* (Figure 3.1A), *G6pc2* (Figure 3.1B), and *G6pc3* (Figure 3.1C), as well as *Slc37a4* (Figure 3.1D). Of the tissues tested, *G6pc2* expression was only detected in pancreas (Figure 3.1B). In contrast, *G6pc1* was expressed predominantly in liver and kidney (Figure 3.1A), whereas *G6pc3* expression was detected in all tissues examined (Figure 3.1C). Similarly, expression of *Slc37a4*, which is known to couple with G6PC1 and G6PC3 [195], was detected in all tissues examined (Figure 3.1D). These real time PCR data are similar to the results of expression analyses for *G6pc1* [122], *G6pc2* [143], *G6pc3* [191] and *Slc37a4* [196] performed using Northern

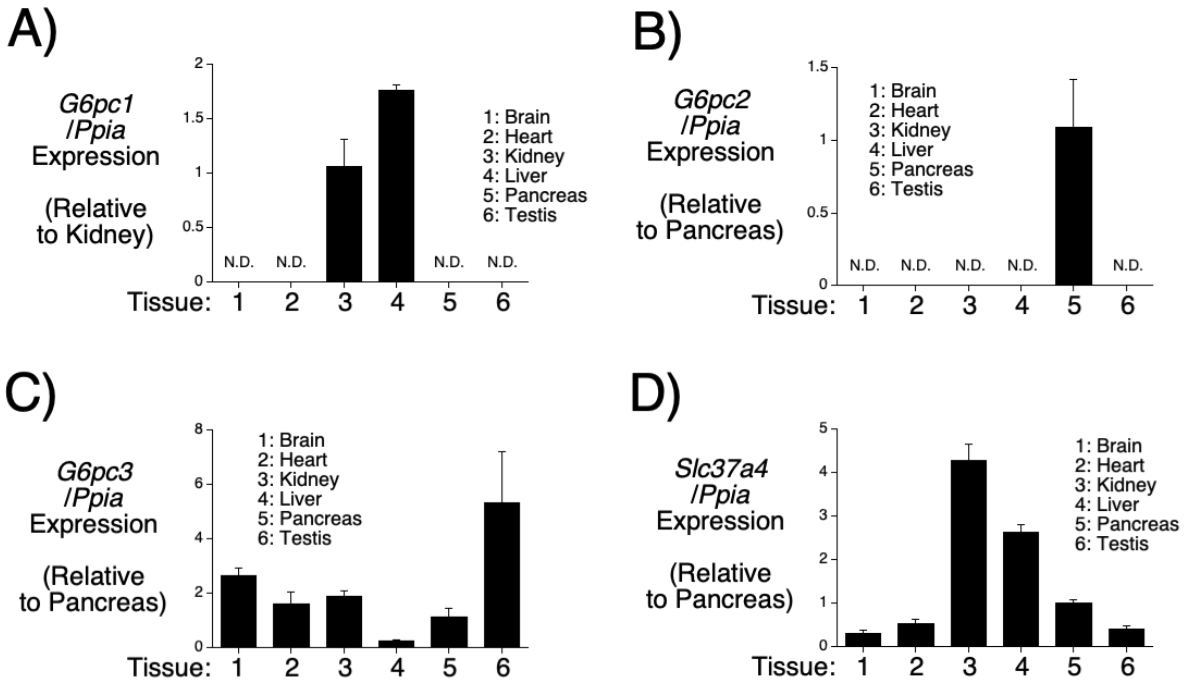

Figure 3.1. Comparison of Tissue-Specific *G6pc* Isoform Expression in Male Mice.

Comparison of *G6pc1* (Panel **A**), *G6pc2* (Panel **B**), *G6pc3* (Panel **C**) and *Slc37a4* (Panel **D**) expression in brain, heart, kidney, liver, pancreas and testis from 2 month old non-fasted male mice. *G6pc* and *Slc37a4* expression were quantitated relative to *Ppia* (cyclophilin A) expression in the indicated tissue and then expressed relative to that in either kidney (Panel **A**) or pancreas (Panels **B-D**). Results represent the mean data ± S.E.M. derived from tissues isolated from 3 male mice.

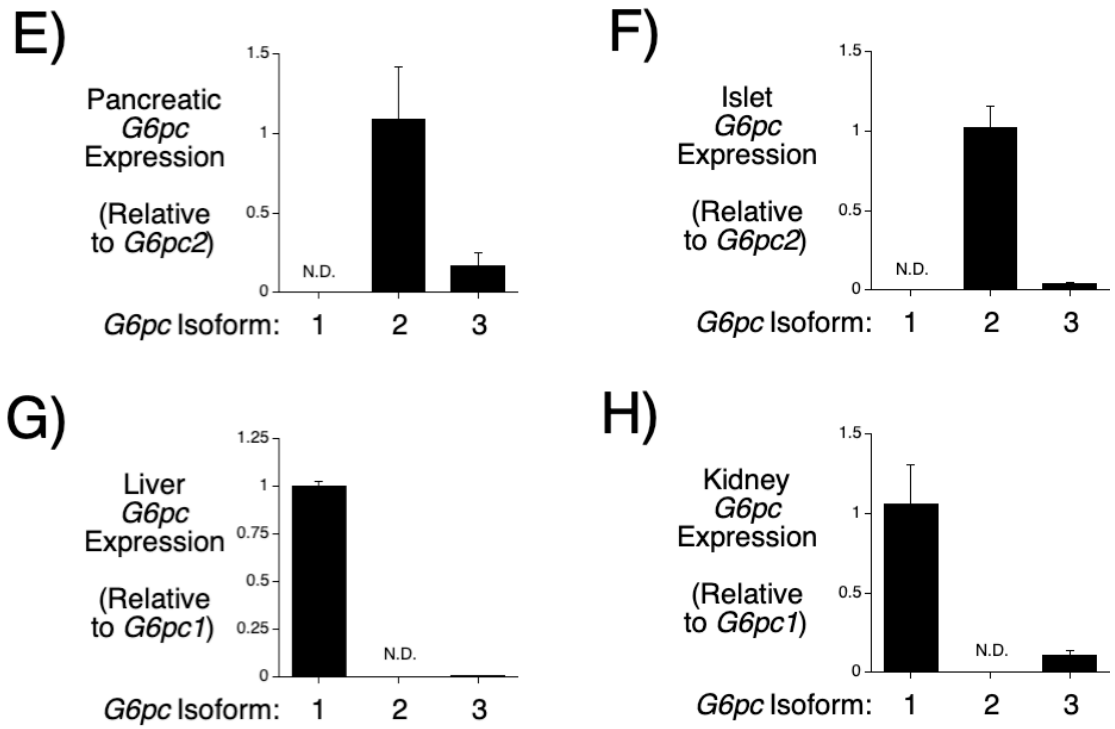

Figure 3.1. Comparison of Tissue-Specific *G6pc* Isoform Expression in Male Mice.

Comparison of *G6pc1*, *G6pc2* and *G6pc3* expression in pancreas (Panel **E**), islets (Panel **F**), liver (Panel **G**) and kidney (Panel **H**) from 2 month old non-fasted male mice. *G6pc* expression was quantitated relative to *G6pc2* expression in pancreas (Panel **E**) or islet (Panel **F**) or relative to *G6pc1* expression in liver (Panel **G**) or kidney (Panel **H**). Results represent the mean data ± S.E.M. derived from tissues isolated from 3 male mice.

blotting. These results may indicate that the pattern of *G6pc2* expression differs between mouse and human or, more likely, that this apparent difference simply reflects the increased sensitivity of RNA-Seq versus real time PCR with the former method being able to detect extremely low expression. For example, RNA-Seq data demonstrate that *G6PC2* is expressed in liver at ~0.018% of the level in islets [197], a difference too small to easily detect using real time PCR. Even if *G6pc2* is expressed at trace levels in these non-pancreatic tissues, because both G6PC1 [124] and G6PC3 [4] have much higher catalytic activity than G6PC2 [6], these results suggest that G6PC2 is highly unlikely to directly affect metabolism in these tissues.

The Relative Expression of *G6pc* Isoforms Varies within Specific Tissues in Male Mice

We next examined the relative expression of *G6pc* isoforms within individual tissues. Within pancreas (Figure 3.1E) and islets (Figure 3.1F) *G6pc2* expression is higher than that of *G6pc3,* and *G6pc1* expression is not detected. These results suggest that G6PC3 is unlikely to compensate for the absence of G6PC2 in pancreatic islets (see Figure 3.7). Indeed, glucose-6-phosphatase activity [1] and glucose cycling [7] are abolished rather than reduced in germline *G6pc2* KO islets. Similarly, *G6pc1* expression is higher than that of *G6pc3* in both liver (Figure 3.1G) and kidney (Figure 3.1H) suggesting that G6PC3 is unlikely to be able to compensate for the absence of G6PC1 in either tissue, explaining why inactivating mutations in G6PC1 result in glycogen storage disease type 1a despite the presence of G6PC3 [127].

G6pc Isoform Expression, FBG and FPI Change with Aging in Male Mice

To potentially further establish a critical role for pancreatic G6PC2 in the regulation of FBG, we examined the correlation between the timing of the induction of *G6pc2* expression during

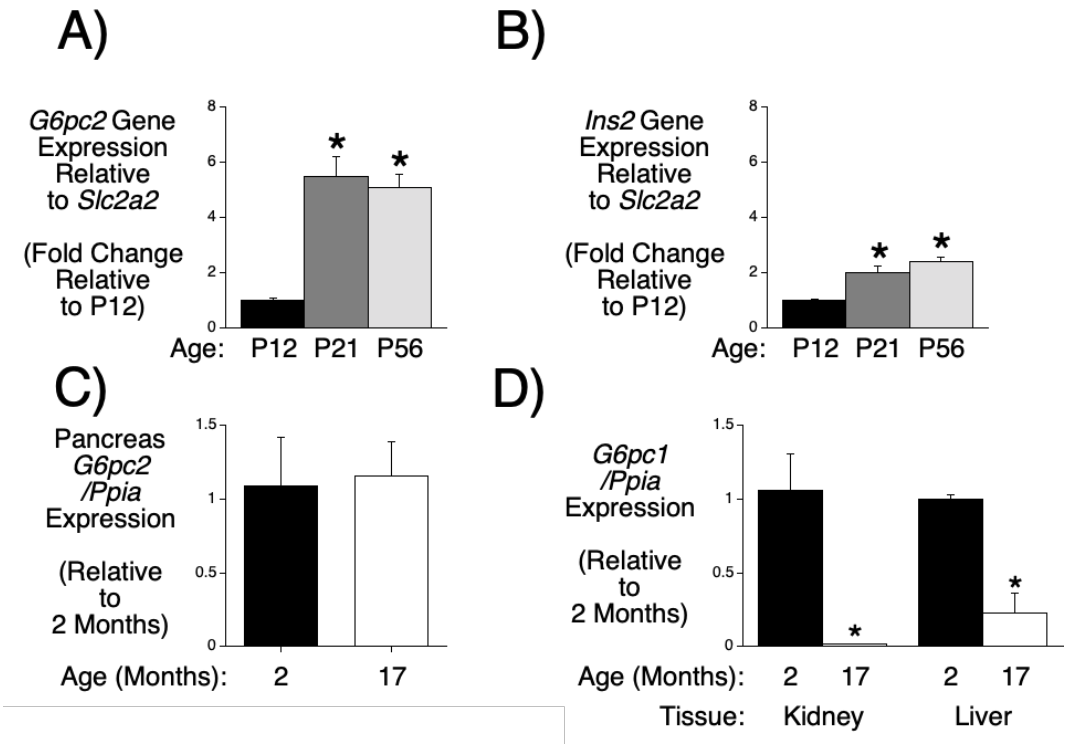

Figure 3.2. Analysis of Changes in *G6pc* Isoform Expression, FBG and FPI with Aging in Male Mice.

Comparison of pancreatic *G6pc2* (Panel **A**) and *Ins2* (Panel **B**) expression in P12 (non-fasted) and 6 hour fasted P21 and P56 male mice. *G6pc2* and *Ins2* expression were quantitated relative to *Slc2a2* expression and then expressed relative to that at P12. Results represent the mean data ± S.E.M. derived from pancreata isolated from 3-5 mice. *$p < 0.05$ vs P12, one-way ANOVA. Comparison of *G6pc2* (Panel **C**) and *G6pc1* (Panel **D**) expression in pancreas, kidney or liver in 2 versus 17 month old non-fasted male mice. *G6pc1* was quantitated relative to *Ppia* (cyclophilin A) expression in the indicated tissue and then expressed relative to expression at 2 months. Results represent the mean data ± S.E.M. derived from tissues isolated from 3 male mice. *$p < 0.05$ vs 2 months, t-test.

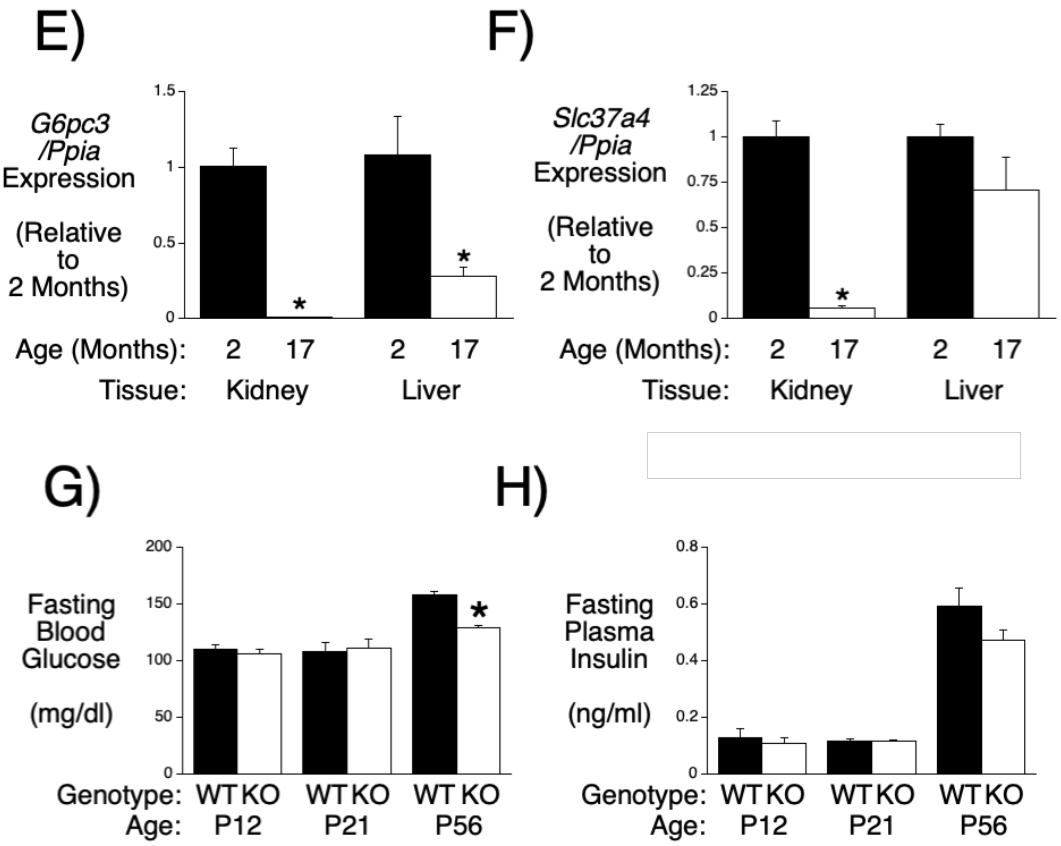

Figure 3.2. Analysis of Changes in *G6pc* Isoform Expression, FBG and FPI with Aging in Male Mice.

Comparison of *G6pc3* (Panel **E**) and *Slc37a4* (Panel **F**) expression in kidney or liver in 2 versus 17 month old non-fasted male mice. *G6pc3* and *Slc37a4* expression were quantitated relative to *Ppia* (cyclophilin A) expression in the indicated tissue and then expressed relative to expression at 2 months. Results represent the mean data ± S.E.M. derived from tissues isolated from 3 male mice. *$p < 0.05$ vs 2 months, t-test. Comparison of pancreatic FBG (Panel **G**) and FPI (Panel **H**) in P12 (non-fasted) and 6 hour fasted P21 and P56 male WT and germline *G6pc2* KO mice. FBG data represent the mean ± S.E.M. derived from WT, n=24; KO, n=14 (P12), WT, n=9; KO, n=9 (P21) and WT, n=21; KO, n=24 (P56) mice. FPI data represent the mean ± S.E.M. derived from WT, n=23; KO, n=14 (P12), WT, n=9; KO, n=9 (P21) and WT, n=15; KO, n=23 (P56) mice. *$p < 0.05$ vs WT, t-test.

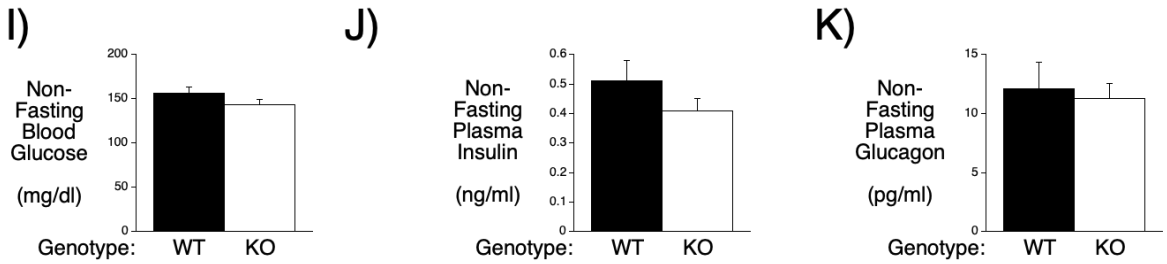

Figure 3.2. Analysis of Changes in *G6pc* Isoform Expression, FBG and FPI with Aging in Male Mice.

Comparison of glucose (Panel **I**), insulin (Panel **J**) and glucagon (Panel **K**) in 14-16 week old non-fasted WT (n=7) and germline *G6pc2* KO (n=7) mice. Data represent the mean ± S.E.M.

postnatal beta cell maturation with the ability of G6PC2 to regulate FBG. *G6pc2* expression is markedly induced during the weaning period between days 12 and 21 after birth relative to *Slc2a2*, which encodes the GLUT2 glucose transporter (Figure 3.2A). *Ins2* expression shows a modest induction over this same time period (Figure 3.2B). *G6pc2* expression changes little between day 21 and day 56 (2 months) (Figure 3.2A) and remains unchanged even in old mice (17 months) (Figure 3.2C). In contrast, expression of *G6pc1* (Figure 3.2D) and *G6pc3* (Figure 3.2E) decline markedly in liver and kidney in old mice. *G6pc3* expression remains unchanged in other tissues in old mice (Figure 3.3) while *Slc37a4* expression is selectively reduced in kidney (Figure 3.2F). The induction of *G6pc2* expression at P21 did not correlate with a reduction in FBG in germline *G6pc2* KO relative to WT mice; a reduction was only apparent at P56 (Figure 3.2G). Since FBG (Figure 3.2G) and especially FPI (Figure 3.2H) increase markedly between P21 and P56, we hypothesize that the absence of a difference in FBG between WT and germline *G6pc2* KO mice at P21 is simply because the dose response curve for GSIS is at a low point where it is not affected by G6PC2 (Figure 3.4). A trend towards reduced blood glucose levels is also observed in non-fasted *G6pc2* KO mice (Figure 3.2I), with no change in plasma insulin (Figure 3.2J) or glucagon (Figure 3.2K). Since the weaning period is associated with the switch to a relatively high carbohydrate diet, we hypothesize that this induction of *G6pc2* represents part of the beta cell maturation process [198] and is important for enabling the independent offspring to tightly regulate blood glucose levels.

FBG is Reduced in Male Beta Cell-Specific (BCS) *G6pc2* KO Mice

We reasoned that a second approach for addressing whether G6PC2 is also active in other tissues would be through the generation and analysis of beta cell-specific (BCS) *G6pc2* KO mice.

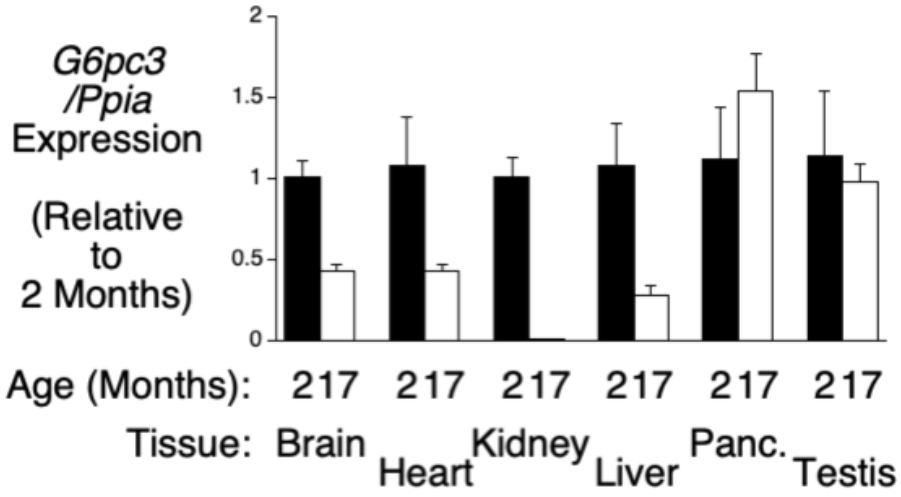

Figure 3.3. Analysis of Changes in *G6pc3* Isoform Expression with Aging in Male Mice.

Comparison of *G6pc3* expression in multiple tissues in 2 versus 17 month old non-fasted male mice. *G6pc3* expression was quantitated relative to *Ppia* (cyclophilin A) expression in the indicated tissue and then expressed relative to expression at 2 months. Results represent the mean data ± S.E.M. derived from tissues isolated from 3 male mice. *$p < 0.05$ vs 2 months.

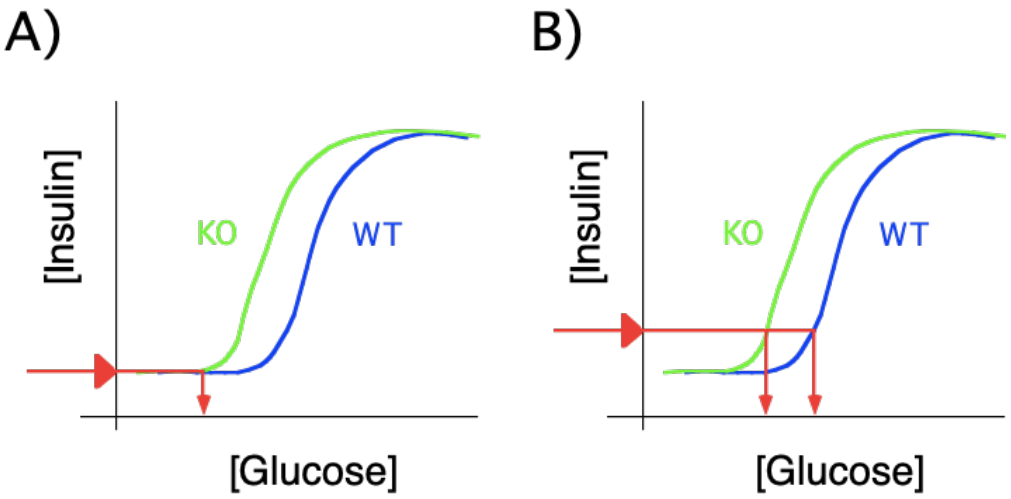

Figure 3.4. Effect of *G6pc2* Deletion on the Sensitivity of GSIS to Glucose.

Panel A: Schematic proposing that in P21 mice very low FPI is associated with very low FBG such that deletion of *G6pc2* has no effect on FBG.

Panel B: Schematic proposing that in P56 mice higher FPI is associated with higher FBG such that deletion of *G6pc2* now has the effect of reducing FBG.

If the effect of *G6pc2* deletion on FBG was also observed with beta cell-specific loss, it would argue that G6PC2 primarily regulates FBG through an islet-dependent mechanism. BCS *G6pc2* KO mice were generated by breeding mice with a floxed *G6pc2* allele in which LoxP sites surround *G6pc2* exon 3, which encodes the third transmembrane domain [143], with *Ins1-CreERT2* knock in mice in which expression of the *CreERT2* recombinase gene is driven by the endogenous mouse *insulin1* promoter [178]. Treatment of these mice with tamoxifen allows for excision of exon 3 from the floxed *G6pc2* allele in beta cells in adult mice thereby inactivating the gene. Sequence analysis indicates that, were splicing of *G6pc2* exon 2 to exon 4 to occur, an in-frame G6PC2 variant lacking only exon 3 encoded amino acids would not be generated.

Neither the presence of LoxP sites in the *G6pc2* gene nor the presence of the *Ins1-CreERT2* gene prior to tamoxifen treatment had major effects on *G6pc2*, *Slc37a4* or *Ins2* RNA expression in homozygous floxed relative to WT mice (Figure 3.5A-F). In contrast, tamoxifen treatment (by three days of IP injections) of homozygous floxed mice expressing the *Ins1-CreERT2* gene led to a selective ~60% reduction in *G6pc2* RNA (Figure 3.5G-I) and protein (Figure 3.5J & K) expression in floxed mice relative to WT mice, similar to the efficiency of gene deletion reported by Thorens et al. [178] using these *Ins1-CreERT2* mice.

Neither the presence of LoxP sites in the *G6pc2* gene nor the presence of the *Ins1-CreERT2* gene prior to tamoxifen treatment affected FBG and FPI (Figure 3.6A-D). In contrast, tamoxifen treatment led to a clear reduction in FBG in floxed mice (Figure 3.6E) with no change in FPI (Figure 3.6F) indicating that the loss of G6PC2 selectively in beta cells is sufficient to regulate FBG. As expected, the difference in FBG between WT and floxed mice (~15 mg/dl; WT n=14; floxed n=17) (Figure 3.6E) is slightly less than that observed in germline *G6pc2* KO mice (~21 mg/dl; WT n=29; KO n=16) [1, 147], consistent with the difference between a partial reduction in

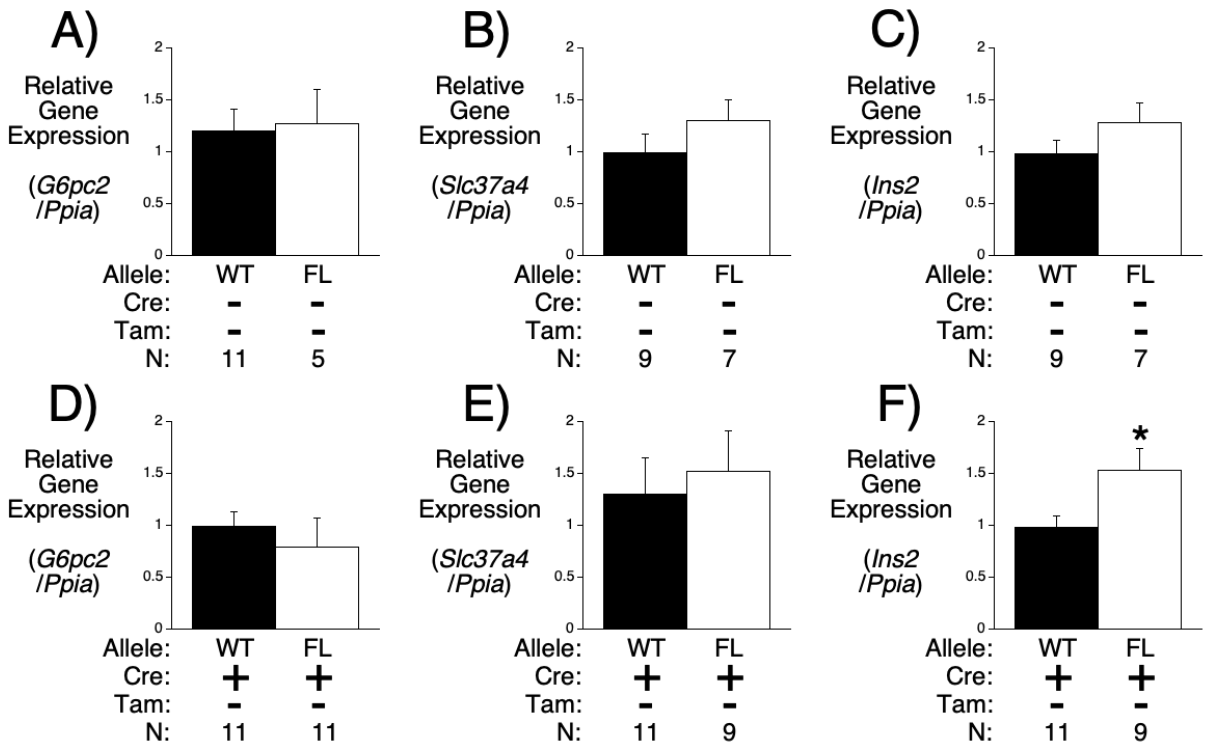

Figure 3.5. Analysis of *G6pc2* RNA and G6pc2 protein expression in Floxed *G6pc2* Male Mice.

Comparison of pancreatic *G6pc2* (Panels **A and D**), *Slc37a4* (Panels **B and E**) and *Ins2* (Panels **C and F**) expression in 16 week old 6 hour fasted male mice in the presence or absence of the *Ins1-CreERT2* allele and in the presence or absence of tamoxifen (Tam) treatment. *G6pc2*, *Ins2* and *Slc37a4* expression were quantitated relative to *Ppia* (cyclophilin A) and then expressed relative to that in WT mice. Results represent the mean data ± S.E.M. derived from tissues isolated from the indicated number of male mice. *$p < 0.05$ vs WT, t-test.

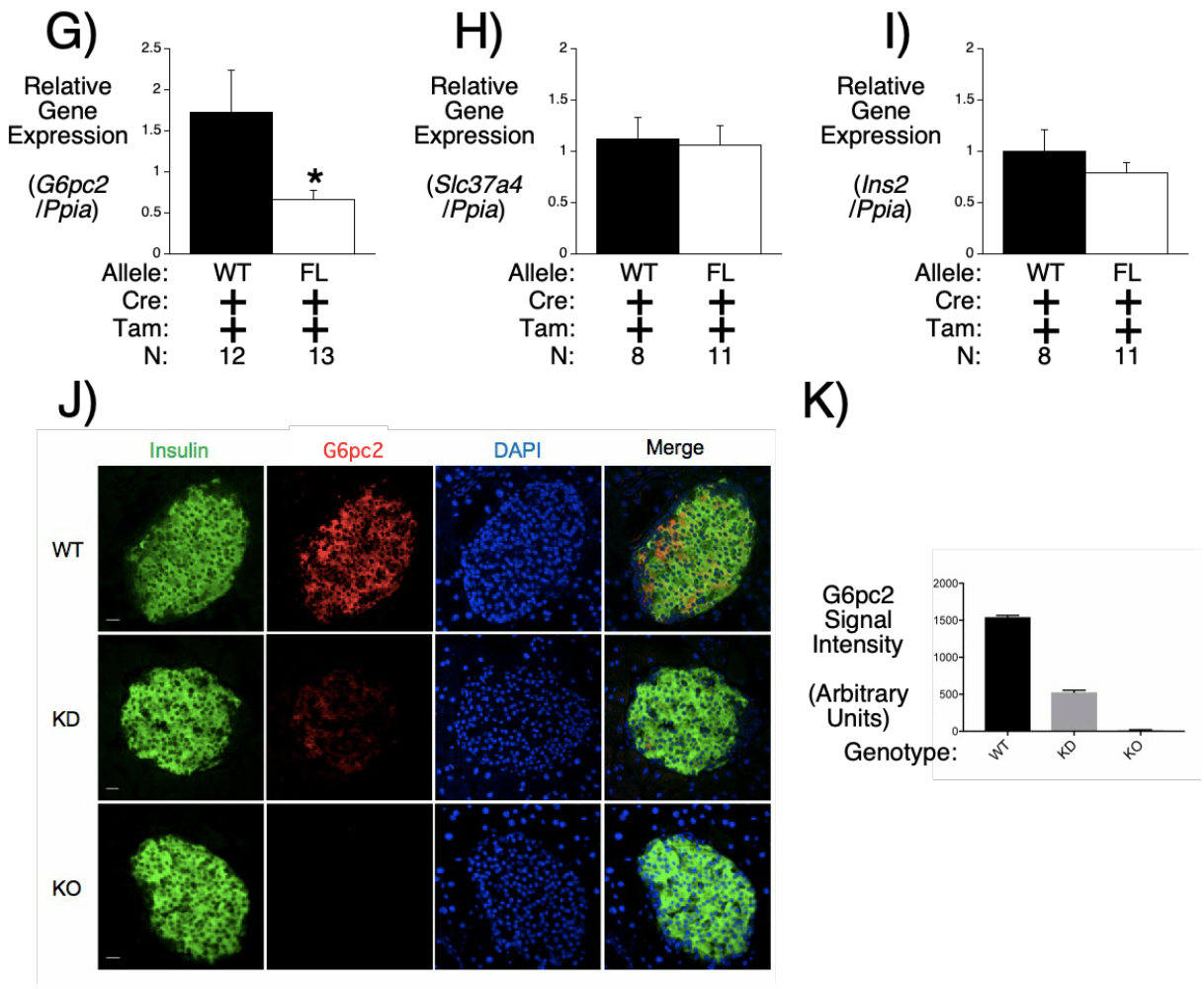

Figure 3.5. Analysis of *G6pc2* RNA and G6pc2 protein expression in Floxed *G6pc2* Male Mice.

Comparison of pancreatic *G6pc2* (Panel **G**), *Slc37a4* (Panel **H**) and *Ins2* (Panel **I**) expression in 16 week old 6 hour fasted male mice in the presence or absence of the *Ins1-CreERT2* allele and in the presence or absence of tamoxifen (Tam) treatment. *G6pc2*, *Ins2* and *Slc37a4* expression were quantitated relative to *Ppia* (cyclophilin A) and then expressed relative to that in WT mice. Results represent the mean data ± S.E.M. derived from tissues isolated from the indicated number of male mice. *$p < 0.05$ vs WT, t-test. Comparison of insulin and G6PC2 protein expression in representative sections of pancreas isolated from WT, germline and BCS *G6pc2* KO mice (Panel **J**). Quantitation of G6PC2 protein expression (Panel **K**). Data represent the mean ± S.E.M. from 100 cells for each group. FL, floxed; KD, knockdown.

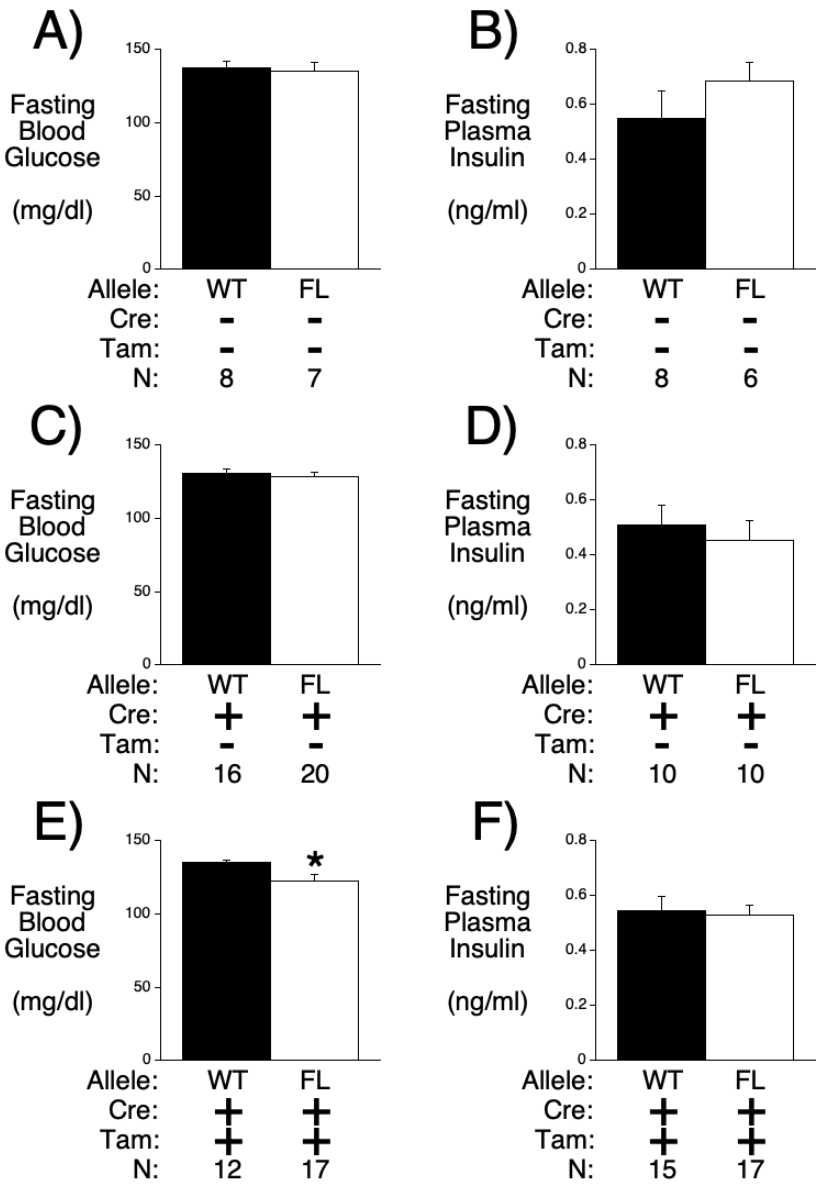

Figure 3.6. Analysis of FBG and FPI in Floxed *G6pc2* Male Mice.

Comparison of FBG (Panels **A, C & E**) and FPI (Panels **B, D & F**) in 16 week old 6 hour fasted male mice in the presence or absence of the *Ins1-CreERT2* allele and in the presence or absence of tamoxifen (Tam) treatment. Results represent the mean data ± S.E.M. derived from the indicated number of male mice. *$p < 0.05$ vs WT, t-test.

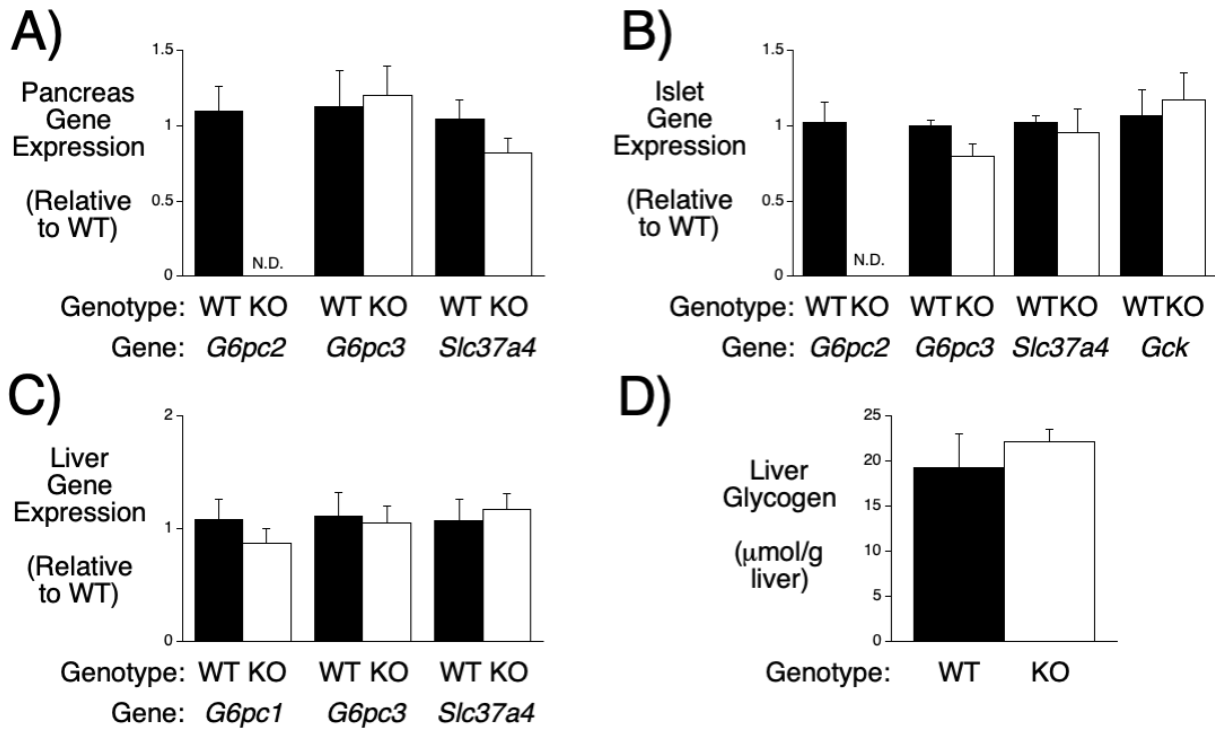

Figure 3.7. Analysis of Compensatory Changes in Gene Expression and Hepatic Glycogen in Male *G6pc2* KO mice

Panel A: Comparison of *G6pc2*, *G6pc3* and *Slc37a4* expression in pancreas from 2 month old 6 hour fasted WT and germline *G6pc2* KO mice. Gene expression was quantitated relative to *Ppia* (cyclophilin A) and then expressed relative to WT. Results represent the mean data ± S.E.M. derived from 6-7 male mice.

Panel B: Comparison of *G6pc2*, *G6pc3, Slc37a4* and *Gck* expression in isolated islets from 2 month old non-fasted WT and germline *G6pc2* KO mice. Gene expression was quantitated relative to *Ppia* (cyclophilin A) and then expressed relative to WT. Results represent the mean data ± S.E.M. derived from 3-6 islet samples.

Panel C: Comparison of *G6pc1*, *G6pc3* and *Slc37a4* expression in liver from 2 month old 6 hour fasted WT and germline *G6pc2* KO mice. Gene expression was quantitated relative to *Ppia* (cyclophilin A) and then expressed relative to WT. Results represent the mean data ± S.E.M. derived from 6-7 male mice.

Panel D: Comparison of glycogen levels in liver from 2 month old 6 hour fasted WT and germline *G6pc2* KO mice. Results represent the mean data ± S.E.M. derived from 4 male mice.

G6pc2 expression in BCS *G6pc2* KO mice compared to a complete loss of *G6pc2* expression in germline KO mice. These data also suggest that developmental compensation, a common feature in germline KO mouse studies, has not affected the phenotype of germline *G6pc2* KO mice, consistent with the absence of evidence for compensatory changes in pancreatic, islet and liver gene expression comparing WT and *G6pc2* KO mice (Figure 3.7).

Human Biobank Studies Find No Evidence for Extra-Pancreatic Actions of G6PC2

To complement our mouse studies, we searched for evidence for potential extra-pancreatic functions of G6PC2 in humans using Vanderbilt University's Medical Center (VUMC) BioVU Biobank, a DNA biobank linked to a de-identified version of the Vanderbilt electronic health records, called the Synthetic Derivative (SD) [183, 184]. Systematic and efficient approaches have been developed that involve screening the SD with specific SNPs to identify both novel phenotype-variant associations and plasma hormone/metabolite associations, referred to as PheWAS and LabWAS analyses, respectively [185, 186, 199-201]. For these analyses we used the *G6PC2* rs560887 SNP that has been shown to affect *G6PC2* RNA splicing [171] and has been linked by GWAS to variations in FBG [167, 168] and hemoglobin A1c (HbA1c) [173]. PheWAS analyses showed that the *G6PC2* rs560887 'A' allele is associated with increased risk for acute pancreatitis in non-diabetic European Americans (EAs) (G6PC2 OR = 1.39, CI = 1.20 – 1.62, p = 2.05E-05) after Bonferroni correction for the 1212 phenotypes tested (Table 3.1). Similar, though less statistically significant, trends were observed in the African American sample and in the total (multi-ancestry) population (Table 3.1). The association with acute pancreatitis was not observed in EAs with T2D (Table 3.1) or in African Americans with T2D (data not shown). Because *G6PC2* is not expressed in pancreatic exocrine or ductal tissue [27], this suggests that reduced islet *G6PC2*

Gene	SNP	Population	Phecode	Description	Beta	SE	OR	P	N_total	N_cases	N_controls	N_no_snp	LCI	UCI	Bonferroni	FDR
G6PC2	rs560887	Total	577.1	Acute pancreatitis	0.13	0.05	1.14	0.00709997	37343	411	36932	10	1.04	1.26	FALSE	FALSE
G6PC2	rs560887	All EA	577.1	Acute pancreatitis	0.15	0.05	1.16	0.00606234	31878	339	31539	6	1.04	1.28	FALSE	FALSE
G6PC2	rs560887	EA Non-T2D	577.1	Acute pancreatitis	0.33	0.08	1.39	2.05E-05	21357	145	21212	5	1.20	1.62	TRUE	TRUE
G6PC2	rs560887	EA T2D	577.1	Acute pancreatitis	2.5E-03	0.09	1.00	0.97696475	6155	140	6015	0	0.85	1.19	FALSE	FALSE
G6PC2	rs560887	Total	250.2	Type 2 diabetes	0.01	0.01	1.01	0.43847308	32759	7026	25733	9	0.98	1.04	FALSE	FALSE
SLC30A8	rs13266634	Total	250.2	Type 2 diabetes	-0.06	0.01	0.94	3.56E-05	32782	7035	25747	16	0.92	0.97	TRUE	TRUE

Table 3.1. Analysis of the Association Between *G6PC2* SNP rs560887 with Disease Phenotypes Using Electronic Health Record (EHR)-Derived Analyses.

Data show an association between *G6PC2* SNP rs560887 and acute pancreatitis in European Americans (EAs) without T2D and no association with T2D, in contrast to *SLC30A8* SNP rs13266634. ‘ All’ refers to the total EHR population. ‘ Phecodes’ refer to the numerical abbreviation for individual phenotypes in the Vanderbilt EHRs. All associations were adjusted for the covariates median age of record, sex, and EHR-reported race using linear regression. SE, standard error; OR, odds ratio; N_no_SNP, number of records with a missing predictor; FDR, false discovery rate; LCI, lower confidence interval; UCI, upper confidence interval.

Gene	SNP	Population	Analyte	Effect Estimate	SE	OR	P	N	LCI	UCI	Bonferroni	FDR
G6PC2	rs560887	Total	GLUCOSE BLOOD	-0.05	0.01	0.95	6.56E-24	38301	0.94	0.96	TRUE	TRUE
G6PC2	rs560887	Total	HGB A1C GLYCATED	-0.01	0.01	0.99	0.21060335	14328	0.97	1.01	FALSE	FALSE
G6PC2	rs560887	Total	TAURINE	0.32	0.08	1.38	7.28E-05	158	1.22	1.53	TRUE	TRUE
G6PC2	rs560887	All EA	GLUCOSE BLOOD	-0.05	0.01	0.95	2.08E-22	32686	0.94	0.96	TRUE	TRUE
G6PC2	rs560887	All EA	HGB A1C GLYCATED	-0.01	0.01	0.99	0.15780832	12271	0.97	1.00	FALSE	FALSE
G6PC2	rs560887	All EA	TAURINE	0.27	0.08	1.31	0.00171088	132	1.15	1.47	FALSE	FALSE
G6PC2	rs560887	Non T2D EA	GLUCOSE BLOOD	-0.07	0.01	0.93	3.97E-38	21728	0.92	0.94	TRUE	TRUE
G6PC2	rs560887	Non T2D EA	HGB A1C GLYCATED	-0.05	0.01	0.96	3.83E-05	4353	0.93	0.98	TRUE	TRUE
G6PC2	rs560887	Non T2D EA	TAURINE	0.29	0.09	1.34	0.00243233	114	1.16	1.53	FALSE	FALSE
G6PC2	rs560887	T2D EA	GLUCOSE BLOOD	0.01	0.01	1.01	0.18306124	6444	0.99	1.04	FALSE	FALSE
G6PC2	rs560887	T2D EA	HGB A1C GLYCATED	0.02	0.01	1.02	0.18513367	5159	0.99	1.04	FALSE	FALSE
G6PC2	rs560887	T2D EA	TAURINE	0.30	0.51	1.35	0.58240028	12	0.36	2.35	FALSE	FALSE

Table 3.2. Analysis of the Association Between *G6PC2* SNP rs560887 with Laboratory Analytes Using Electronic Health Record (EHR)-Derived Analyses.

Data show an association between *G6PC2* SNP rs560887 and blood glucose, hemoglobin A1c (HbA1c) and blood taurine in either the total EHR population (All) or specific European American (EA) sub-populations. No associations were observed in the African American (AA) population or separately in AAs with or without T2D (data not shown). SE, standard error; FDR, false discovery rate. For each laboratory value, we tested for associations between the median of all lab values for an individual against the number of minor alleles for that individual. All associations were adjusted for covariates median age of record, sex, and EHR-reported race using linear regression. The units for all measurements in any given lab were consistent within the lab (e.g. all blood glucose values were reported in mg/dL).

expression can influence non-islet pancreatic tissue function. *G6PC2* was not associated with T2D in the total population (Table 3.1). In contrast, BioVU analyses using the established rs13266634 T2D-associated SNP in the *SLC30A8* gene [202] did detect an association with T2D (Table 3.1).

LabWAS analyses showed that the *G6PC2* rs560887 'A' allele was associated with reduced blood glucose (Effect estimate = -0.05, SE = 0.01, p = 6.56E-24) in the total population. Similar trends were observed in the total EA population and in non-diabetic EAs but not EAs with T2D (Table 3.2) or in African Americans (data not shown). Given the differences in sample sizes we cannot rule out the possibility that the lack of association in these groups is simply related to power. The *G6PC2* rs560887 'A' allele was also associated with reduced HbA1c but only in non-diabetic EAs (Table 3.2). These results are consistent with GWAS data [167, 168, 173] and suggest that the influence of G6PC2 on blood glucose and HbA1c is lost under diabetic conditions. Surprisingly, the *G6PC2* rs560887 'A' allele was associated with increased taurine levels in the total population (Effect estimate = 0.32, SE = 0.08, p = 7.28E-05) with similar trends in the total EA and non-diabetic EA populations (Table 3.2). It is well established that insulin regulates amino acid metabolism [203], so the simplest hypothesis is that reduced islet *G6PC2* expression influences the kinetics of insulin secretion which then affects amino acid metabolism. Overall these PheWAS and LabWAS results complement the conclusions of the mouse studies by not finding evidence for extra-pancreatic functions of G6PC2.

To follow up on these observations from human population studies, we examined whether germline deletion of *G6pc2* results in pancreatitis in mice. Pancreatic sections from ~8 month old 6 hour fasted mice showed no evidence of pancreatitis, with no necrosis, edema, hemorrhage, steatosis, or fibrosis within the pancreatic parenchyma and no increase in inflammatory infiltrate compared to WT controls. Furthermore, acinar cell morphology appeared normal with no evidence

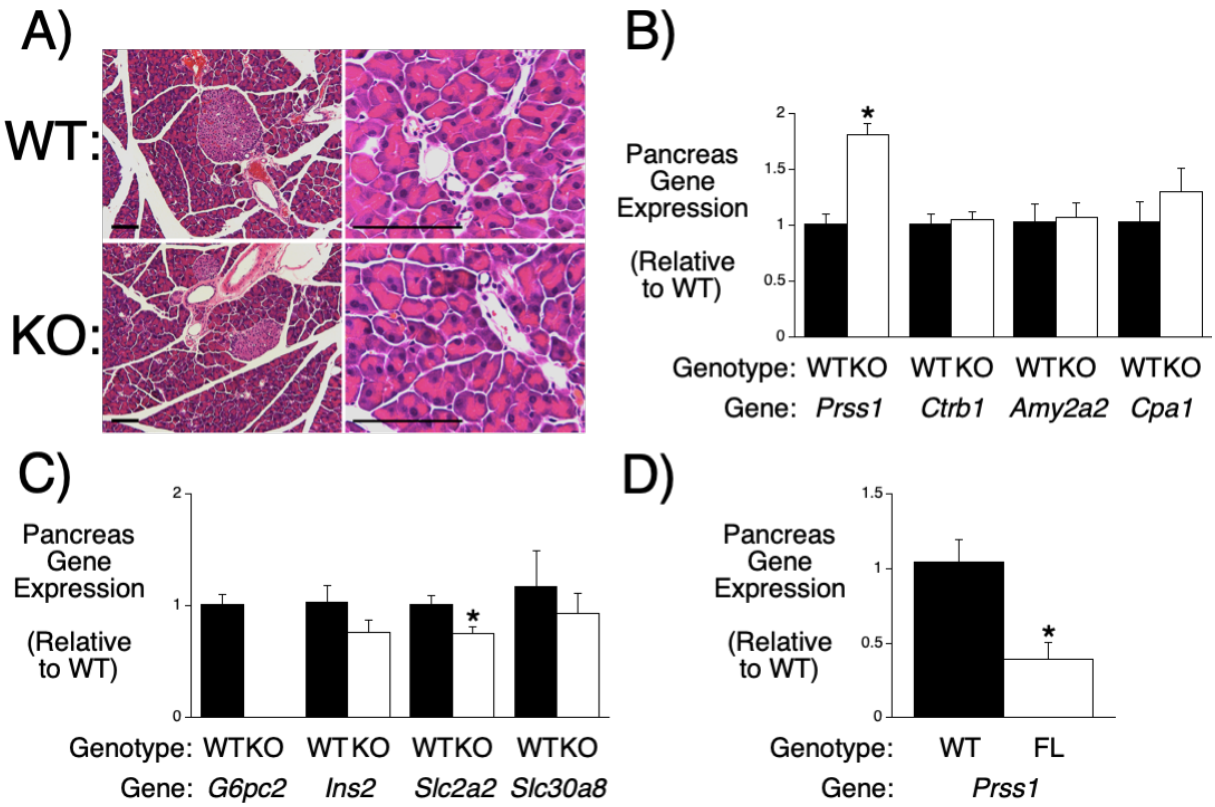

Figure 3.8. Analysis of Pancreatitis and Acinar Gene Expression in Germline *G6pc2* KO and Floxed *G6pc2* Male Mice.

Panel A: Comparison of pancreatic tissue in WT and germline *G6pc2* KO mice. Results are representative of sections analyzed from 3 WT and 3 KO mice. Size bars represent 100 µm. **Panels B & C:** Comparison of pancreatic acinar gene expression in 6 hour fasted 16 week old male WT and germline *G6pc2* KO mice. Gene expression was quantitated relative to *Ppia* (cyclophilin A) and then expressed relative to that in WT mice. Results represent the mean data ± S.E.M. derived from pancreata isolated from 5 mice. *p < 0.05 vs WT, t-test. **Panel D:** Comparison of pancreatic gene expression in 6 hour fasted 16 week old male WT and BCS *G6pc2* KO mice following tamoxifen treatment. The RNA samples were a subset of those used in **Fig. 3.5 Panels G-I**. Gene expression was quantitated relative to *Ppia* (cyclophilin A) and then expressed relative to that in WT mice. Results represent the mean data ± S.E.M. derived from pancreata isolated from 5 mice. *p < 0.05 vs WT, t-test.

of degranulation, vacuolization, or luminal dilation (Figure 3.8A). However, expression of *Prss1*, which encodes trypsinogen, was elevated in 16 week old 6 hour fasted germline *G6pc2* KO mice (Figure 3.8B). The expression of *Ctrb1* (chymotrypsinogen), *Amy2a2* (amylase) and *Cpa1* (carboxypeptidase A1) were unchanged (Figure 3.8B) as were *Ins2*, *Slc30a8* (ZnT8) and *Slc37a4*, though *Slc2a2* expression was slightly reduced (Figure 3.8C). Surprisingly the opposite result was observed in 16 week old 6 hour fasted BCS *G6pc2* KO mice in which expression of *Prss1* was reduced (Figure 3.8D).

We also examined whether germline deletion of *G6pc2* affects circulating amino acid levels in mice. Surprisingly, the levels of several amino acids were significantly lower in 8 month old 6 hour fasted germline KO mice compared to WT controls, which is the opposite of the results of the LabWAS analysis (Figure 3.9).

Glycolysis is Enhanced in Germline *G6pc2* KO Relative to WT Islets

Our model predicts that deletion of *G6pc2* will increase glycolytic flux in islets. While glucose cycling analyses can quantitate G6P production [7], such experiments do not quantitate the rate of glycolysis. It is important to address this key difference because glycolysis, rather than the rate of G6P production, is the determinant of the magnitude of GSIS [164, 165]. This distinction arises because G6P has multiple alternate metabolic fates, including conversion to fructose-6-phosphate, glucose-1-phosphate, and inositol-3-phosphate. The well-established glycolytic assay that measures the generation of $^{3}H_2O$ from D-[5-^{3}H]glucose [187-189] was used to compare glycolytic rates in WT and germline *G6pc2* KO islets. Consistent with our model, glycolysis was elevated in KO islets at 5.6 mM glucose (Figure 3.10).

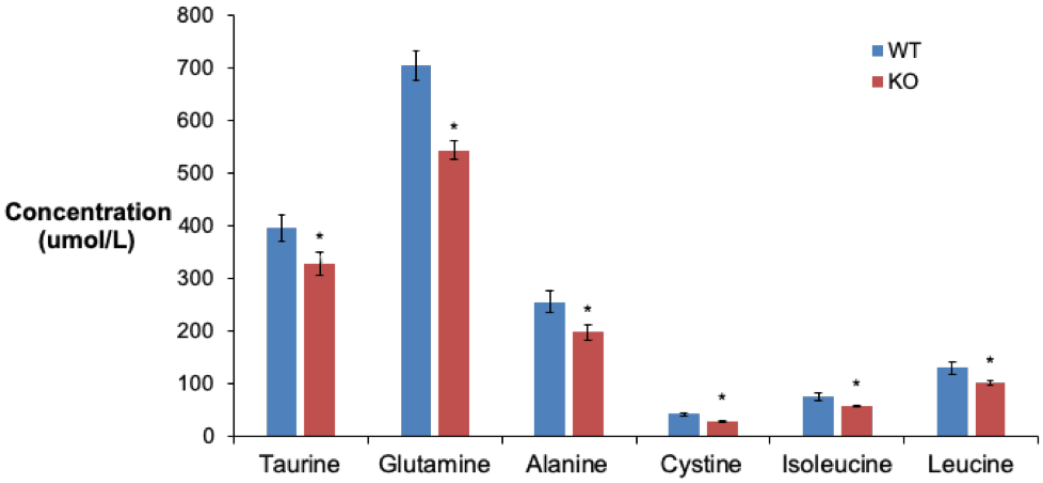

Figure 3.9. Analysis of Plasma Amino Acid Levels in WT and Germline *G6pc2* KO Male Mice. Comparison of amino acid levels in plasma from 8 month old 6 hour fasted WT and germline *G6pc2* KO mice. Results represent the mean data ± S.E.M. derived from plasma isolated from 5 WT and 5 KO male mice. *$p < 0.05$ vs WT, t-test

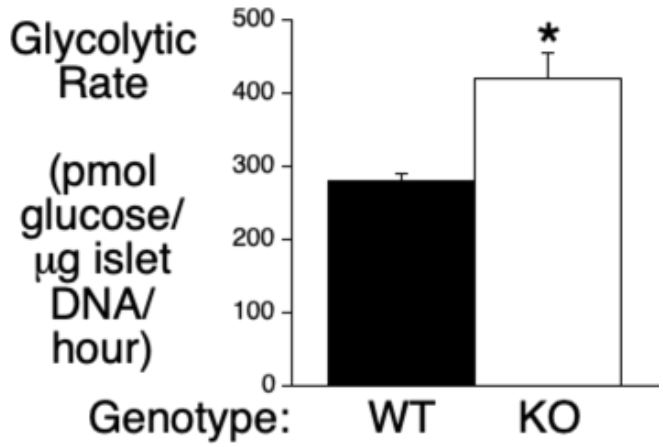

Figure 3.10. Comparison of Glycolytic Rates in WT and Germline *G6pc2* KO Islets.

Data show the rates of glycolysis in isolated islets from WT and germline *G6pc2* KO mice at 5 mM glucose and represent the mean ± S.E.M. of 5-7 islet samples. *$p < 0.05$ vs WT, t-test.

Glucose Cycling Exists in Human Islets

Using a novel stable isotope-based methodology that eliminates assumptions associated with the use of radioisotopes, we have recently shown that mouse islets exhibit significant rates of glucose cycling [7]. The same methodology was used to address the key question as to whether glucose cycling also occurs in human islets. Kayton et al. [3] have recently used islet perifusion assays to define 5 patterns of GSIS in human islets, designated as Group 1- 5. Group 1 islets exhibit optimal responses to secretagogues whereas GSIS shows distinct abnormalities in Group 2-5 islets [3]. Glucose uptake and cycling were compared at both 5 mM and 11 mM glucose in human islet preparations from four donors (Table 3.3) that were defined as Group 1 using perifusion assays (Figure 3.11). Significant rates of glucose uptake and glucose cycling were detected and were typically greater at 11 mM than 5 mM though, for reasons that are unclear, this was not uniform and the islet preparation that exhibited decreased glucose uptake at 11 mM was distinct from the preparation that exhibited decreased glucose cycling at 11 mM (Figure 3.12). At 5 mM glucose the level of glucose uptake inversely correlated with the level of glucose cycling (Figure 3.12). Since the rate of glucose cycling is determined by quantitating the glucose isotopomers generated by cycling that are transported out of the islets and back into the media, one possible interpretation of this observation is that in cells with high glycolytic flux, re-cycled glucose preferentially re-enters the glycolytic pathway rather than leaving the cell, leading to an underestimate of the rate of cycling. Another possible interpretation is that the rate of G6P dephosphorylation is fairly constant despite changes in glucose uptake, so glucose cycling represents a smaller percentage of glucose uptake when the glucose uptake rate is high. The mean rate of glucose cycling is clearly lower in human (Figure 3.12) than mouse [7] islets. This correlates with higher basal GSIS [204]

Islet preparation	A	B	C	D
MANDATORY INFORMATION				
Unique identifier	ADBN085	ACKB319	ACEA213	ABG2385
Donor age (years)	19	49	52	30
Donor sex (M/F)	M	F	M	M
Donor BMI (kg/m^2)	27.2	31.6	33.25	43.7
Donor HbA_{1c} or other measure of blood glucose control	N.R	5.2	4.6	N.R.
Origin/source of islets[b]	NDRI	IIDP	IIDP	IIDP
Islet isolation centre	University of Pittsburgh	University of Pennsylvania	University of Wisconsin	University of Wisconsin
Donor history of diabetes? Please select yes/no from drop down list	No	No	No	No
RECOMMENDED INFORMATION				
Donor cause of death	Head trauma	Cerebrovascular/ Stroke	Head trauma	Anoxia
Warm ischaemia time (h)	N.R.	N.R.	N.R.	N.R.
Cold ischaemia time (h)	N.R.	5.3	9.3	N.R.
Estimated purity (%)	N.R.	95%	95%	95%
Estimated viability (%)	N.R.	94%	97%	95%
Total culture time (h)[d]	N.R.	39	72	N.R.
Glucose-stimulated insulin secretion or other functional measurement[e]	Yes	Yes	Yes	Yes
Handpicked to purity? Please select yes/no from drop down list	Yes	Yes	Yes	Yes

Table 3.3. Checklist for Reporting Human Islet Preparations Used in Research. This table provides information on the individual donors used for the glucose cycling studies in **Figure 3.12** and the islet perifusion studies in **Figure 3.11**. Adapted from [5].

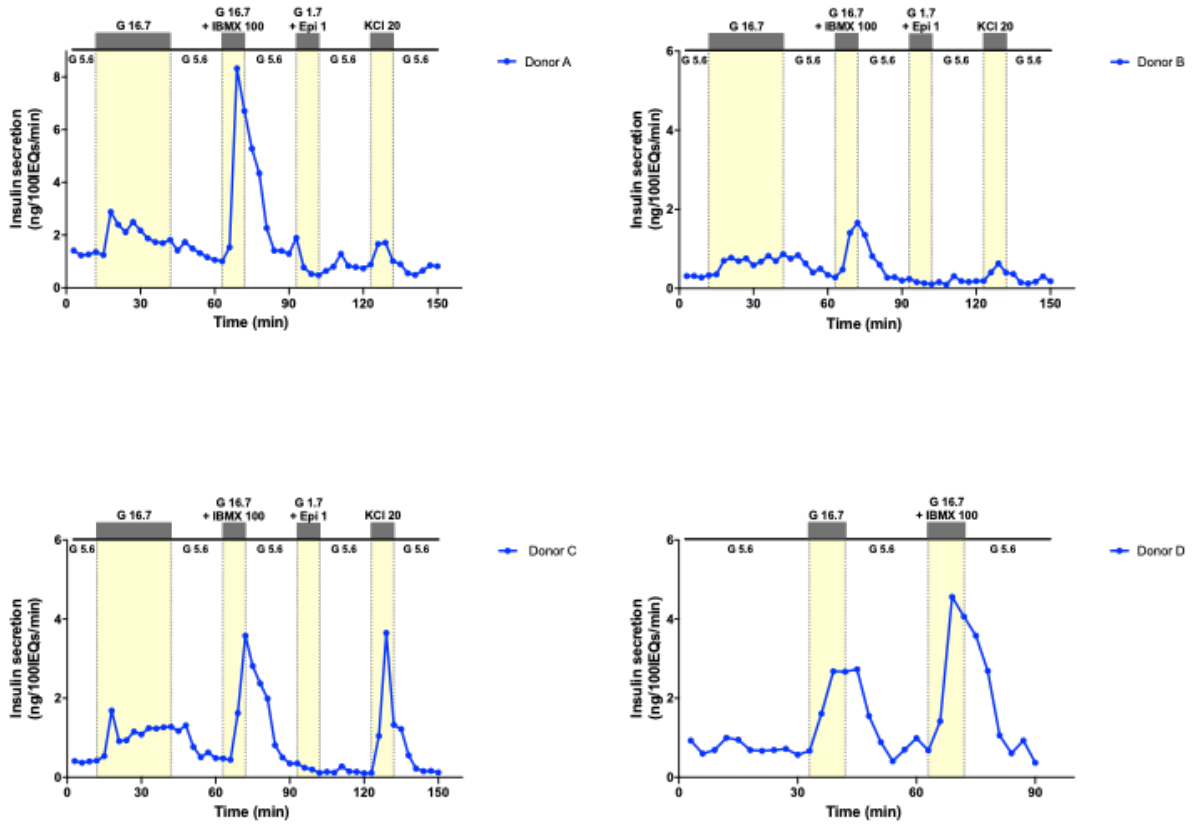

Figure 3.11. Insulin Secretory Profiles in Isolated Human Islets.

Insulin secretion by human islets was assessed using perifusion as previously described [3]. Based on the insulin secretory profile, human islet donor samples A-D are classified as Group 1 [3].

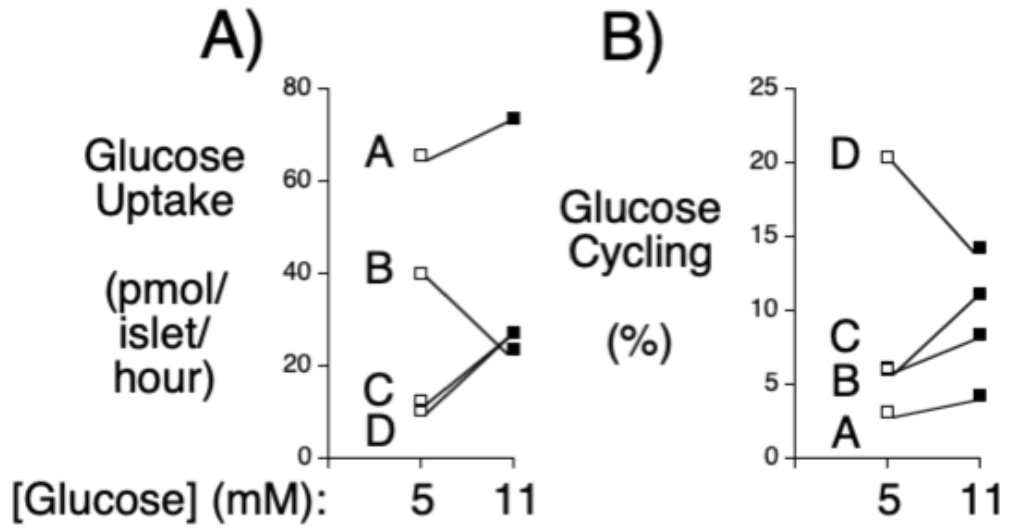

Figure 3.12. Comparison of Glucose Uptake Cycling Rates in Group 1 Human Islets.

Data show the rates of glucose uptake (Panel **A**) and cycling (Panel **B**) in individual preparations of Group 1 islets at either 5 mM or 11 mM glucose from four donors (designated A-D). Information on the individual human donors is presented in **Table 3.3** and information of the insulin secretory profile of each islet preparation, as assessed by islet perifusion, is presented in **Figure 3.11.**

and lower *G6PC2* expression [205] in human versus mouse islets as well as lower FBG in healthy humans [206] than C57BL/6J mice [1].

Discussion

The experiments described here provide further support for the concept that G6PC2 activity in pancreatic islets creates a glucokinase/G6PC2 futile cycle that determines the rate of beta cell glycolytic flux and hence the sensitivity of GSIS to glucose rather than this rate being determined by glucokinase alone. Specifically, we show from gene expression analyses that G6PC2 is unlikely to be important in non-islet tissues where the more active G6PC isoforms, G6PC1 and G6PC3, are more abundantly expressed (Figure 3.1) and that deletion of *G6pc2* specifically in beta cells is sufficient to reduce FBG (Figures 3.5 & 3.6). Consistent with our model, deletion of *G6pc2* enhances glycolysis in mouse islets (Figure 3.10) and glucose cycling also exists in human islets (Figure 3.12).

Several interesting observations arose from the human biobank studies. First, we observed a strong association between *G6PC2* and blood glucose levels (Table 3.2) even though the BioVU population represents individuals who visit VUMC with a wide range of medical issues and who were not all under overnight fasting conditions when blood was isolated. This suggests that G6PC2 can influence blood glucose under non-fasting conditions, consistent with the concept that altered *G6PC2* expression affects the sensitivity of GSIS to glucose over a range of glucose concentrations rather than just at fasting glucose levels (Figure 3.4).

Second, the results show that altered *G6PC2* expression in humans can affect the risk of acute pancreatitis (Table 3.1) and that deletion of *G6pc2* in mice alters *Prss1* expression (Figure 3.8B & D). Since altered *Prss1* expression may affect the risk of pancreatitis [207, 208] this

provides a potential mechanistic link between these observations. Since *G6PC2* is expressed selectively in pancreatic islet cells [27], the mechanism by which it affects *Prss1* expression and especially why the direction of the effect differs with germline and BCS deletion is unclear but will be the subject of future studies.

Third, the results show that altered *G6PC2* expression in humans can affect the levels of circulating amino acids in plasma (Figure 3.9). One possible explanation for this is that altered *G6PC2* expression affects amino acid metabolism by altering the kinetics of insulin secretion. Additionally, it is unclear why the mouse and human data differ in the direction of the effect, but this, along with the mechanism by which *G6PC2* expression affects amino acid metabolism, will be the subject of future studies.

Finally, we observed that *G6PC2* was not associated with altered risk for T2D (Table 3.1), matching GWAS data that have failed to establish a consistent link with T2D risk [209]. It will be of considerable interest to identify individuals with mutations that have a major effect on G6PC2 function to determine whether an association with T2D risk then emerges. Elevations in FBG in the prediabetic state correlate with [210] and appear sufficient to drive [211, 212] the decline in beta cell function, likely mediated by reactive oxygen species (ROS), that underlies the progression from prediabetes to T2D [213, 214]. However, unless G6PC2 has unknown additional effects on beta cell metabolic flux, a therapy designed to inhibit G6PC2 and thereby lower FBG may fail to prevent this progression because the reduced FBG is associated with the same level of insulin secretion, and would be associated with unchanged glycolytic flux and therefore unchanged generation of damaging ROS (Figure 3.13). While a therapy directed at G6PC2 may not affect T2D risk it would likely still be beneficial in preventing cardiovascular-associated mortality (CAM) in individuals with elevated FBG. Thus, in Europeans, an increase in FBG levels from less

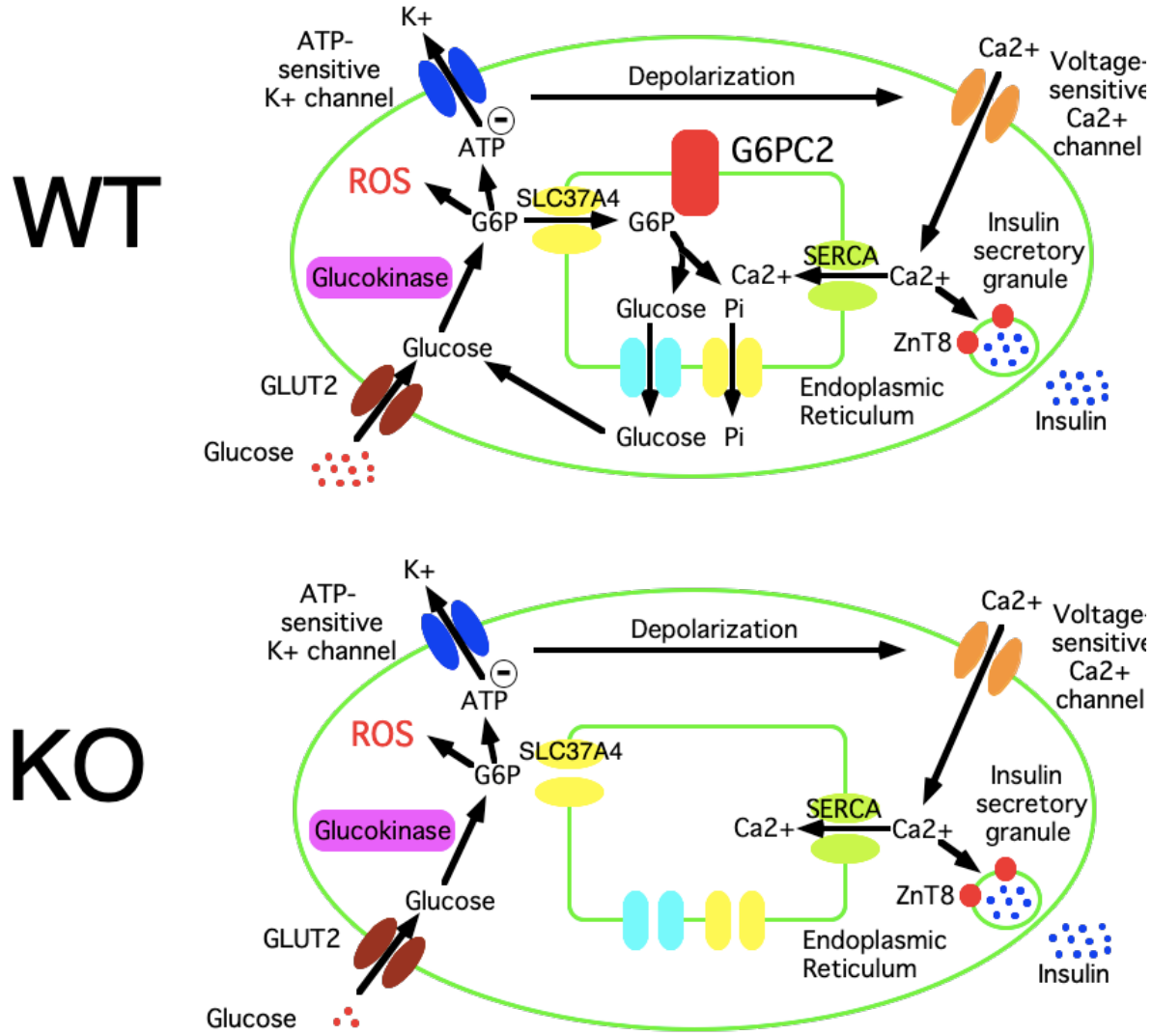

Figure 3.13. Effect of *G6pc2* Deletion on the Generation of Reactive Oxygen Species. Schematic proposing that in the absence of G6PC2, a reduced level of glucose is required to achieve the same level of insulin secretion while glycolytic flux remains unchanged, explaining why FBG is reduced in *G6pc2* KO mice with no change in FPI. However, because glycolytic flux is unchanged, the schematic proposes that the generation of reactive oxygen species (ROS) is also unchanged in the absence of G6PC2. Therefore, unless G6PC2 has other unknown functions in beta cells, the schematic proposes that while inhibition of G6PC2 would reduce FBG, it would not reduce the deleterious effects of ROS on beta cell function and hence may not slow or prevent the transition from impaired glucose tolerance to T2D.

than 90 mg/dl to between 99-108 mg/dl is associated with 30% increased risk of CAM [157], and in Asians a reduction in FBG from 99 to 90 mg/dl is associated with a 25% reduction in the risk of CAM [158]. The risk of CAM increases still further in individuals with the high FBG levels characteristic of diabetes [157, 158, 215, 216].

In mice, *G6pc2* expression is ~20 fold higher in beta than alpha cells [205], G6PC2 protein is undetectable in alpha cells [27], and glucagon levels are unchanged in germline *G6pc2* KO mice [147]. The reduction in FBG in germline *G6pc2* KO mice with unchanged FPI is therefore solely due to the shift in the sensitivity of GSIS to glucose, consistent with our glycolysis and BCS *G6pc2* KO mouse data. In contrast, in humans *G6PC2* expression is only ~5 fold higher in beta than alpha cells [205] such that altered alpha cell glycolysis could contribute to the reduction in FBG in humans with reduced *G6PC2* expression.

In summary, these studies show that islet-specific G6PC2 activity is sufficient to regulate FBG, although the possibility that G6PC2 plays some role in tissue-specific metabolism outside the pancreas cannot be excluded.

CHAPTER 4

G6PC2 Confers Protection Against Hypoglycemia Upon Ketogenic Diet Feeding and Prolonged Fasting

Introduction

As described in the introduction to this dissertation, G6PC2 acts in conjunction with glucokinase to create a futile substrate cycle that determines the rate of beta cell glycolytic flux [1, 164, 165] (Figure 1.2). In turn, the rate of glycolysis determines the sensitivity of GSIS to glucose and hence the influence of beta cells on FBG [164, 165]. Deletion of *G6pc2* results in a leftward shift in the dose response curve for GSIS [1] such that under fasting conditions, insulin levels are the same in WT and *G6pc2* KO mice but FBG is reduced in KO mice [1, 147]. This model is consistent with genome wide association and molecular studies that have linked the rs560887 'A' allele to reduced *G6PC2* expression and reduced FBG [167, 168, 171].

A key question is the nature of the physiological benefit conferred by this glucokinase/G6PC2 substrate cycle. Experiments in mice in which glucocorticoids were injected [175] or endogenous glucocorticoids were elevated by physical restraint [174] induced *G6pc2* expression, and the associated change in FBG relative to WT suggested that G6PC2 may have evolved, in part, to confer a transient, beneficial elevation in FBG during periods of stress [176]. In contrast, in the modern world, long-term treatment of elderly patients with glucocorticoids is associated with a deleterious hyperglycemic state resembling Cushing's disease [217-220], to which a prolonged elevation in G6PC2 expression would contribute. The experiments described here extend these studies by examining the role of G6PC2 in the response to different nutritional

challenges and suggest that G6PC2 evolved to not only regulate FBG in response to stress but also prevent hypoglycemia associated with prolonged fasting and ketogenic diets.

Results

G6PC2 Confers Protection Against Hypoglycemia Upon Ketogenic Diet Feeding

To understand why the *G6PC2* gene would have been conserved across multiple species over the course of evolution we considered the benefits a glucokinase/G6PC2 futile substrate cycle might confer under different dietary conditions. In winter months when carbohydrate-rich foods were scarce we hypothesized that G6PC2 might have been beneficial by limiting basal GSIS and therefore conferring protection against hypoglycemia. To address this hypothesis, we investigated the response of WT and *G6pc2* KO mice to ketogenic diet feeding.

Switching mice from a chow diet to a ketogenic diet resulted in transient weight loss in both WT and *G6pc2* KO mice (Figure 4.1A). Both WT and *G6pc2* KO mice returned to their initial starting weight after 21 days on the ketogenic diet (Figure 4.1A). After 35 days on the ketogenic diet WT mice gained additional weight and exceeded their initial starting weight whereas KO mice remained at their initial starting weight even after 56 days on the diet (Figure 4.1A). A difference in body weight between WT and *G6pc2* KO mice emerged upon ketogenic diet feeding (Figure 4.1A).

FBG (Figure 4.1B) and FPI (Figure 4.1C) dropped in both WT and *G6pc2* KO mice after 7 days of ketogenic diet feeding and remained lower after 56 days. FPI did not differ between WT and *G6pc2* KO mice at any time (Figure 4.1C). The difference in FBG observed in chow fed WT and *G6pc2* KO mice was still apparent after 7 days of ketogenic diet feeding but a statistically

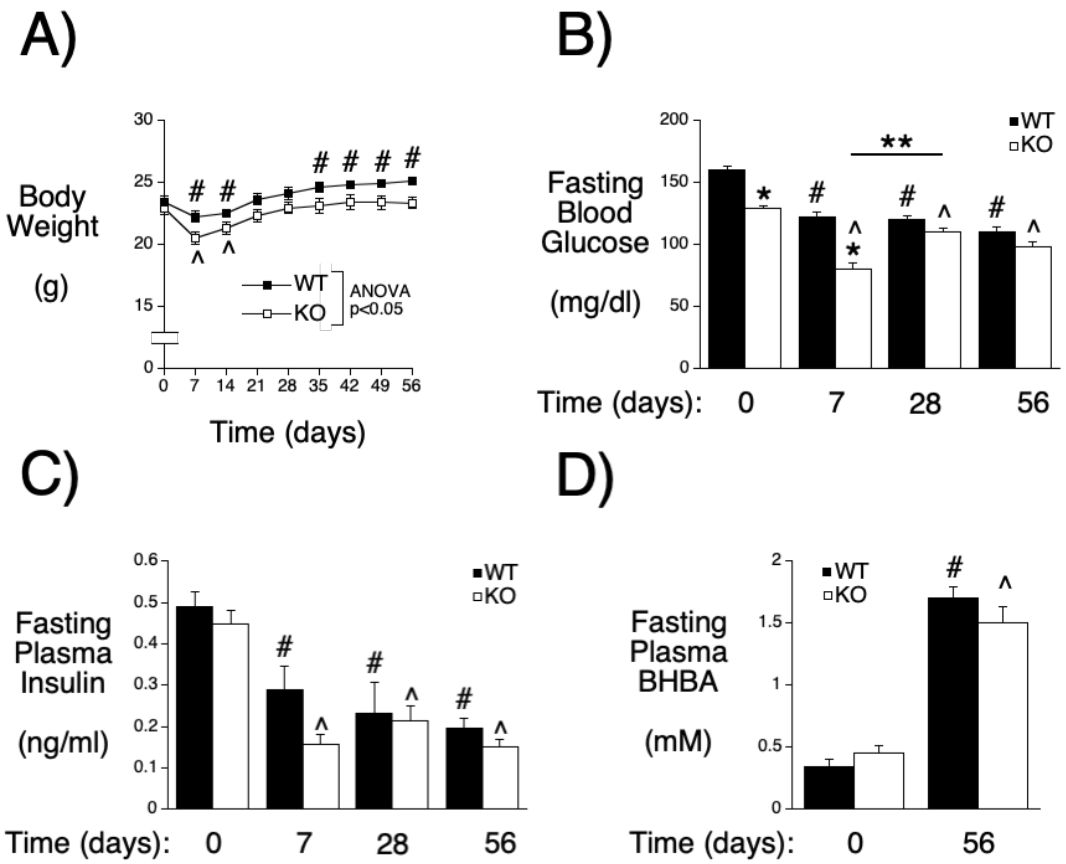

Figure 4.1. Analysis of Metabolic Parameters in Male WT and *G6pc2* KO Mice on a Ketogenic Diet.

Body weight (Panel **A**; WT n = 14; KO n = 15), FBG (Panel **B**; WT n = 14-16; KO n = 15-17), FPI (Panel **C**; WT n = 5-21; KO n = 5-22) and plasma ketones (beta-hydroxybutyric acid; BHBA) (Panel **D**; WT n = 5-8; KO n = 5-8) were compared in non-fasted (Panel **A**) or 6 hour fasted (Panels **C-D**) WT and KO mice that were switched from a chow diet to a ketogenic diet at 8 weeks of age. Results represent the mean data ± S.E.M. Statistical significance was analyzed using ANOVA. *$p < 0.05$ WT vs KO; #$p < 0.05$ WT at day 0 vs WT after ketogenic diet feeding; ^$p < 0.05$ KO at day 0 vs KO after ketogenic diet feeding.

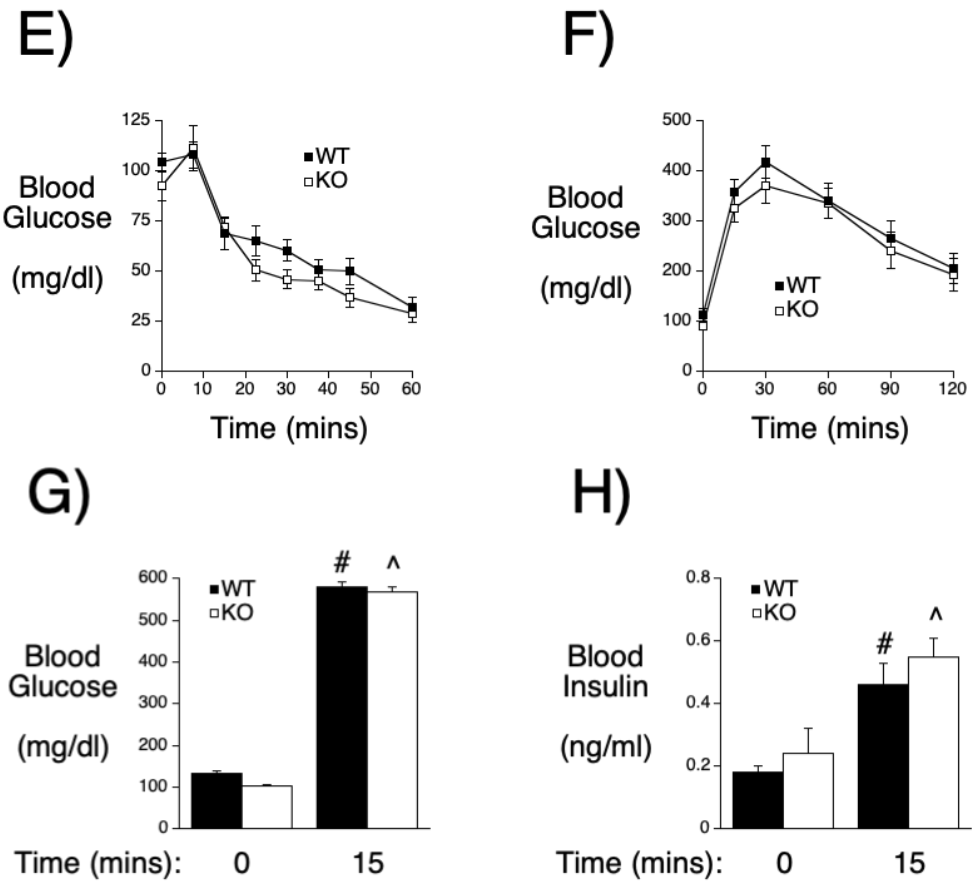

Figure 4.1. Analysis of Metabolic Parameters in Male WT and *G6pc2* KO Mice on a Ketogenic Diet.

Insulin sensitivity (Panel **E**; WT n = 7; KO n = 9), intraperitoneal (IP) glucose tolerance (Panel **F**; WT n = 8; KO n = 9) and both blood glucose (Panel **G**; WT n = 8-9; KO n = 8-10) and plasma insulin (Panel **H**; WT n = 8-9; KO n = 8-10) before and after IP glucose injection (2 g/kg) were compared in 6 hour fasted 16-18 week old WT and KO mice after 8-10 weeks of ketogenic diet feeding. Results represent the mean data ± S.E.M. Statistical significance was analyzed using ANOVA. #$p < 0.05$ WT at day 0 vs WT after ketogenic diet feeding; ^$p < 0.05$ KO at day 0 vs KO after ketogenic diet feeding.

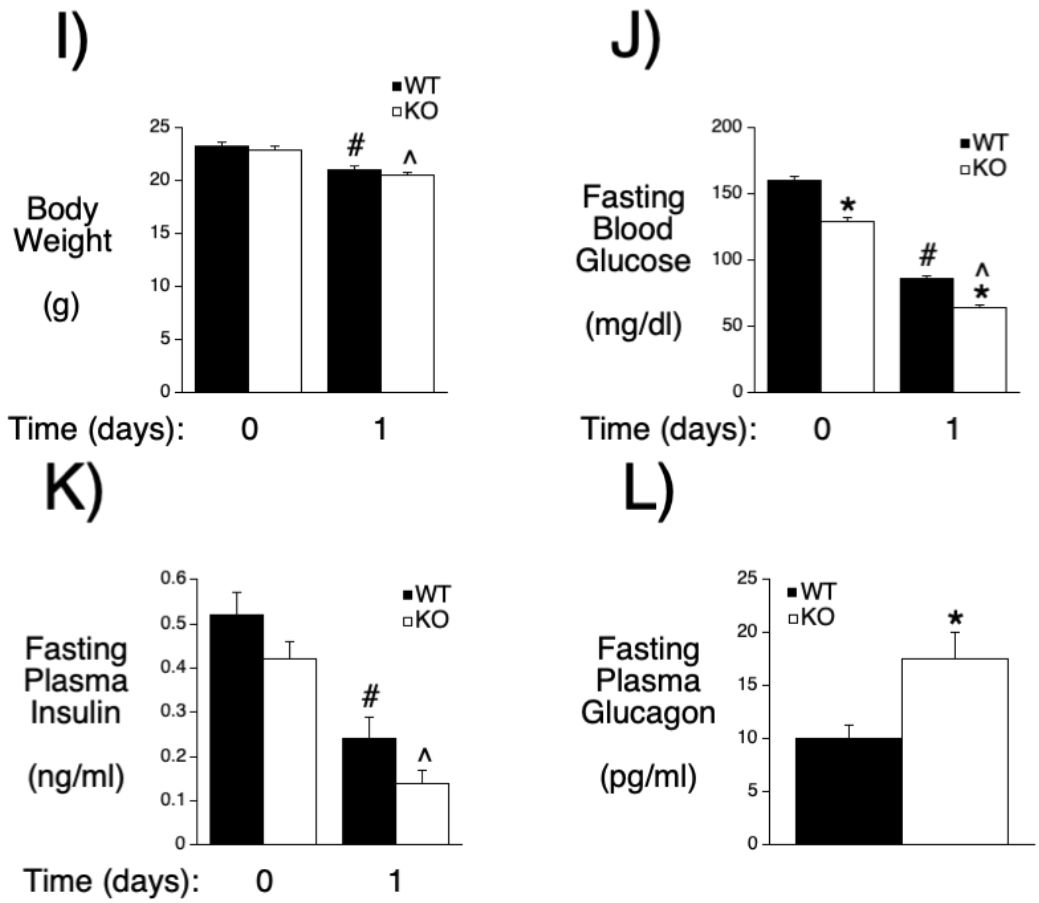

Figure 4.1. Analysis of Metabolic Parameters in Male WT and *G6pc2* KO Mice on a Ketogenic Diet.

Body weight (Panel **I**; WT n = 16; KO n = 20), FBG (Panel **J**; WT n = 16; KO n = 17-19), FPI (Panel **K**; WT n = 13-14; KO n = 14) and plasma glucagon (Panel **L**; WT n = 7; KO n = 11) were compared in 6 hour fasted WT and KO mice before and/or 1 day after switching from a chow diet to ketogenic diet at 8 weeks of age. Results represent the mean data ± S.E.M. Statistical significance was analyzed using ANOVA (Panels **I-K**) or t-tests (Panel **L**). *$p < 0.05$ WT vs KO; #$p < 0.05$ WT at day 0 vs WT after ketogenic diet feeding; ^$p < 0.05$ KO at day 0 vs KO after ketogenic diet feeding.

significant difference was lost after prolonged feeding (Figure 4.1B). Ketone levels were elevated in both WT and KO mice (Figure 4.1D). As in chow fed mice [1], WT and *G6pc2* KO mice on a ketogenic diet showed no differences in insulin sensitivity (Figure 4.1E) or intraperitoneal glucose tolerance (Figure 4.1F) and the rise in blood glucose following intraperitoneal injection of glucose in WT and KO mice (Figure 4.1G) was not associated with a difference in the rise in plasma insulin (Figure 4.1H).

Since the fall in FBG in *G6pc2* KO mice partially recovers between 7 and 28 days of ketogenic diet feeding (Figure 4.1C), we investigated the initial response to the switch to a ketogenic diet. Significant weight loss was observed in WT and *G6pc2* KO mice one day after switching mice from a chow diet to a ketogenic diet (Figure 4.1I) and this was associated with marked decrease in both FBG (Figure 4.1J) and FPI (Figure 4.1K), with KO mice becoming hypoglycemic (64.1 -/+ 2.2 mg/dl glucose). Glucagon levels were elevated in KO mice after 1 day on the ketogenic diet relative to WT mice but this increase was clearly insufficient to prevent hypoglycemia in KO mice (Figure 4.1L). These data suggest that G6PC2 confers protection against transient hypoglycemia upon ketogenic diet feeding.

The switch from a chow to ketogenic diet was associated with only modest changes in pancreatic expression of genes known to be highly expressed in islets, including *G6pc2* (Figure 4.2A). By focusing on the expression of genes highly expressed in islets but not acinar cells, their expression can be analyzed in whole pancreas RNA preparations which then captures expression levels in the *in vivo* islet environment and avoids the confounding issue of gene expression changing during islet isolation. The switch from a chow to ketogenic diet was associated with marked changes in pancreatic acinar gene expression (Figure 4.2B) whereas the expression of key hepatic genes was unchanged (Figure 4.2C). The absence of a marked change in *G6pc2* expression

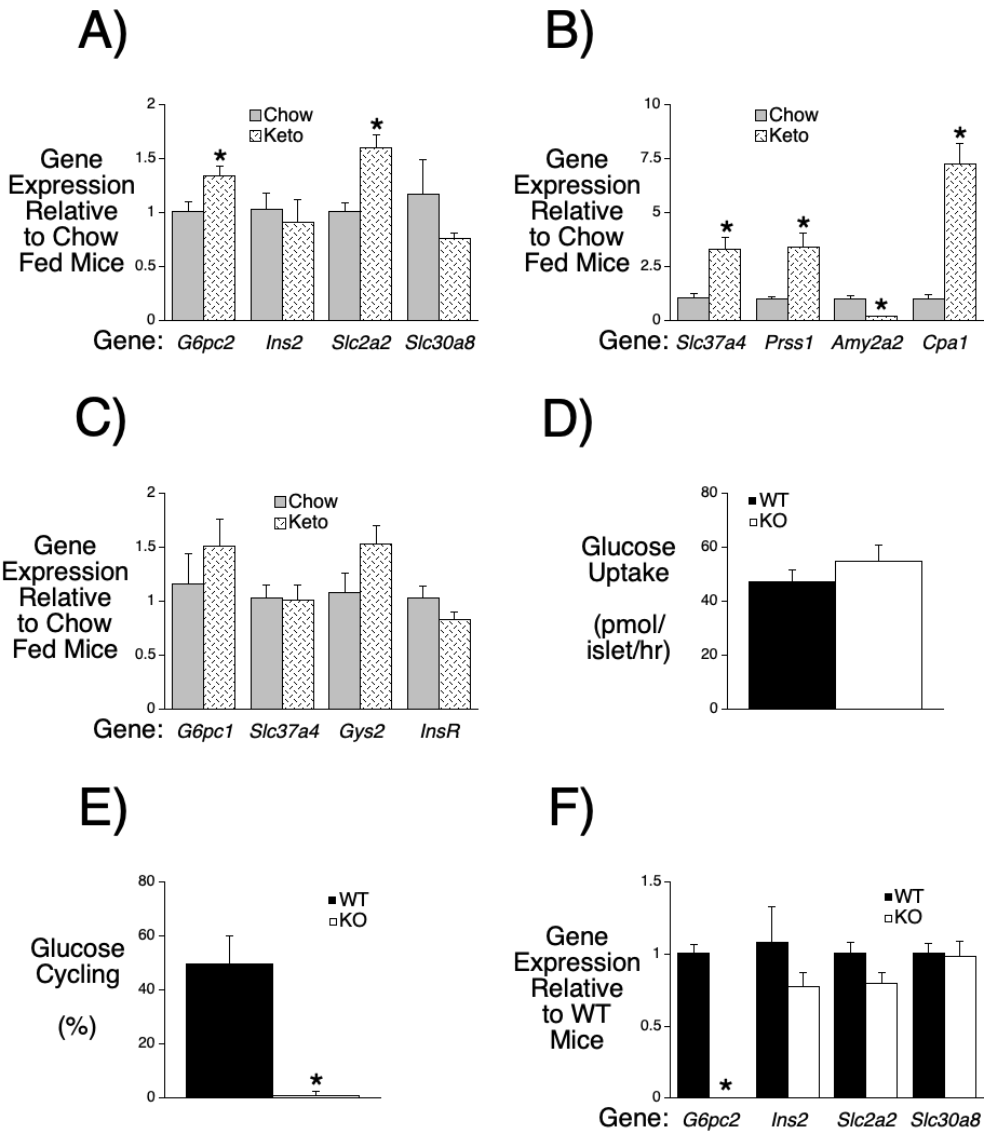

Figure 4.2. Analysis of Gene Expression in Male WT and *G6pc2* KO Mice on a Ketogenic Diet.

Comparison of pancreatic expression of genes known to be highly expressed in islets (Panel **A**; chow n = 5; ketogenic n = 5) or acinar cells (Panel **B**; chow n = 5; ketogenic n = 5) or liver (Panel **C**; chow n = 8; ketogenic n = 10) in 6 hour fasted 16 week old chow fed WT mice versus 6 hour fasted 16 week old WT mice that were switched to a ketogenic diet at 8 weeks of age. Data were corrected relative to *Ppia* (cyclophilin A) expression. Results represent the mean data ± S.E.M. *p < 0.05 chow vs ketogenic diet (Keto). Comparison of glucose uptake (Panel **D**) and glucose cycling (Panel **E**) rates at 11 mM glucose in islets isolated from 16 week old WT and KO mice (n = 3) that were switched to a ketogenic diet at 8 weeks of age. Results represent the mean data ± S.E.M. *p < 0.05 WT vs KO. Comparison of pancreatic expression of genes known to be highly expressed in islets (Panel **F**; WT n = 5; KO n = 5) in 6 hour fasted 16 week old WT and KO mice that were switched to a ketogenic diet at 8 weeks of age. Data were corrected relative to *Ppia* (cyclophilin A) expression. Results represent the mean data ± S.E.M. *p < 0.05 WT vs KO. Statistical significance was analyzed using t-tests.

is consistent with the observation that the rate of glucose uptake (Figure 4.2D) and glucose cycling (Figure 4.2E) in islets isolated from mice on a ketogenic diet is similar to that in islets isolated from mice on a chow diet [7]. As expected, deletion of *G6pc2* abolished glucose cycling (Figure 4.2E). Deletion of *G6pc2* did not result in compensatory changes in the expression of pancreatic genes known to be highly expressed in islets when mice were on a chow (Figure 3.7) or ketogenic (Figure 4.2F) diet.

G6PC2 Confers Protection Against Hypoglycemia Upon Prolonged Fasting

We next investigated the response of chow fed WT and *G6pc2* KO mice to prolonged fasting. A 24 hour fast resulted in weight loss (Figure 4.3A) and a reduction in both FBG (Figure 4.3B) and FPI (Figure 4.3C) relative to both 6 hour fasted WT and *G6pc2* KO mice. FPI did not differ between WT and *G6pc2* KO mice (Figure 4.3C) whereas the difference in FBG observed in 6 hour fasted WT and *G6pc2* KO mice was still apparent after a 24 hour fast (Figure 4.3B) with KO mice becoming hypoglycemic (70 -/+ 1 mg/dl glucose). The occurrence of hypoglycemia with 24 hour fasting was observed with *G6pc2* KO mice on paper (Figure 4.3B) but not corn cob bedding [175]. We also observed that the effect of ketogenic diet feeding on FBG in *G6pc2* KO mice was variable with mice housed on corn cob bedding (Figure 4.4). These observations are consistent with studies showing that metabolic responses in mice are affected by cage bedding materials [221]. A difference in glucagon levels between WT and KO mice was not observed despite the hypoglycemia in KO mice (Figure 4.3D). These data suggest that G6PC2 confers protection against transient hypoglycemia upon prolonged fasting.

Prolonged fasting was associated with a ~50% fall in pancreatic *G6pc2* and *Slc2a2* gene expression, but no change in *Ins2* or *Slc30a8* gene expression (Figure 4.3E), as well as marked

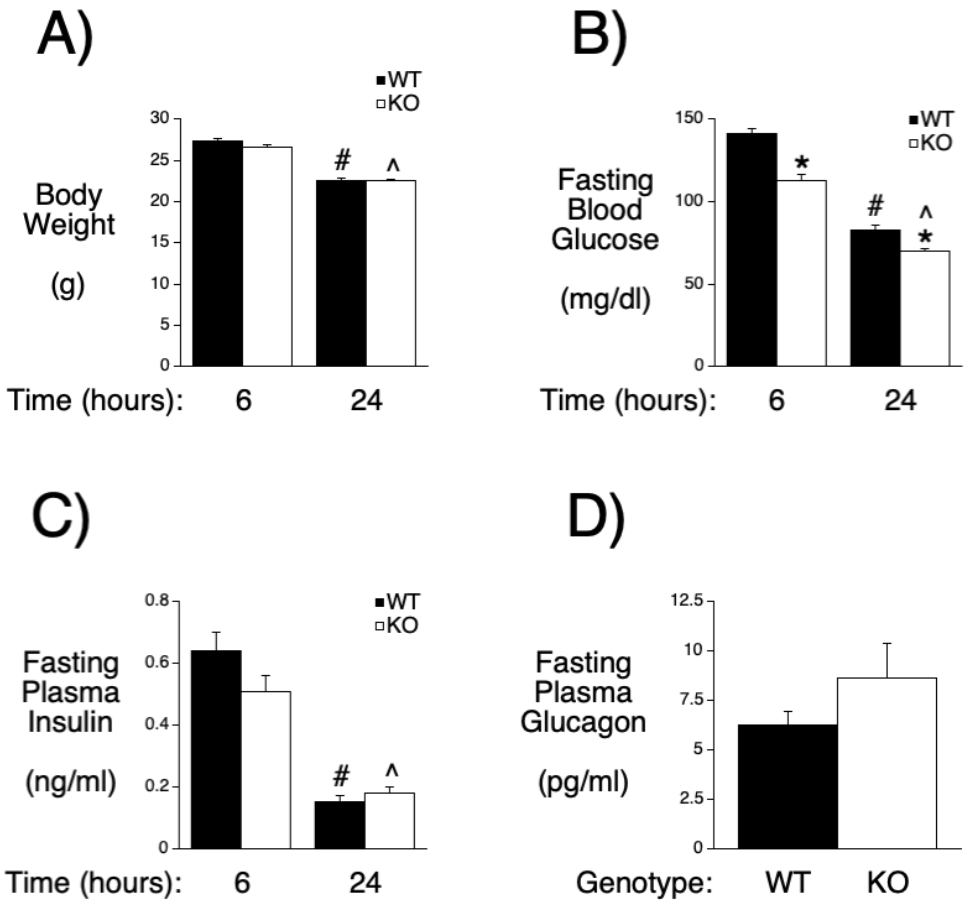

Figure 4.3. Analysis of Metabolic Parameters and Gene Expression in Male WT and *G6pc2* KO Mice After Prolonged Fasting.

Body weight (Panel **A**; WT n = 16-18; KO n = 18-21), FBG (Panel **B**; WT n = 17-24; KO n = 17-20), FPI (Panel **C**; WT n = 19-24; KO n = 17-20) and plasma glucagon (Panel **D**; WT n = 14; KO n = 20) were compared in 6 hour and/or 24 hour fasted 16 week old male WT and KO mice. Results represent the mean data ± S.E.M. Statistical significance was analyzed using ANOVA (Panels **A-C**) or t-tests (Panel **D**). *$p < 0.05$ WT vs KO; #$p < 0.05$ 6 hour fasted WT vs 24 hour fasted WT; ^$p < 0.05$ 6 hour fasted KO vs 24 hour fasted KO.

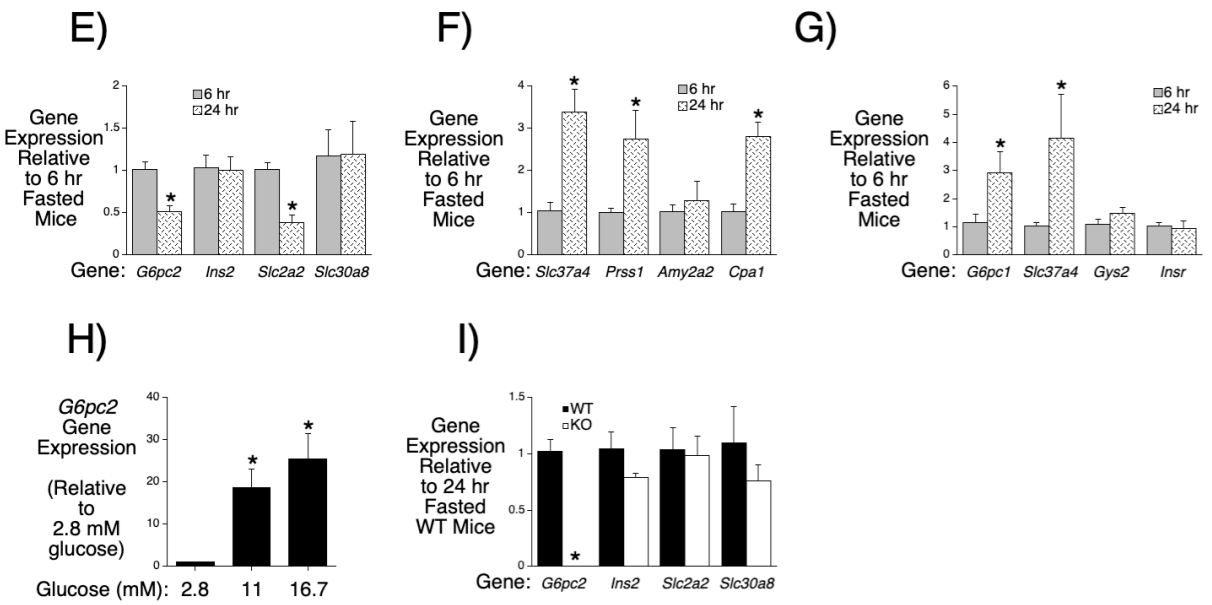

Figure 4.3. Analysis of Metabolic Parameters and Gene Expression in Male WT and *G6pc2* KO Mice After Prolonged Fasting.

Comparison of pancreatic expression of genes known to be highly expressed in islets (Panel **E**; 6 hour n = 5; 24 hour n = 5) or acinar cells (Panel **F**; 6 hour n = 5; 24 hour n = 4) or liver (Panel **G**; 6 hour n = 8; 24 hour n = 5) in 6 hour or 24 hour fasted 16 week old male WT mice. Data were corrected relative to *Ppia* (cyclophilin A) expression. Results represent the mean data ± S.E.M. *$p < 0.05$ 6 hour fasted WT vs 24 hour fasted WT. Effect of glucose on *G6pc2* expression in islets isolated from adult male mice (n=7-8) (Panel **H**). Results represent the mean data ± S.E.M. *$p < 0.05$ vs 2.8 mM glucose. Comparison of pancreatic expression of genes known to be highly expressed in islets (Panel **I**; WT n = 5; KO n = 5) in 24 hour fasted 16 week old WT and KO mice. Data were corrected relative to *Ppia* (cyclophilin A) expression. Results represent the mean data ± S.E.M. Statistical significance was analyzed using ANOVA (Panel **H**) or t-tests (Panels **E-G, I**). *$p < 0.05$ WT vs KO.

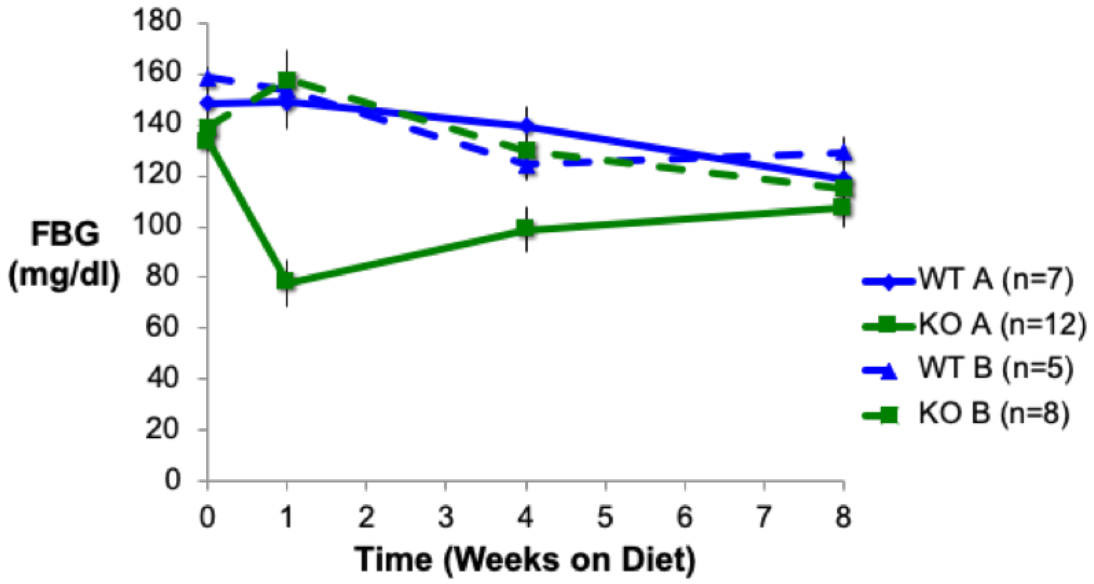

Figure 4.4. Comparison of FBG in Two Cohorts of Male WT and *G6pc2* KO Mice Fasted and Housed on Corn Cob Bedding.
FBG was compared in two separate cohorts (A = Cohort A, solid lines; B = Cohort B, dashed lines) of 6 hour fasted WT and KO mice that were switched from a chow diet to a ketogenic diet at 8 weeks of age. Results represent the mean data ± S.E.M.

increases in the expression of several pancreatic acinar (Figure 4.3F) and hepatic (Figure 4.3G) genes. The mechanisms mediating the induction of hepatic *G6pc1* gene expression by fasting have been studied in detail [120]. Insulin represses *G6pc1* expression whereas glucose stimulates expression [120]. The observation that hepatic *G6pc1* expression increases with fasting (Figure 4.3G) suggests that the effect of reduced repression by insulin (Figure 4.3C) is dominant over the effect of reduced stimulation by glucose (Figure 4.3B). The fall in pancreatic *G6pc2* gene expression is consistent with the observation that glucose stimulates expression of this gene in isolated islets (Figure 4.3H). Prolonged fasting was not associated with compensatory changes in the expression of various pancreatic genes known to be selectively expressed in islets in *G6pc2* KO mice (Figure 4.3I).

G6PC2 Limits Hyperglycemia Upon High Fat Diet Feeding

While prolonged fasting and ketogenic diets may have been common over the course of evolution, in the modern world high fat diets are more prevalent. We therefore investigated the response of WT and *G6pc2* KO mice to high fat diet feeding.

Switching mice from a chow diet to a high fat diet resulted in weight gain in both WT and *G6pc2* KO mice (Figure 4.5A) and, in contrast to ketogenic diet feeding (Figure 4.1A), no difference in body weight emerged between WT and *G6pc2* KO mice. FBG rose in both WT and KO mice after 28 days of high fat diet feeding (Figure 4.5B). After 84 days on the diet FPI was markedly elevated in both WT and *G6pc2* KO mice (Figure 4.5C), consistent with the presence of insulin resistance, but the difference in FBG between WT and *G6pc2* KO mice remained (Figure 4.5B). Plasma cholesterol was elevated in both WT and KO mice after 84 days on the diet with a greater elevation seen in WT mice (Figure 4.5D), as previously reported [177]. These data suggest

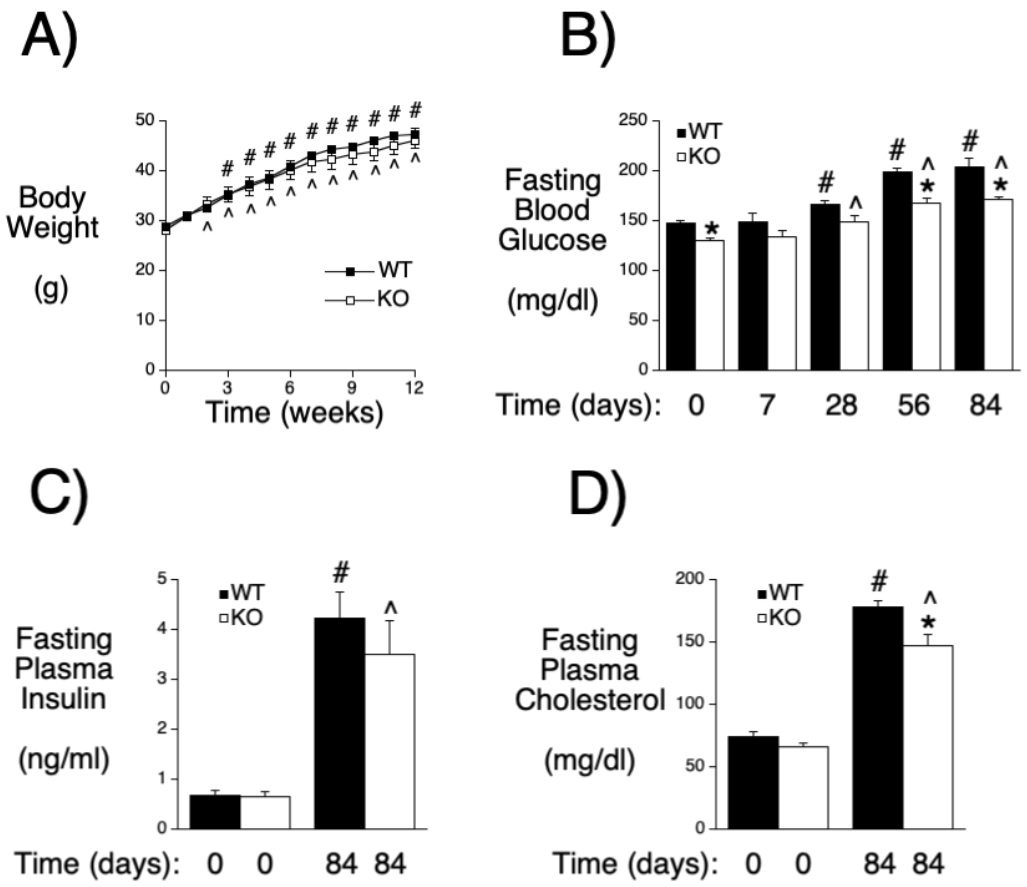

Figure 4.5. Analysis of Metabolic Parameters and Gene Expression in Male WT and *G6pc2* KO Mice on a High Fat Diet.

Body weight (Panel **A**; WT n = 15; KO n = 12), FBG (Panel **B**; WT n = 15-29; KO n = 15-30), FPI (Panel **C**; WT n = 10; KO n = 10) and plasma cholesterol (Panel **D**; WT n = 6-10; KO n = 6-10) were compared in non-fasted (Panel **A**) or 6 hour fasted (Panels **C-D**) mice WT and KO mice that were switched from a chow diet to a high fat (HF) diet at 33 weeks of age. Results represent the mean data ± S.E.M. Statistical significance was analyzed using ANOVA. *$p < 0.05$ WT vs KO; #$p < 0.05$ WT at day 0 vs WT after high fat diet feeding; ^$p < 0.05$ KO at day 0 vs KO after high fat diet feeding.

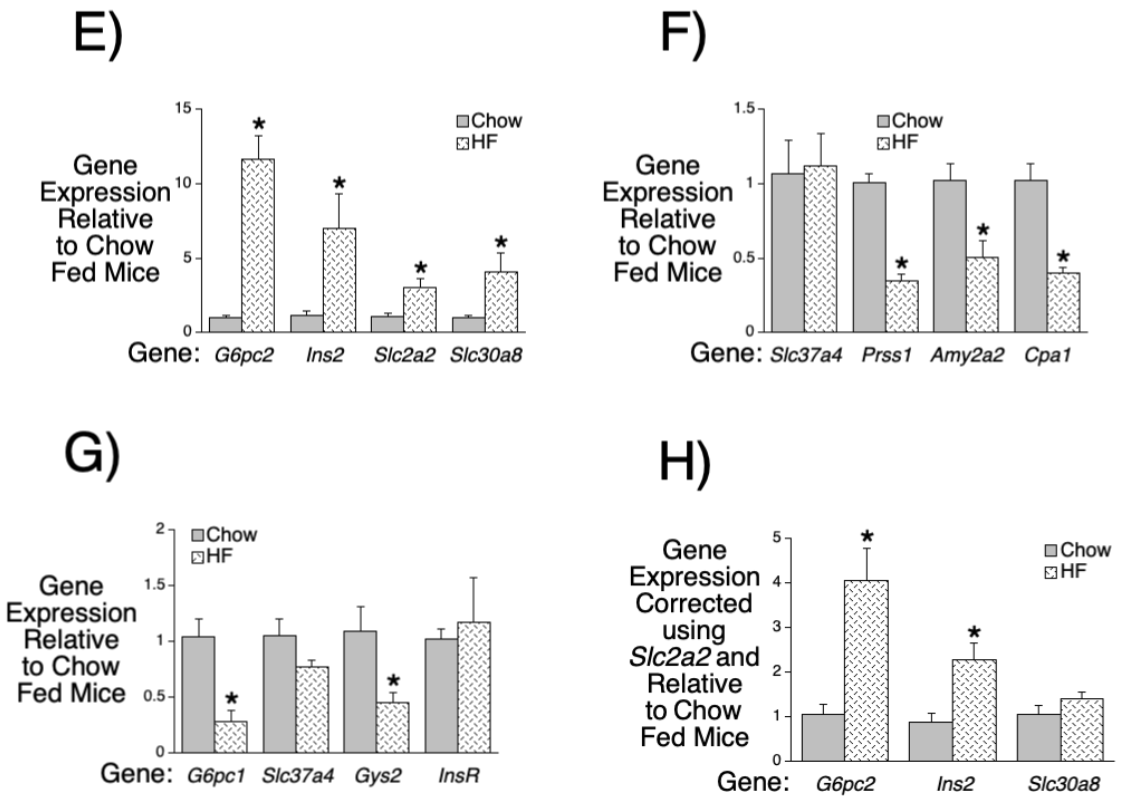

Figure 4.5. Analysis of Metabolic Parameters and Gene Expression in Male WT and *G6pc2* KO Mice on a High Fat Diet.

Comparison of pancreatic expression of genes known to be highly expressed in islets (Panels **E** and **H**; chow n = 5; HF n = 7) or acinar cells (Panel **F**; chow n = 5; HF n = 5) or liver (Panel **G**; chow n = 6; HF n = 5) in 6 hour fasted 33 week old chow fed WT mice versus 6 hour fasted 45 week old WT mice that were switched to a high fat diet at 33 weeks of age. Data were either corrected relative to *Ppia* (cyclophilin A) (Panels **E-G**) or *Slc2a2* (Panel **H**) expression. Results represent the mean data ± S.E.M. Statistical significance was analyzed using t-tests. *$p < 0.05$ chow vs high fat fed (HFF).

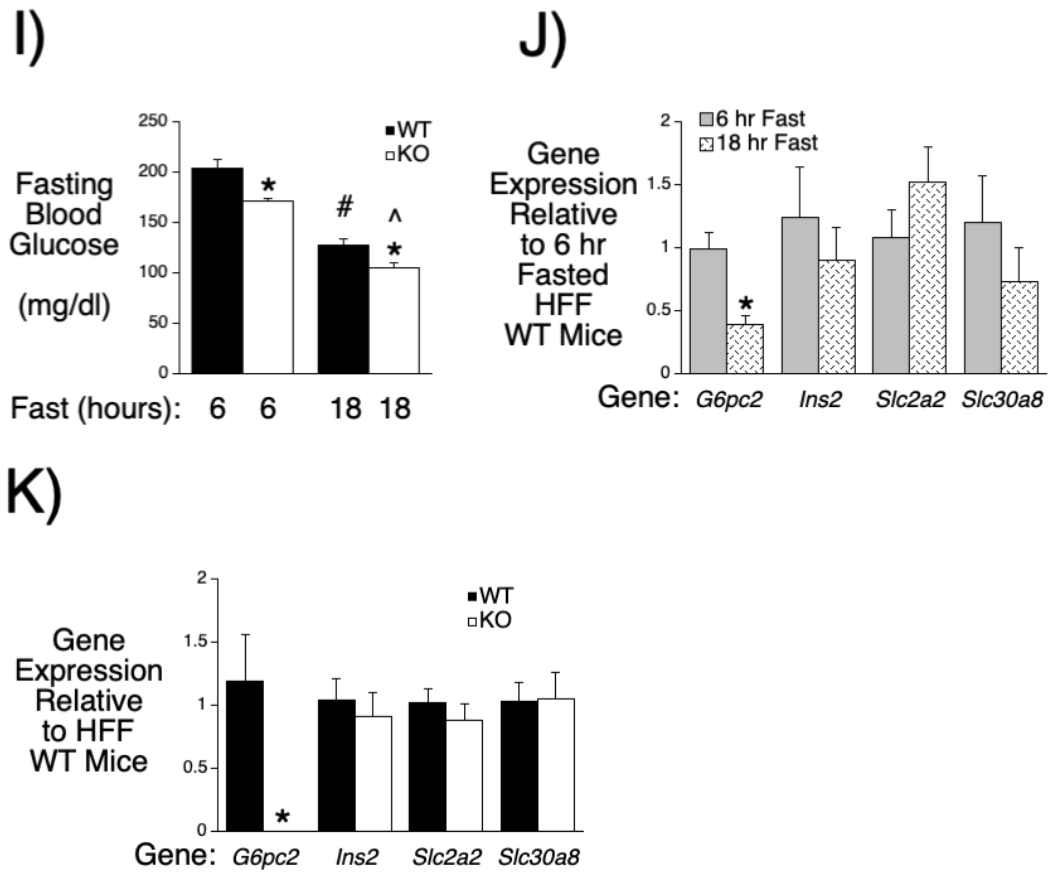

Figure 4.5. Analysis of Metabolic Parameters and Gene Expression in Male WT and *G6pc2* KO Mice on a High Fat Diet.

FBG (Panel **I**) after a 6 hour (WT n = 20; KO n = 25) or 18 hour (WT n = 14; KO n = 19) fast in 45 week old male WT and KO mice that were placed on a high fat diet at 33 weeks of age. Comparison of pancreatic expression of genes known to be highly expressed in islets in 45 week old 6 hour fasted male WT mice that were placed on a high fat diet at 33 weeks of age (n = 7) versus 24 week old 18 hour fasted male WT mice that were placed on a high fat diet at 24 weeks of age (n = 5) (Panel **J**). Comparison of pancreatic expression of genes known to be highly expressed in islets (Panel **K**; WT n = 5; KO n = 5) in 6 hour fasted 45 week old WT and KO mice that were switched to a high fat diet at 33 weeks of age. Results represent the mean data ± S.E.M. *$p < 0.05$ WT vs KO. Statistical significance was analyzed using ANOVA (Panel **I**) or t-tests (Panels **J-K**).

that inhibition of G6PC2 would limit but not prevent the hyperglycemia associated with high fat diet feeding.

The switch from a chow diet to a high fat diet was associated with marked changes in pancreatic expression of genes known to be highly expressed in islets (Figure 4.5E) as well as pancreatic acinar (Figure 4.5F) and hepatic (Figure 4.5G) gene expression. The induction of *G6pc2*, *Ins2*, *Slc2a2* and *Slc30a8* gene expression are highly likely to be due in part to the well characterized effects of high fat diet feeding on pancreatic islet mass [91]. However, using *Slc2a2* rather than the ubiquitously expressed *Ppia* to correct for expression suggests a more marked induction of *G6pc2* expression beyond that associated with increased islet mass (Figure 4.5H), which would again be consistent with a stimulatory action of hyperglycemia (Figure 4.3H). Indeed, fasting previously high fat fed mice for 18 hours rather than 6 hour results in reduced FBG (Figure 4.5I) and a marked decrease in *G6pc2* expression with little change in *Ins2*, *Slc2a2* and *Slc30a8* expression (Figure 4.5J). These data suggest that *G6pc2* expression is particularly sensitive to changes in glucose concentrations. High fat diet feeding was not associated with compensatory changes in the expression of various pancreatic genes known to be selectively expressed in islets in *G6pc2* KO mice (Figure 4.5K).

Discussion

The experiments described here suggest that G6PC2 may have evolved to not only confer a beneficial elevation in FBG in response to stress [174, 175] but also to prevent hypoglycemia in response to ketogenic diet feeding (Figure 4.1) or prolonged fasting (Figure 4.3). In contrast, in response to high fat diet feeding, as is common in the modern world, the absence of G6PC2 is beneficial by limiting hyperglycemia (Figure 4.5).

Elevated FBG and HbA1c levels in humans have been associated with increased risk for the development of CAM [157, 158, 215] and T2D [222, 223]. This correlation with CAM is observed in both women and men [158] and even at glucose concentrations in the non-diabetic range, though the risk of CAM increases still further in individuals with the high FBG levels characteristic of diabetes [157, 158, 215, 216]. Even small differences in FBG have a profound effect over time. For example, in Europeans an increase in FBG levels from less than 90 mg/dl to between 99-108 mg/dl is associated with 30% increased risk of CAM [157]. In Asians a reduction in FBG of approximately 9 mg/dl is associated with a 25% reduction in the risk of CAM [158]. Similarly, Gerstein et al. [159] have shown that individuals with FBG between 100-125 mg/dl are 5 times more likely to develop T2D that individuals whose FBG is <100 mg/dl. Elevations in FBG in the prediabetic state correlate with [210] and appear sufficient to drive [211, 212] the decline in beta cell function that underlies the progression from prediabetes to T2D. As such, a therapy designed to inhibit G6PC2 and thereby lower FBG could have a major impact by preventing this progression. Since deletion of *G6pc2* is associated with a ~20 mg/dl reduction in FBG [1, 147, 174] the magnitude of this effect, relative to the human data described above, suggests that inhibition of G6PC2 should already be considered as a novel therapeutic strategy for lowering FBG and hence preventing both CAM and T2D. However, the potential risk of hypoglycemia under specific conditions (Figures 4.1 and 4.3) suggests that achieving partial inhibition may be the optimal approach.

We hypothesized that *G6pc2* would be induced by fasting and ketogenic diet feeding to protect against hypoglycemia, however, *G6pc2* expression was surprisingly reduced in response to fasting (Figure 4.3) and little changed in response to ketogenic diet feeding (Figure 4.2). In contrast, *G6pc2* expression was markedly induced in response to high fat diet feeding (Figure 4.5).

Since glucose stimulates *G6pc2* expression in isolated islets (Figure 4.3) this could explain why *G6pc2* expression is elevated in response to the hyperglycemia associated with high fat diet feeding (Figure 4.5) and reduced in response to the hypoglycemia associated with fasting (Figure 4.3). However, other factors must be involved since *G6pc2* expression did not fall in response to the hypoglycemia associated with ketogenic diet feeding (Figure 4.2). Future experiments will explore whether this regulation by glucose occurs at a transcriptional or post-transcriptional level.

It is not clear why the marked induction of *G6pc2* in mice on a high fat diet (Figure 4.5E) has little effect on the difference in FBG between WT and KO mice (Figure 4.5B). One possibility is that the beneficial glucose-lowering effect of *G6pc2* deletion is countered by insulin resistance in peripheral tissues caused by the high-fat diet. Pound et al demonstrated that deletion of *G6pc2* improved the sensitivity of GSIS at submaximal glucose concentrations, but not at maximal glucose concentrations [1]. Therefore, when under conditions of insulin resistance when glucose levels are increased and the dose-response curve for GSIS is at a maximal point, there may not be an increased difference in FBG between WT and *G6pc2* KO mice (Figure 1.5). Interestingly, our LabWAS data suggest that the influence of *G6PC2* on FBG is lost under diabetic conditions (Table 3.2), suggesting that alterations in beta cell function or peripheral insulin action, both of which are affected in T2D, can modulate the effect of G6PC2 on FBG. Therefore, a second possible explanation for the lack of enhanced FBG in the high fat fed mice despite the induction of *G6pc2* expression, is that G6PC2 function is impaired.

CHAPTER 5

Analysis of *G6PC2* SNPs that Potentially Affect Enzyme Activity and/or Protein Expression

Introduction

Elevated FBG is associated with an increased risk of developing T2D and CAM. Previous studies have found that an increase in FBG of 9-18 mg/dL is associated with a 30% increased risk of CAM, whereas a decrease in FBG of 9 mg/dL is associated with a 25% reduction in the risk of CAM [157, 158]. Patients with an FBG between 100-125 mg/dL were five times more likely to develop T2D than patients with an FBG below 100 mg/dL [159]. As mentioned previously, multiple groups have performed GWAS to identify genes associated with variations in FBG. The rs560887 SNP in the third intron of the *G6PC2* locus was identified as the strongest common genetic determinant of FBG levels, and accounts for ~1% of the total variance in FBG [168, 169, 172].

While the rs560887 *G6PC2* SNP was associated by multiple GWA studies with variations in FBG, multiple groups have worked to determine if this SNP and others in the *G6PC2* locus are causative. This is important for several reasons. First, GWAS typically identify common SNPs that only have a modest effect on disease manifestation. It is likely that a disease or phenotype is manifested by the presence of either rare, high-impact variants, or multiple common low-impact variants; additionally, the effect of either of these categories of SNPs may only be manifest through an interaction between those SNPs and environmental factors or other genetic loci [224]. Secondly, SNPs identified by GWAS are frequently present in non-coding regions and are assumed to be associated with the gene closest in proximity. This assumption has two caveats. First, the SNP may

be causative, but it may be altering the activity of a long-range enhancer, thus affecting the expression of a distal gene rather than the proximal one. Second, the SNP may not be causative but instead it may exist in linkage disequilibrium with the true causative SNP. It is therefore crucial to design and perform functional studies that establish that a SNP is truly causative and identify the gene affected by the SNP.

Studies have been performed that sought to characterize four common *G6PC2* SNPs: rs560887, rs13431652, rs2232316, and rs573225. The goal of these studies was to determine the mechanism by which each SNP contributes to the association signal with FBG. Minigene analyses demonstrated that the rs560887 SNP is located at a splicing branch site 26 nucleotides upstream of exon 4, and affects G6PC2 protein expression by altering splicing efficiency [171]. The G allele enhances splicing and the inclusion of exon 4, while the A allele reduces inclusion of exon 4, thus decreasing the production of full-length functional G6PC2. This is consistent with the genetic association between the G allele, elevated FBG, and the function of G6PC2, which supports rs560887 as the causative SNP [171]. Each A allele of this SNP is associated with an approximate 1mg/dL reduction in FBG [168], meaning that homozygosity for the A allele results in a 2 mg/dL difference in FBG relative to homozygosity for the G allele.

The other three SNPS, rs13431652, rs2232316, and rs573225, are known to be in high linkage disequilibrium with rs560887, and are all associated with FBG as part of the same signal [171, 225]. However, it was still important to characterize the effect of these SNPs on *G6PC2* expression. All three SNPs are located in the *G6PC2* promoter, and studies were done in cell lines to determine the effect of these SNPs on transcription factor binding and promoter activity. The minor alleles of rs13431652 and rs2232316 enhance the binding of the transcription factors NF-Y and FOXA2, respectively, to the *G6PC2* promoter, increasing *G6PC2* promoter activity and gene

expression, which may explain the association of the minor alleles with elevated FBG [225]. The rs573225 A allele slightly increases the affinity of Foxa2 binding, but surprisingly was associated with decreased *G6PC2* promoter activity, which was the opposite of what was predicted given the association between this allele and elevated FBG [225]. There are two possible explanations for this discrepancy between the GWAS data and the functional data. First, the functional data were obtained in tissue culture cells derived from rodents, which may not be representative of human biology or physiology. Second, if the functional studies in fact reflect gene transcription regulation *in vivo*, it would imply that this SNP opposes the action of those other SNPs with which it is in high linkage disequilibrium and that the association signal is driven by the other SNPs.

While GWAS have been highly successful in identifying common variants associated with complex diseases and human traits, in most cases they have only identified a small fraction of the heritability for these traits. A variety of explanations for this missing heritability have been proposed and debated, including unidentified common variants with very small effects, gene-gene interactions, or inadequate accounting for the effect of environment [224, 226]. Another possibility is that there are low-frequency (MAF <5%) or rare variants (MAF <0.5%) with a large effect; these variants would be undetected in large GWAS due to their low frequency and absence from genotyping arrays [224, 226]. The identification of such high impact rare variants has previously provided insight into beta cell biology. For example, rare inactivating variants in *GCK* cause neonatal diabetes or MODY, and rare activating variants cause persistent hyperinsulinemic hypoglycemia of infancy (PHHI) [164]. Also, total deletion of *GCK* is lethal in mice [227]. However, the common SNP rs1799884 in the *GCK* locus has a relatively modest effect on FBG of only 1mg/dL whether heterozygous or homozygous for the minor allele [166]. The common SNP rs560887 in *G6PC2* has a larger, though still modest, effect on FBG of 2 mg/dL when homozygous

for the minor allele [168], but deletion of *G6pc2* in mice leads to a mild metabolic phenotype with a decrease in FBG of nearly 20 mg/dL [1]. These data illustrate an important caveat in the interpretation of GWAS data, in that the effect size of common variants does not necessarily reflect the importance of the gene in the phenotype or disease being studied. However, the difference in the effect size between the common *G6PC2* SNP rs560887 and deletion of *G6pc2* also suggest that a rare variant that inhibits G6PC2 activity would have a larger impact on FBG in humans.

Studies have begun to examine the functional consequences of low-frequency or rare variants (minor allele frequency (MAF) <5%) in *G6PC2* in the hopes of identifying other causal variants for FBG and elucidating the mechanisms by which these variants influence FBG. One group identified three *G6PC2* coding variants (His177Tyr, Tyr207Ser, and Val219Leu) that were potential causal variants for the association between *G6PC2* and FBG [228]. The minor alleles of these variants were associated with reduced FBG levels independent of the rs560887 SNP. Transient transfections of FLAG-tagged *G6PC2* constructs showed that each variant reduced G6PC2 expression as assessed by Western blot, indicating that these SNPs exert their effects on FBG by reducing G6PC2 protein levels [228].

A previous study from the O'Brien lab also examined the effect of G6PC2 variants on protein expression and activity [2]. These studies also analyzed non-synonymous *G6PC2* SNPs that altered amino acids that are conserved in mouse and human G6PC1 and mouse G6PC2, and assessed the effects of these variants on mouse G6PC1 expression and activity [2]. Six variants, Ser30Phe, Asn68Ile, Arg79Gln, Gly114Arg, Phe256Leu, and Ser324Pro, were found to reduce mouse G6PC1 activity in a luciferase reporter assay without reducing protein expression, and three other variants (Gly8Glu, Arg293Trp, and Pro340Leu) reduced protein expression [2]. However,

this study was unable to examine the direct effect of these variants on human G6PC2 activity, due to the low V_{max} of G6PC2 and low protein expression from the transfected expression vectors.

A recent study extended these analyses to include seven other coding variants [229]. Seven of the ten variants were found to reduce G6PC2 protein expression in transient transfections of 832/13 cells, and three of those (His177Tyr, Tyr207Ser, and Ser324Pro) were further found to increase ER stress as assessed using reporter assays, indicating that these variants might also have an impact on ER homeostasis in beta cells. These results were entirely consistent with the genetic studies that associated these variants with decreased FBG [229].

We obtained a new plasmid vector from the Jacobson lab that gives very high levels of G6PC2 expression. This chapter describes our efforts to use this vector to continue the assessment of the impact of rare variants in *G6PC2* on protein expression and enzyme activity.

Results

Analysis of G6PC2 Expression from the pJPA5 Plasmid

Previous work assessing the impact of non-synonymous coding G6PC2 variants on G6PC2 enzyme activity has been hindered by low protein expression of human G6PC2 driven by the pcDNA3 plasmid vector. Analysis of G6PC2 expression was successfully assessed in COS cells, but the caveat to assessing G6PC2 expression in a non-islet-derived cell line is that there may be factors that affect G6PC2 stability or activity that are present in islet cells, but which may be absent in other cell types.

To address this concern, we sought to generate a vector that would give greater G6PC2 expression and allow us to examine the effects of G6PC2 SNPs on human G6PC2 protein

expression and enzyme activity in 832/13 cells. We chose to modify an existing vector, pJPA5, which was known to give high levels of protein expression [230]. G6PC2 cDNA coding sequences with additional sequence encoding a C-terminal V5-His tag were sub-cloned from the original pcDNA3 plasmid into the pJPA5 plasmid. We then compared the expression of various G6PC2 variants conferred by the following plasmids to determine the relative expression of each: mouse WT G6PC2 in pcDNA3, human WT G6PC2 in pcDNA3, human WT G6PC2 in pJPA5, and a catalytically dead mutant of human G6PC2 in pJPA5 (Figure 5.1). In the catalytically-dead variant, amino acid (AA) 174, which is analogous to the amino acid identified as the phosphate acceptor in G6PC1 [231], is changed from a histidine to an alanine, abolishing phosphatase activity. Expression of both WT human G6PC2 and catalytically-dead human G6PC2 was significantly higher when driven using the pJPA5 vector than human G6PC2 or mouse G6PC2 driven using the pcDNA3 vector (Figure 5.1).

Since we were able to achieve high expression of human G6PC2 using the new pJPA5 vector, we then sought to examine the effects of various SNPs on G6PC2 expression in 832/13 cells. Previous work from our lab examined the effects of 23 non-synonymous coding variants directly on human G6PC2 expression in COS cells and indirectly on mouse G6PC1 enzyme activity in 832/13 cells [2]. Of those twenty-three SNPs, nine of them (Gln16His, Val53Ile, Asn68Ile, Tyr124Cys, Ser203Arg, Phe215Ser, Tyr222His, His250Tyr, and Leu301Ser) resulted in a less than 25% change in mouse G6PC1 activity in an *in situ* assay, and were not reanalyzed in the context of the pJPA5 vector. The remaining fourteen SNPs were re-analyzed using the pJPA5 vector. We also analyzed an additional six non-synonymous coding SNPs, identified in various databases since our previous study, that affect amino acids 59, 64, 73, 148, 174, and 186. All of these SNPs affect amino acids that are conserved in mouse G6PC1, mouse G6PC2, human G6PC1,

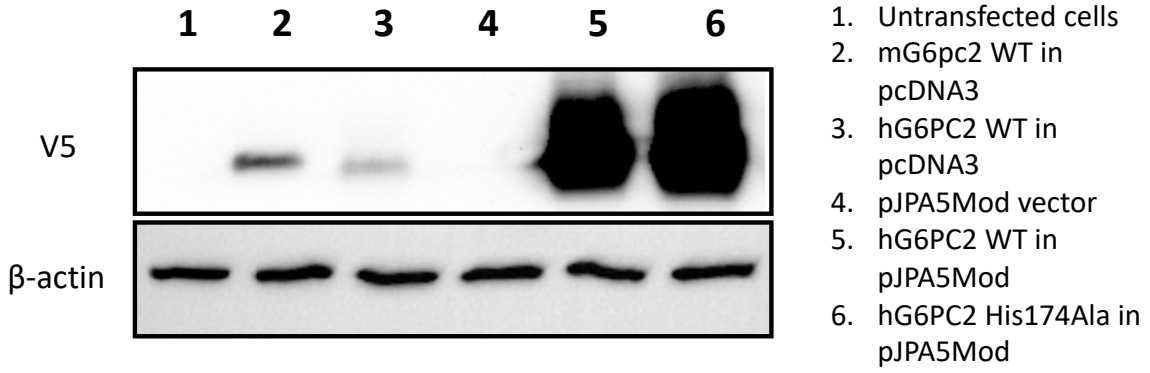

Figure 5.1. Analysis of Human G6PC2 Protein Expression Driven Using pJPA5. 832/13 cells were transiently transfected with either empty pJPA5 vector (lane 4) or one of the following expression vectors: mouse (m) G6pc2 in pcDNA3 (lane 2), human (h) WT G6PC2 in pcDNA3 (lane 3), human WT G6PC2 in pJPA5 (lane 5), or human catalytically-dead G6PC2 (His174Ala) in pJPA5 (lane 6). Following transfection, cells were incubated for 18-20 hours in serum-containing media. Cells were subsequently harvested and protein expression assayed by Western blot as described in Materials and Methods.

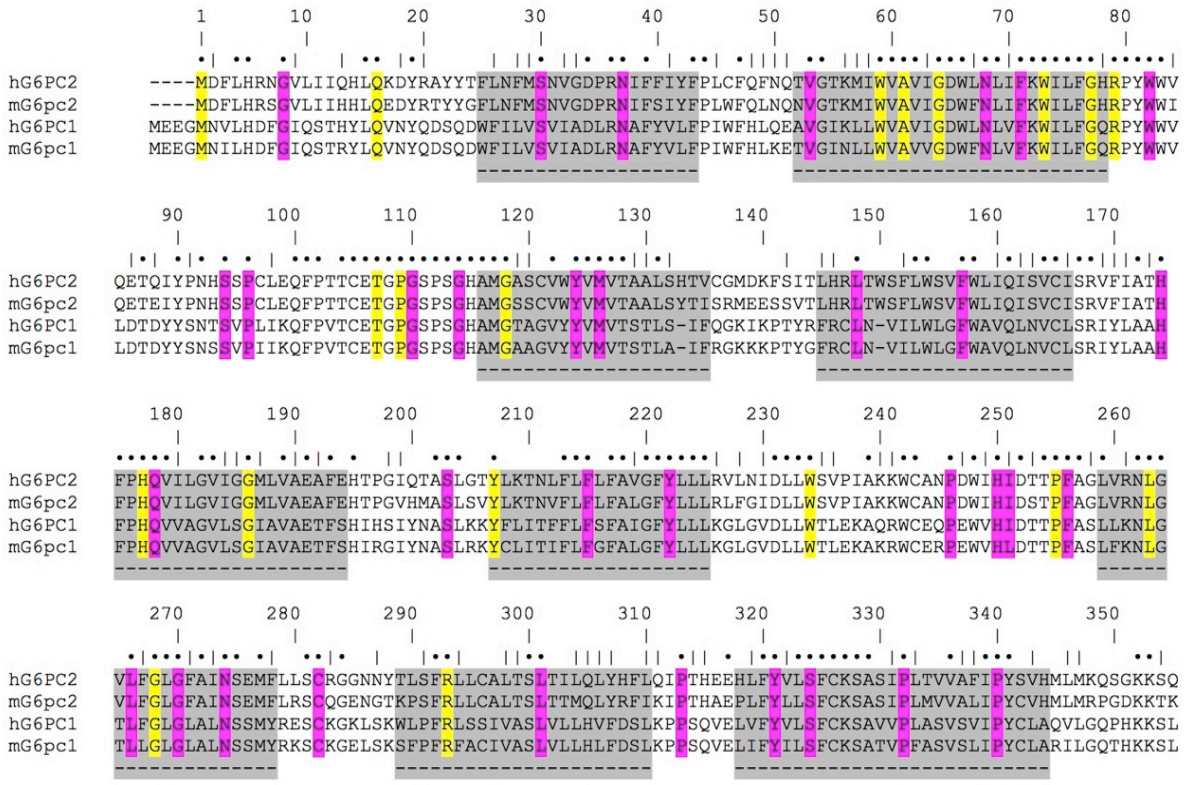

Figure 5.2. Conservation of Amino Acids between Human and Mouse G6PC2 and Human and Mouse G6PC1. Sequence alignment showing the conservation of amino acids between human G6PC2 (hG6PC2), mouse G6PC2 (mG6pc2), human G6PC1 (hG6PC1), and mouse G6PC1 (mG6PC1). Residues highlighted in pink represented amino acids conserved between the four isoforms that are changed by human G6PC2 SNPs identified through database searches. Residues highlighted in yellow represent amino acids conserved between the four isoforms that are changed by human G6PC2 SNPs and where a mutation in human G6PC1 is known to cause GSD1a. Gray boxes represent putative transmembrane domains. Adapted from [2]

and human G6PC2. We hypothesized that this conservation of amino acids meant these were likely to be functionally important (Figure 5.2, in pink). In addition, as mentioned previously, mutations in G6PC1 have been found to cause glycogen storage disease type 1a (GSD1a). Therefore, we were particularly interested in a subset of nine of these twenty SNPs that affect conserved amino acids where a mutation in human G6PC1 has been shown to cause GSD1a, again indicating they are functionally important (Figure 5.2, in yellow). It should be noted that for these variants, the amino acid that is changed in human G6PC2 is the one associated with the *G6PC2* SNP, and does not necessarily match the amino acid change associated with GSD1a (Table 5.1).

We used the SIFT algorithm to predict the effects of the amino acid changes on human G6PC2 function [232]. This algorithm assesses the conservation of the protein sequence using homologous sequences and the severity of the amino acid change, and uses these data to predict if the change is likely to have little effect on protein function ("tolerated"), or if the change is likely to be deleterious ("damaging"). The SIFT algorithm does not specifically predict whether the deleterious impact of a specific mutation will be on protein function or expression, but follow-up studies have shown it can predict the deleterious effects of amino acid changes on protein function with approximately 80% accuracy [232]. The SIFT predictions for all twenty variants can be found in Table 5.1 and Table 5.2.

We first assessed the impact of the nine human *G6PC2* SNPs, that affect amino acids that are associated with GSD1a in the context of human G6PC1, on G6PC2 protein expression in 832/13 cells using Western blotting. All nine amino acid changes shown in Table 5.1 were associated with significantly reduced protein expression when compared to WT (Figures 5.3 and 5.5). This is consistent with predictions from the SIFT algorithm that indicated that these amino acid changes would be damaging to the protein (Table 5.1). Next, we examined the impact of the

hG6PC2 SNP	AA#	Mutation in Human G6PC1 causing GSD1a	Domain Location	Protein Expression (%WT)	SIFT Prediction
rs369755574	Trp59Arg	Arg	TM 2	35.7±9.6*	Damaging
rs762205787	Gly64Arg	Arg	TM 2	25.0±12.3*	Damaging
rs756028690	Trp73Arg	Arg	TM 2	19.6±8.5*	Damaging
rs144254880	Arg79Gln	His or Cys	Loop	26.6±4.9*	Damaging
rs371234742	Thr107Arg	Ile	Loop	19.1±3.2*	Damaging
rs138726309	His177Tyr	Pro	TM 5	36.2±16.5*	Damaging
rs764817338	Gly186Asp	Asp or Arg or Ser	TM 5	9.1±2.7*	Damaging
rs2232323	Tyr207Ser	Cys	TM 6	22.4±9.7*	Damaging
rs374055555	Arg293Trp	Cys	TM 8	18.3±3.8*	Damaging

Table 5.1: Human *G6PC2* SNPs That Affect Conserved Amino Acids Associated with GSD1a in the Context of Human G6PC1. Human G6PC2 SNPs were identified that affect amino acids conserved between mouse and human G6PC1 and mouse and human G6PC2 where a mutation is known to cause GSD1a in the context of human G6PC1. The amino acid change associated with GSD1a is shown in parentheses. Domain locations were predicted by comparison with the putative structure of G6PC1 [9]; TM = transmembrane domain. SIFT predictions were obtained by entering SNP rs numbers into the SIFT algorithm (https://sift.bii.a-star.edu.sg). Protein expression was assessed by Western blot, quantified by densitometric analysis, and then expressed as a percentage of WT expression. Results show mean ± SEM. n=4 *$p<0.05$

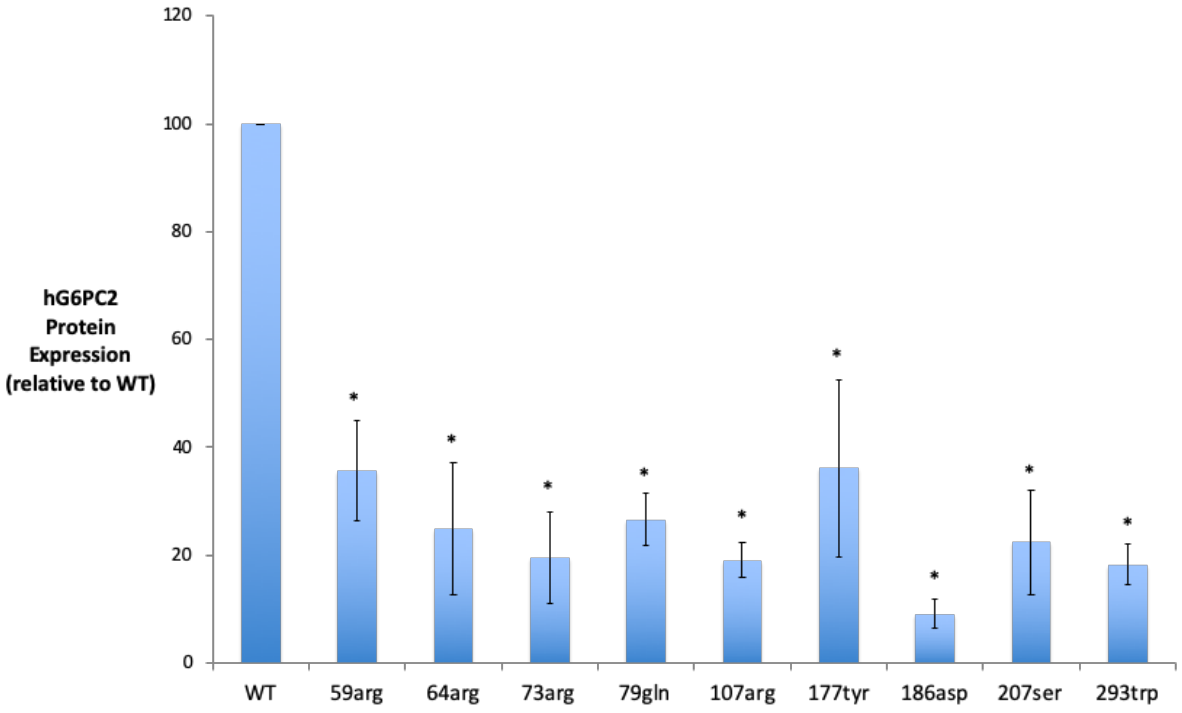

Figure 5.3: Analysis of the Effect on G6PC2 Protein Expression of Human *G6PC2* SNPs That Affect Conserved Amino Acids Associated with GSD1a in the Context of Human G6PC1. 832/13 cells were transiently transfected (as described in Materials and Methods) with expression vectors encoding either human WT G6PC2 or G6PC2 variants where the indicated amino acid was changed (see Table 5.1). Cells were then harvested and protein expression was assessed by Western blot, quantified by densitometric analysis, and expressed as a percentage of WT expression. Results show mean ± SEM. n=4 *$p<0.05$

hG6PC2 SNP	AA#	Domain Location	Protein Expression (%WT)	SIFT Prediction
rs368382511	Gly8Glu	NH2 terminus	182.9±56.9*	Tolerated
rs142189264	Ser30Phe	TM 1	32.9±13.5*	Damaging
rs149663725	Gly114Arg	Loop	99.3±17.9	Damaging
rs367930047	Met126Val	TM 3	85.7±18.3	Damaging
rs761866606	Leu148Pro	TM 4	30.5±12.0*	Tolerated
rs746984825	His174Tyr	Loop	29.0±13.2*	Damaging
rs492594	Leu219Val	TM 6	236.4±77.3*	Tolerated
rs150538801	Phe256Leu	Loop	132.9±27.5	Damaging
rs137857125	Pro313Leu	Loop	34.3±12.1*	Damaging
rs2232326	Ser324Pro	TM 9	40.0±14.5*	Damaging
rs2232327	Pro340Leu	TM 9	33.5±9.6*	Damaging

Table 5.2: Human *G6PC2* SNPs That Do Not Affect Conserved Amino Acids Associated with GSD1a in the Context of Human G6PC1. Human G6PC2 SNPs were identified that affect amino acids conserved between mouse and human G6PC1 and mouse and human G6PC2. Domain locations were predicted by comparison with the putative structure of G6PC1 [9]. TM = transmembrane domain. SIFT predictions were obtained by entering SNP rs numbers into the SIFT algorithm (https://sift.bii.a-star.edu.sg). Protein expression was assessed by Western blot, quantified by densitometric analysis, and expressed as a percentage of WT expression. Results show mean ± SEM. n=4 *$p<0.05$

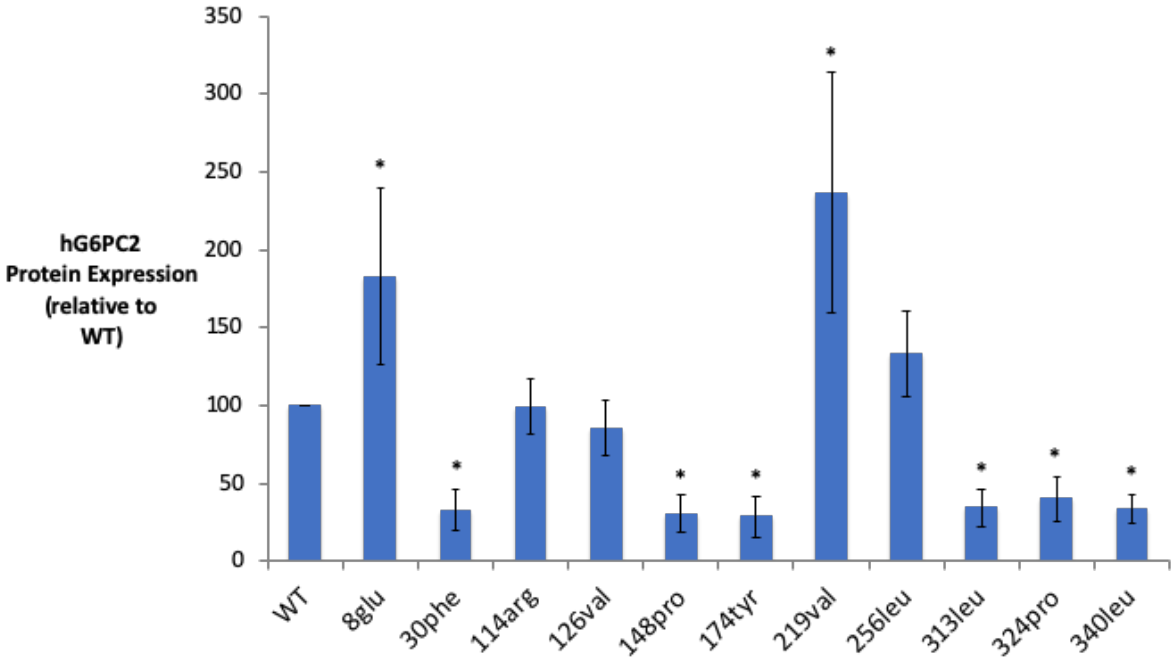

Figure 5.4: Analysis of the Effect on G6PC2 Protein Expression of Human *G6PC2* SNPs That Do Not Affect Conserved Amino Acids Associated with GSD1a in the Context of Human G6PC1. 832/13 cells were transiently transfected (as described in Materials and Methods) with expression vectors encoding either human WT G6PC2 or G6PC2 variants where the indicated amino acid was changed (see Table 5.2). Cells were then harvested and protein expression was assessed by Western blot, quantified by densitometric analysis, and expressed as a percentage of WT expression. Results show mean ± SEM. n=4 *p<0.05

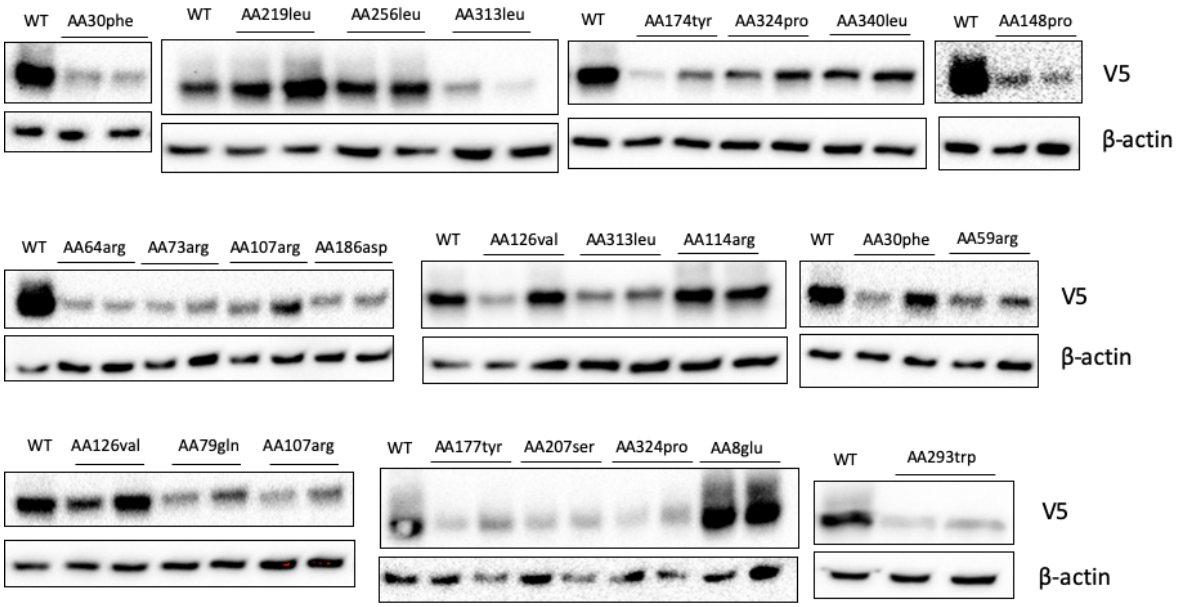

Figure 5.5. Western Blot Analysis of the Effect of Human G6PC2 Variants on Protein Expression. 832/13 cells were transiently transfected (as described in Materials and Methods) with expression vectors encoding either human WT G6PC2 or G6PC2 variants where the indicated amino acid was changed (see Tables 5.1 and 5.2). Cells were then harvested and protein expression was assessed by Western blot, as described in Materials and Methods. Representative blots are shown.

remaining eleven human *G6PC2* SNPs, that affect amino acids that are not associated with mutations in human G6PC1 that cause GSD1a, on human G6PC2 protein expression in 832/13 cells. For the amino acid changes of the variants shown in Table 5.2, we saw no significant change in expression for three variants (Gly114Arg, Met126Val, and Phe256Leu). Protein expression was significantly decreased by six variants (Ser30Phe, Leu148Pro, His174Tyr, Pro313Leu, Ser324Pro, and Pro340Leu), and two variants significantly increased expression (Gly8Glu and Leu219Val) (Figures 5.4 and 5.5).

Analysis of the Effect of *G6PC2* SNPs on ER Stress

Given the high levels of human G6PC2 expression from the pJPA5 vector, we sought to determine if this increased expression also increased ER stress in transfected 832/13 cells. To test this, a plasmid encoding a fusion gene sensitive to ER stress [194] was co-transfected with the empty pJPA5 vector or pJPA5 plasmids encoding either WT or dead (His174Ala) human G6PC2. This fusion gene plasmid contains five repeats of a consensus ATF6 binding site upstream of a minimal promoter ligated to the luciferase reporter gene [194]. Neither WT nor dead G6PC2 significantly increased ER stress relative to the empty pJPA5 vector (Figure 5.6).

We then assessed a range of SNPs in human G6PC2 to determine their effects on ER stress. Figure 5.6 shows that four variants (Gly114Arg, Met126Val, Ser30Phe, and His177Tyr) modestly increased ER stress. The effect of the amino acid variant on ER stress does not correlate with the effect of the SNP on G6PC2 expression; two of the variants (Gly114Arg and Met126Val) that increased ER stress did not affect G6PC2 expression, and the other two (Ser30Phe and His177Tyr) reduced G6PC2 expression. Interestingly, Gly8Glu and Leu219Val, which increase G6PC2 expression, had no effect on ER stress in this assay. This contrasts with previously published data

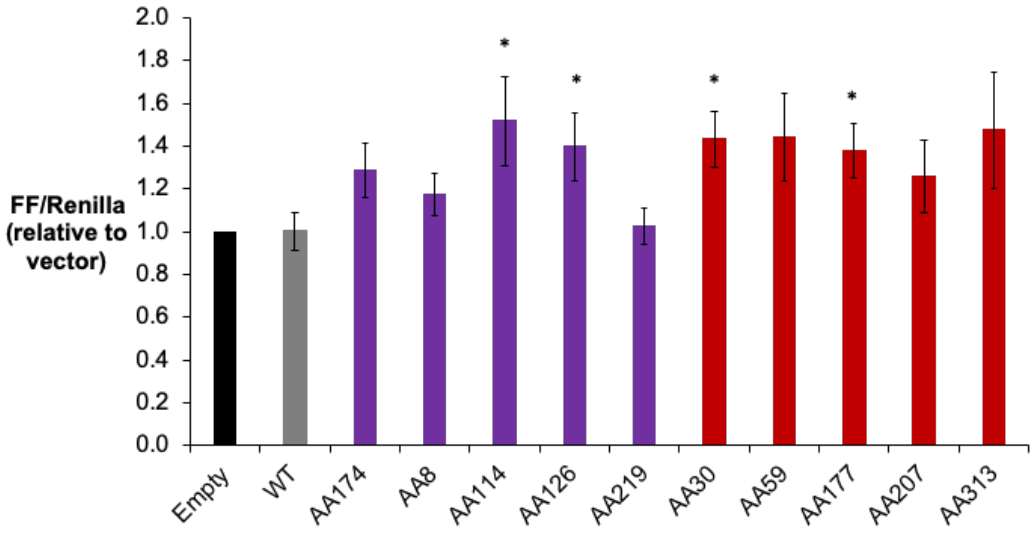

Figure 5.6. Analysis of the Effect of G6PC2 Amino Acid Variants on ER Stress. 832/13 cells were transiently co-transfected (described in Materials and Methods) with an expression vector encoding Renilla luciferase (0.5 μg), a plasmid encoding an ATF6-luciferase fusion gene (2μg), and expression vectors encoding either WT G6PC2 or G6PC2 variants where the indicated amino acid was changed (2μg), (see Tables 5.1 and 5.2). Following transfection, cells were incubated in serum-containing media. Cells were then harvested and luciferase activity assayed as described in Materials and Methods. Results were calculated as the ratio of firefly:Renilla luciferase activity and are presented as a fold change relative to that of cells transfected with the empty pJPA5 vector. Results represent mean ± SEM of 4 experiments where each variant was assayed in triplicate. Black bar, empty vector; gray bar, WT G6PC2; purple bars, variants that did not decrease G6PC2 protein expression; red bars, variants that decreased G6PC2 protein expression. *$p<0.05$

showing that transgenic overexpression of WT human G6PC2 in mice increases ER stress and leads to beta cell death [233]. This difference could be due to the relative levels of expression of human G6PC2 in the transiently transfected cells and the transgenic mice, since the transgenic mice had as much as 25-fold greater expression of human G6PC2 as compared to the endogenous mouse G6PC2 protein [233].

Analysis of the Effect of *G6PC2* SNPs on Enzyme Activity

We next tested the activity of human G6PC2 in an *in situ* assay previously developed by our lab to study the effect of G6PC1 mutations on G6PC1 enzyme activity [2]. For this assay, we use 832/13 cells; since this cell line is derived from rat islets, they do not express endogenous *G6pc2* because in rats *G6pc2* is a pseudogene. These cells were transiently transfected with a plasmid containing a luciferase reporter gene under the control of a promoter that binds two glucose-responsive transcription factors, CREB and ChREBP. Under high glucose conditions, G6P levels within the cell will rise as glucokinase converts glucose to G6P. Increasing levels of G6P activate ChREBP and CREB, which leads to increased luciferase expression [2]. However, when a plasmid encoding an active G6Pase, such as G6PC1 or G6PC2, is present, it will hydrolyze G6P, decreasing the amount of G6P present in the cell and thus luciferase expression. Therefore, in these experiments, as a control for ER stress, cells are transfected with either WT or catalytically dead G6Pase. Under low glucose conditions, when the cells are transfected with a catalytically-dead form of G6PC1, luciferase activity is low, and increases when the cells are incubated in high glucose. However, when the cells are transfected with wild-type G6PC1, luciferase activity is decreased (Figure 5.7).

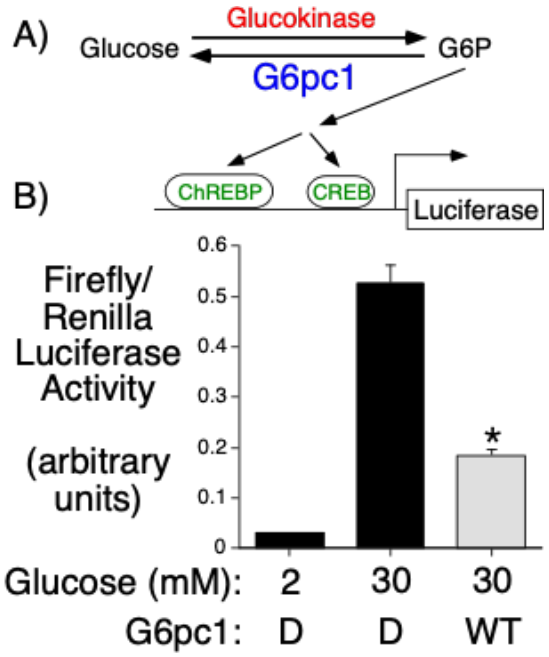

Figure 5.7. Overexpression of Mouse G6PC1 Suppresses Glucose-Stimulated Fusion Gene Expression in 832/13 Cells [2]. Panel A: Schematic illustrating how glucose cycling catalyzed by GCK and G6PC1 determines intracellular G6P levels and thus activation of fusion gene expression through activation of CREB and ChREBP. **Panel B**: Example of results from an *in situ* assay where 832/13 cells were transiently co-transfected with an expression vector encoding Renilla luciferase, a plasmid encoding a glucose-responsive promoter-luciferase fusion gene, and an expression vector encoding either WT or catalytically dead mouse G6PC1. Luciferase activity from cells transfected with dead G6PC1 increases with increasing glucose concentration, but activity is decreased when cells are transfected with WT G6PC1.

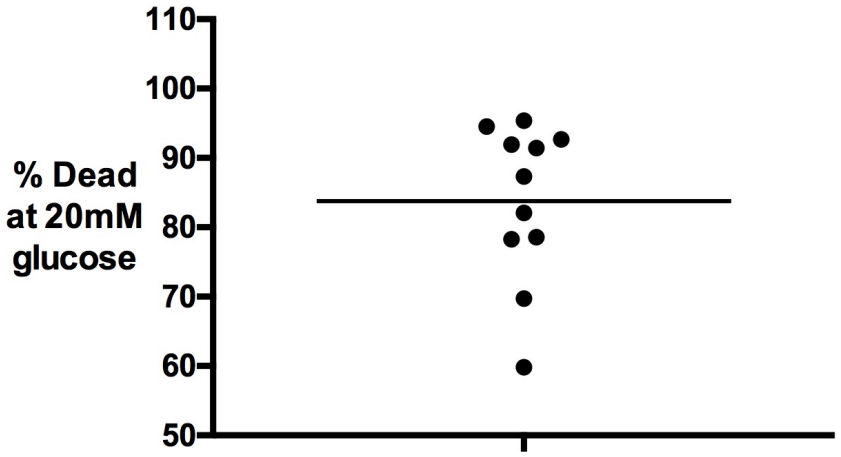

Figure 5.8. Overexpression of Human G6PC2 Driven by the pJPA5 Vector Does Not Consistently Repress Glucose-Stimulated Fusion Gene Expression. 832/13 cells were transiently co-transfected (described in Materials and Methods) with an expression vector encoding Renilla luciferase (0.5 μg), a plasmid encoding a glucose-responsive promoter-luciferase fusion gene (2μg), and an expression vector encoding either WT or catalytically-dead human G6PC2 (2μg). Following transfection, cells were incubated in serum-free media. Cells were then harvested and luciferase activity assayed as described in Materials and Methods. Results were calculated as the ratio of firefly:Renilla luciferase activity and are presented as a percentage of luciferase activity in cells transfected with the catalytically-dead G6PC2. Results represent mean ± SEM of 11 experiments with WT G6PC2 assayed in triplicate.

Despite the marked increase in human G6PC2 expression achieved using the pJPA5 vector, it was still insufficient to achieve consistent detection of glucose-6-phosphatase activity using this *in situ* assay (Figure 5.8). There are two likely explanations for this observation. First, G6PC2 activity is approximately 40-fold lower than that of G6PC1, and its activity has therefore been difficult to assess in previous studies using other assays [6, 143, 146]. Secondly, the level of G6PC2 expression achieved using the pJPA5 vector is only the same as that achieved with G6PC1 using the pcDNA3 vector, meaning the activity of G6PC2 would still be difficult to detect, given the lower inherent activity of G6PC2 (Figure 5.9). Interestingly, while G6PC1 expression is much higher when expressed using the pJPA5 vector versus the pcDNA3 vector (Figure 5.9), this does not result in a corresponding increase in activity, as assessed using our *in situ* assay (Figure 5.10). These data suggest that when G6PC1 is expressed from the pJPA5 vector it does not result in the expected increase in activity; this is perhaps due to misfolding or lack of post-translational modifications such as glycosylation which may be necessary for G6PC1 to be fully functional [234]. Additionally, the level of endogenous SLC37A4 expression may be insufficient to allow the functional coupling between G6PC1 and SLC37A4 that is required for optimal G6P hydrolysis [235].

Discussion

This study focused on the effects of twenty human *G6PC2* SNPs that affect amino acids conserved between human and mouse G6PC1 and human and mouse G6PC2. Of these twenty variants, fifteen were found to decrease human G6PC2 expression (Ser30Phe, Trp59Arg, Gly64Arg, Trp73Arg, Arg79Gln, Thr107Arg, Leu148Pro, His174Tyr, His177Tyr, Gly186Asp, Tyr207Ser, Arg293Trp, Pro313Leu, Ser324Pro, Pro340Leu). Only three variants had no effect on

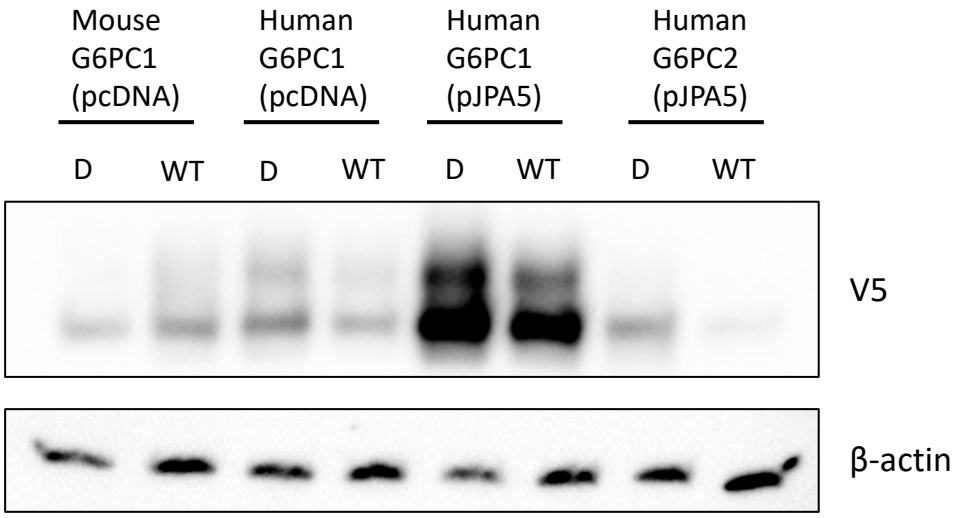

Figure 5.9. Analysis of Mouse and Human G6PC1 and Human G6PC2 Protein Expression Driven Using pJPA5. 832/13 cells were transiently transfected (as described in Materials and Methods) with an expression vector encoding either WT or catalytically dead mouse G6PC1 from pcDNA3, WT or catalytically dead human G6PC1 from pcDNA3, WT or catalytically dead human G6PC1 from pJPA5, or WT or catalytically dead human G6PC2 from pJPA5. Following transfection, cells were incubated for 18-20 hours in serum-containing media. Cells were subsequently harvested and protein expression assayed by Western blot as described in Materials and Methods. A representative blot is shown. D = catalytically dead; WT = wild-type

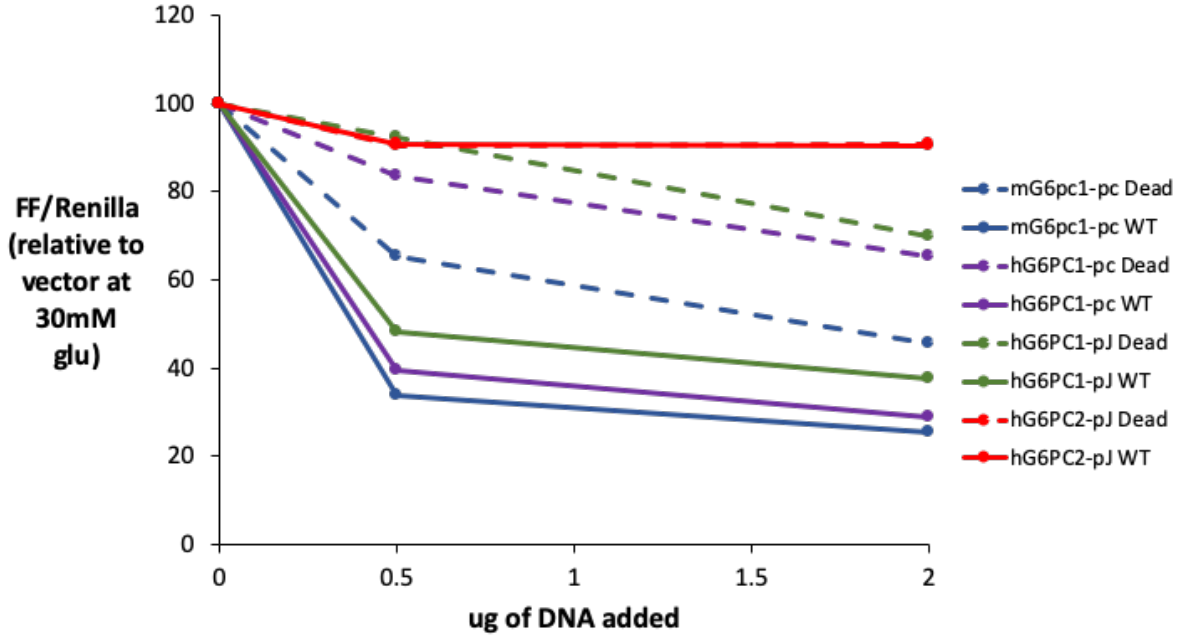

Figure 5.10. Mouse and Human G6PC1 but not Human G6PC2 Suppress Glucose-Stimulated Fusion Gene Expression. 832/13 cells were transiently co-transfected (described in Materials and Methods) with an expression vector encoding Renilla luciferase (0.5 μg), a plasmid encoding an glucose-responsive promoter-luciferase fusion gene (2μg), and an expression vector encoding either WT or catalytically dead mouse G6PC1 from pcDNA3 (mG6PC1-pc), WT or dead human G6PC1 from pcDNA3 (hG6PC1-pc), WT or dead human G6PC1 from pJPA5 (hG6PC1-pJ), or WT or dead human G6PC2 from pJPA5 (hG6PC2-pJ) (0.5 or 2μg). Following transfection, cells were incubated in serum-free media. Cells were then harvested and luciferase activity assayed as described in Materials and Methods. Results were calculated as the ratio of firefly:Renilla luciferase activity and are presented as a percentage of luciferase activity from cells transfected with empty vector. Results represent mean ± SEM of 4 experiments where each variant was assayed in triplicate.

G6PC2 expression (Gly114Arg, Met126Val, Phe256Leu), and two variants led to increased expression (Gly8Glu and Leu219Val). These results broadly replicate what we previously observed in COS cells, in that the amino acid changes shown in Tables 5.1 and 5.2 for AAs 177, 207, 293, 313, 324, and 340 all resulted in decreased human G6PC2 expression [2].

Similarly, Ng et al also found that the variants affecting AAs 177, 207, 219, 313, and 324 all decreased human G6PC2 expression when expressed in islet-derived cell lines [229]. They also reported that the variants in AAs 30, 219, and 256 confer reduced, increased, or no change in G6PC2 expression, respectively, which matches our results reported here, though it should be noted that for AA219, Ng et al reported the result for the alternate amino acid change, and hence they reported a decrease in expression. Importantly, several of the variants that cause decreased protein expression (AAs 30, 177, 207, 219, 256, & 324) have been linked to decreased FBG levels, indicating that the effect of these variants to decrease G6PC2 expression has physiological significance [228, 229, 236]. We did not analyze the effects of changes in AA171, which Ng et al found affected enzyme activity in the context of G6PC1 rather than protein expression, because this amino acid is not conserved between G6PC1 and G6PC2 (Figure 5.2) [229].

Our present results differ from our previous results in COS cells in two instances. First, the AA219 variant results in increased expression in 832/13 cells but showed little difference in expression in COS cells. Second, changing AA8 also resulted in increased expression in 832/13 cells, whereas in COS cells decreased expression was observed. This suggests that for these particular variants, unidentified cell line-dependent factors exert effects on G6PC2 expression, and highlights the importance of studying the effects of variants, when possible, in a cell type representative of the endogenous cell type or types for that protein. One caveat with these studies is that *in vivo* data has demonstrated that G6PC2 can affect beta cell function, with loss of G6PC2

increasing flux through glycolysis (Figure 3.10) and elevating basal cytoplasmic calcium levels [1]. Overexpressing G6PC2 in islet-derived cell lines could result in secondary effects on cellular functions that could then feed back to impact the effect of altered of protein expression or enzyme activity. In contrast, studies in non-islet-derived cell lines would be less affected by variations in G6PC2 activity since such cells would likely express either of the two more enzymatically-active G6PC isoforms.

Future studies will use VUMC's BioVU biobank to explore whether SNPs that affect human G6PC2 expression are associated with altered phenotypes in humans. As described previously in Chapter 3, approaches have been developed to screen the BioVU SD with SNPs of interest to identify novel phenotype-variant associations and variant-plasma hormone/metabolite associations, known as PheWAS and LabWAS, respectively. Of particular interest will be whether an association between *G6PC2* SNPs and T2D risk emerges from these analyses. Studies on a smaller Chinese population have reported an association between rs16856187, a SNP located 3' of the *G6PC2* gene that is common in Chinese populations (MAF=0.29), and both FBG and T2D risk [237, 238]. However, studies on the rs560887 SNP common to European populations have reported conflicting results, with some studies reporting no association between this SNP and T2D risk [169, 172, 236], while others reported a slight protective effect of the glucose-raising G allele, which would also increase *G6PC2* expression, against T2D development [209, 239]. Additionally, Mahajan et al reported an association between rs492594, the SNP that affects amino acid 219, and T2D risk, in which the allele that decreased G6PC2 expression was linked to a decreased risk of T2D [228]. Together these studies serve to illustrate that the relationship between G6PC2 expression or function and T2D risk is complex, and may also indicate that the effects of each

variant on G6PC2 has unique effects on beta cell function unrelated to the control of glycolytic flux and FBG by G6PC2.

CHAPTER 6

Summary and Future Directions

Thesis Summary

The work described in this dissertation aimed to further elucidate the role played by G6PC2 in beta cell function and the regulation of FBG. Previous work had demonstrated an association between SNPs in *G6PC2* and variations in FBG [228, 229], and demonstrated that global germline deletion of *G6pc2* abolishes glucose cycling within islets [7] and shifts the dose-response curve for GSIS to the left, thus lowering FBG [1]. A physiological role for G6PC2 in the response to stress was also uncovered, with the presence of G6PC2 conferring a transient beneficial elevation in FBG with both a physical restraint paradigm [174] and exogenous glucocorticoid administration [175]. These data all suggest that G6PC2 could be a potential novel therapeutic target to lower FBG and thereby reduce the risk of developing CAM; as discussed in Chapter 3, the ability of G6PC2 inhibition to lower the risk of T2D is less clear. The work detailed here aimed to determine if G6PC2 should continue to be pursued as a novel therapeutic target by addressing three goals: (1) determining if G6PC2 mediates its action solely through islet beta cells; (2) identifying additional beneficial effects of inhibiting G6PC2 besides reducing FBG; and (3) identifying adverse effects of inhibiting G6PC2.

While previously published data strongly suggest the G6PC2 is active in islets, the observation from GTEx data that *G6PC2* is expressed at low levels in multiple tissues raises the possibility that G6PC2 may be active in other non-islet tissues. We addressed this possibility through the gene expression analyses and the generation of a beta cell-specific *G6pc2* KO mouse

model and through further studies in our global KO mouse model. Briefly, gene expression analyses of major organs showed that mouse *G6pc2* expression is only detected in the pancreas (Figure 3.1B), at much higher levels than either *G6pc1* or *G6pc3* (Figure 3.1E). This implies that, even if *G6pc2* was expressed at some trace level in non-pancreatic tissues, because both G6PC1 and G6PC3 have greater catalytic activity [4, 6, 124], it is unlikely that G6PC2 would be able to directly affect metabolism in those tissues. Additionally, our BCS model demonstrated that deletion of *G6pc2* specifically in beta cells is sufficient to reduce FBG (Figure 3.6E). These data implicate the islet as the primary tissue through which G6PC2 mediates its action.

We further extended our studies into the role of G6PC2 in beta cell function by characterizing the effect of *G6pc2* deletion on glycolysis. We found that deletion of *G6pc2* enhances glycolysis in mouse islets (Figure 3.10), consistent with our model of G6PC2 function in beta cells (Figure 1.2). We also showed that glucose cycling exists in human islets, which had not previously been established (Figure 3.12). While the mean rate of cycling is lower in humans than in mice, the presence of cycling in human islets suggests the possibility that the effects of modulating G6PC2 seen in mouse studies may be physiologically relevant in humans as well.

We sought to complement these mouse studies with human data, and turned to two approaches, PheWAS and LabWAS, to identify novel phenotype-variant associations and plasma hormone/metabolite associations, respectively. While the BioVU population represents individuals with a wide range of medical conditions who are not necessarily under overnight fasted conditions when blood was isolated, the LabWAS confirmed an association between the rs560887 SNP and blood glucose levels (Table 3.2). This suggests that G6PC2 may be able to influence blood glucose levels under non-fasting conditions, which is consistent with the idea that altered *G6PC2* expression affects the sensitivity of GSIS over a range of concentrations (Figure 3.4).

Surprisingly, the PheWAS analysis uncovered a potential adverse effect of inhibiting G6PC2, identifying an association between reduced *G6PC2* expression and an increased risk of acute pancreatitis (Table 3.1). Follow-up studies in mice demonstrated that deletion of *G6pc2* alters *Prss1* expression, providing a potential mechanistic link since altered *Prss1* expression can affect the risk of pancreatitis [207, 208].

We also continued our previous studies into the physiological benefit conferred by the GCK/G6PC2 substrate cycle by examining the role of G6PC2 in the response to various nutritional challenges. While the absence of *G6PC2* was beneficial in limiting the hyperglycemia seen in mice on a high-fat diet (Figure 4.5), the presence of G6PC2 conferred protection against hypoglycemia upon ketogenic diet feeding (Figure 4.1) or prolonged fasting (Figure 4.3). This suggests that a possible adverse effect of G6PC2 inhibition would be an increased incidence of hypoglycemic events. However, no association between the *G6PC2* SNP rs560887 and hypoglycemic events was identified in the PheWAS analysis. Because this SNP only results in a small change in *G6PC2* expression [171], and the *G6pc2* KO mice represent total loss of G6PC2 activity, this suggests that partial inhibition of G6PC2 may be the optimal approach to lower FBG with minimal risk of hypoglycemia.

Finally, we sought to expand our efforts to identify rare G6PC2 variants that have significant effects on protein expression and/or enzyme activity. We were unsuccessful in evaluating the effects of G6PC2 variants on G6PC2 enzyme activity; despite achieving increased human G6PC2 expression from a new vector, our *in situ* glucose-stimulated fusion gene assay was unable to consistently detect glucose-6-phosphatase activity (Figure 5.8). This could be due to the inherently low activity of G6PC2 relative to the other G6PC isoforms, which has made detecting its phosphatase activity difficult in previous studies [27, 143, 147]. However, our results showing

that human G6PC1 does not display increased activity despite a large increase in protein expression when driven by the pJPA5 expression vector suggests that there may be factors that limit the generation of fully functional protein, which could also contribute to our inability to detect G6PC2 activity in this assay. Future studies into the effect of amino acid variants on G6PC2 activity may require the development of a more sensitive assay to detect glucose-6-phosphatase activity, or an alternate method of increasing functional protein expression or improving transfection efficiency. Studies to determine the crystal structure of G6PC2 may also be helpful in determining the effect of amino acid variation on protein structure or function.

We were, however, successful in identifying a total of fourteen amino acid variants in highly conserved amino acids that significantly decreased G6PC2 expression and two variants that increased expression (Tables 5.1 and 5.2, Figures 5.3 and 5.4). Future studies will use the BioVU database to determine if these SNPs are associated with variations in FBG, and if these SNPs have a greater effect on FBG levels than the common SNP rs560887, since they reduce G6PC2 protein expression to a greater extent than rs560887. It would also be enlightening to perform PheWAS and LabWAS analyses with these SNPs, though the power to detect any associations may presently be limited by the size of the BioVU population and the rarity of these SNPs.

Future Directions

The work described in this dissertation has contributed to the field's knowledge of the role of G6PC2 in beta cell function, the regulation of FBG, and the response to nutritional challenges. While these studies suggest that G6PC2 would be a novel potential therapeutic target to lower FBG, more work needs to be done to examine the effects of *G6pc2* deletion on beta cell metabolism

and ROS generation, and to explore the mechanisms by which G6PC2 function in the beta cell may be altering gene expression or metabolism in other tissues.

Effects on Beta Cell Metabolism and ROS Generation

Our analysis of glycolytic flux demonstrates that deletion of *G6pc2* enhances glycolytic flux relative to that in WT islets; this increased flux through glycolysis will ultimately lead to increased concentration of ATP generated by mitochondrial respiration, which will stimulate insulin secretion, as shown in Figure 1.2. However, this increase in mitochondrial respiration will also lead to increased ROS generation [95]. ROS are a normal byproduct of mitochondrial respiration, and are typically detoxified by enzymatic antioxidants such as superoxide dismutase (SOD), catalase (CAT), or glutathione peroxidase (GPx) [240]. However, beta cells express very low levels of these enzymes, and are therefore particularly susceptible to oxidative stress [240]. Indeed, it is thought that chronic overnutrition leads to increased glycolytic flux, increased ROS, and hence oxidative stress on the beta cell and contributes to beta cell failure as part of the pathogenesis of T2D [92].

Under post-prandial conditions, inhibition of G6PC2 would transiently increase glycolytic flux and ROS generation as shown in Figure 3.13, and would therefore increase oxidative stress on the beta cell. To address this prediction, we would need to first measure ROS levels in islets isolated from WT and *G6pc2* KO mice to determine if ROS are increased in *G6pc2* KO islets. This could be assessed using a fluorescent indicator such as MitoSOX (ThermoFisher Scientific) to assess levels of mitochondrial-generated ROS in islets isolated from WT and *G6pc2* KO mice. However, loss of G6PC2 function would also enhance the timing of GSIS and speed the return to basal euglycemia. Therefore, the total ROS generation in WT islets should be equal to that in KO

islets. To address this prediction, the timing of GSIS could be assessed *in vivo* by rapid sampling of mice after a glucose bolus [241], or *in vitro* through islet perifusion analysis. In contrast, under fasting conditions, ROS levels would be the same in WT and *G6pc2* KO mouse islets (Figure 3.13); this may explain in part why *G6PC2* has not been associated with altered risk for T2D

It is important to note that there are pathways that may be able to compensate for the increased ROS levels in the beta cell. Recent work has identified that the Nrf2/Keap1 pathway plays an important role in mediating the response of beta cells to oxidative stress by regulating the expression of genes related to oxidative stress and cell survival [240]. Under basal conditions, Keap1 forms a dimer with the transcription factor Nrf2, targeting it for ubiquitination and degradation [242]. The presence of oxidative stress causes changes in Keap1 that lead to dissociation of the dimer, allowing Nrf2 to translocate to the nucleus where it forms heterodimers with other transcription factors and acts to upregulate genes involved in antioxidant defense, among others [242]. Induction of *Nrf2* expression in mice reduced beta cell damage and ROS accumulation in a mouse model of oxidative damage [243]. Conversely, Nrf2 depletion in this same mouse model enhanced beta cell damage [243], implicating the Nrf2/Keap1 pathway in the protection of beta cells from damaging ROS. It is therefore possible that the Nrf2/Keap1 pathway is transiently upregulated in *G6pc2* KO mice to prevent beta cell damage from the increased ROS resulting from increased glycolytic flux, but this would need to be assessed in islets from these mice.

Intriguingly, recent work has elucidated a role for Nrf2 in the regulation of metabolic genes as well. Chromatin immunoprecipitation (ChIP) experiments found that binding sites for Nrf2 were enriched proximal to genes related to glycolysis and pyruvate metabolism, suggesting Nrf2 may be important for the expression of those genes [244]. Additionally, in cancer cells, Nrf2 regulates

the expression of genes involved in purine nucleotide synthesis, and the pentose phosphate pathway [245]. Increasing metabolic flux through pathways other than glycolysis could also serve to limit the generation of ROS in the mitochondria by diverting metabolites away from oxidative phosphorylation, as well as generate NADPH which is important for redox balance within the cell. Therefore, it would be interesting to examine the relative rates of flux through metabolic pathways in islets from WT and *G6pc2* KO mice using isotope tracers, to determine if other pathways have been upregulated in KO mice to divert metabolites away from glycolysis and thereby potentially decrease ROS.

Effects on Non-islet Tissues

While G6PC2 is expressed in beta cells, our data suggest that altering its function in beta cells can affect tissues other than the islet. Our PheWAS data suggest that decreased *G6PC2* expression is associated with an increased risk of pancreatitis (Table 3.1). Intracellular trypsin activation is believed to be a primary mechanism by which acute pancreatitis develops [246]. This is supported by a number of genetic studies. Gain-of-function mutations in *PRSS1*, the gene that encodes trypsinogen, the precursor to trypsin, enhance trypsinogen autoactivation or confer resistance to proteolysis, and have been associated with hereditary forms of pancreatitis [247]. Copy number variants in the *PRSS1* locus have also been shown to increase trypsinogen expression and are associated with pancreatitis [208, 248, 249]. Association studies have also found links between common variants in the *PRSS1* locus and susceptibility to acute pancreatitis [250, 251]. Finally, loss-of-function mutations that decrease trypsinogen may be protective against the development of pancreatitis [207, 252]. Our mouse data showing that *G6pc2* KO mice have

increased *Prss1* expression (Figure 3.8) may provide a link between *G6PC2* expression and susceptibility to pancreatitis.

However, further work needs to be done to determine the mechanism by which loss of G6PC2 function leads to increased *PRSS1* expression, particularly since *G6PC2* is not expressed in acinar cells [27, 143, 146]. One possibility is that the effects of G6PC2 within the islet on insulin secretion or blood glucose levels affects the local concentration of insulin or glucose in the surrounding acinar tissue, stimulating changes in gene expression. Insulin in particular has been shown to potentiate secretion of digestive enzymes [253, 254] and to increase the levels of trypsinogen protein within acinar cells [255]. However, this effect of insulin on trypsinogen appears to be mediated by regulation of translation rather than an increase in mRNA levels [256], though studies in rats indicate that mRNA levels for trypsinogen are increased after treatment with insulin secretogogues [257]. Other studies have demonstrated the stimulation of trypsinogen expression by low glucose levels. Glucose starvation of a rat exocrine pancreas cell line causes a selective increase in trypsinogen mRNA levels [258]. Additionally, long-term fasting induces an increase in trypsinogen mRNA in zebrafish [259]. Because FPI levels do not differ in *G6pc2* KO mice relative to WT, glucose is the likely factor that explains these data. It is not clear why *PRSS1* expression was not increased but instead decreased in our BCS *G6pc2* KO mice relative to their wild-type counterparts (Figure 3.8D). This could reflect some form of developmental compensation in our global KO mice that would not be present in our BCS KO mice, but this too will require further investigation.

Finally, our LabWAS showed an association between *G6PC2* and plasma amino acid levels, specifically increased taurine levels (Table 3.2), though data from *G6pc2* KO mice showed the opposite effect (Figure 3.9). It is not clear why the mouse data differs from the human data;

one possible explanation is that the LabWAS data was derived from humans who were not necessarily fasted at the time of blood collection, whereas we collected data from fasted mice. The simplest hypothesis that might explain our results in humans or in mice is that reduced islet *G6PC2* expression influences the kinetics of insulin secretion, which in turn affects amino acid metabolism. It has been established that pulsatile insulin secretion has a greater effect than continuous delivery, causing a greater hypoglycemic effect [260], possibly due to better inhibition of endogenous glucose production [261]. These pulses are impaired in humans with T2D [262, 263]. It is thought that oscillations in calcium levels, oscillations in glycolysis, or a combination of the two accounts for the pulsatile nature of insulin secretion [264]. Since G6PC2 can modulate glycolytic flux (Figure 3.10) and basal cytoplasmic calcium levels [1], it will be important to assess the effects of *G6pc2* deletion on pulsatile insulin secretion as well as the downstream effects on hepatic function, including amino acid metabolism.

Studies of pulsatile insulin secretion would also address two paradoxical observations from human studies. The A allele of the *G6PC2* SNP rs560887, which decreases *G6PC2* expression, is also associated with reduced hepatic glucose production (HGP) and with reduced insulin levels at the 30 minute time point in an oral glucose tolerance test (OGTT) [265-267], and the G allele is associated with increased HGP and increased insulin levels at the 30 minute time point in an OGTT. These observations are paradoxical because (1) *G6PC2* is expressed at trace levels in liver [197] so changes in *G6PC2* expression should not affect HGP and (2) based on static isolated islet experiments showing higher GSIS in KO islets at sub-maximal glucose [1], our model suggests that the rs560887-A allele should be associated with increased, not reduced, insulin levels in the OGTT. These observations could be explained by *G6PC2* regulating pulsatile GSIS; decreased *G6PC2* expression is predicted to enhance pulsatile GSIS and improve the repression of HGP by

insulin, as well as reduce the level of required insulin secretion in an OGTT, due to enhanced efficacy of insulin action [265]. In contrast, increased G6PC2 expression is predicted to impair pulsatile GSIS impairing the repression of fasting HGP by insulin and increasing insulin secretory requirements in the OGTT [265]. HGP and pulsatile GSIS could be assessed using a mild hyperglycemic clamp in chronically catheterized conscious mice, with rapid sampling to measure pulsatile GSIS [241] and tracers to quantify HGP [268]. Plasma insulin levels during an OGTT could also be assessed in chronically catheterized mice to allow for collection of multiple samples.

It is important to note that because neither the rs560887 SNP or loss of G6PC2 affects FPI [1, 265-267], this change in fasting HGP cannot be explained by a difference in insulin levels *per se*. Similarly, the effect of G6PC2 on HGP cannot be a compensatory response to its effect on FBG; if compensation occurred to offset the influence of G6PC2 on FBG, then one would expect that the rs560887-A allele (associated with decreased G6PC2 and decreased FBG) would be associated with higher, not lower, HGP whereas the rs560887-G allele (associated with increased G6PC2 and increased FBG) would be associated with lower, not higher, HGP. Instead the opposite effects are observed. Additionally, enhanced insulin action by enhanced pulsatile GSIS could explain the decreased amino acid levels in *G6pc2* KO mice (Figure 3.9), since increased insulin action would be predicted to enhance amino acid uptake and protein synthesis [203].

REFERENCES

1. Pound, L.D., et al., *G6PC2: a negative regulator of basal glucose-stimulated insulin secretion.* Diabetes, 2013. **62**(5): p. 1547-56.
2. Boortz, K.A., et al., *Functional Analysis of Mouse G6pc1 Mutations Using a Novel In Situ Assay for Glucose-6-Phosphatase Activity and the Effect of Mutations in Conserved Human G6PC1/G6PC2 Amino Acids on G6PC2 Protein Expression.* PLoS One, 2016. **11**(9): p. e0162439.
3. Kayton, N.S., et al., *Human islet preparations distributed for research exhibit a variety of insulin-secretory profiles.* Am J Physiol Endocrinol Metab, 2015. **308**(7): p. E592-602.
4. Shieh, J.J., et al., *A glucose-6-phosphate hydrolase, widely expressed outside the liver, can explain age-dependent resolution of hypoglycemia in glycogen storage disease type Ia.* J Biol Chem, 2003. **278**(47): p. 47098-103.
5. Hart, N.J. and A.C. Powers, *Use of human islets to understand islet biology and diabetes: progress, challenges and suggestions.* Diabetologia, 2019. **62**(2): p. 212-222.
6. Petrolonis, A.J., et al., *Enzymatic characterization of the pancreatic islet-specific glucose-6-phosphatase-related protein (IGRP).* J Biol Chem, 2004. **279**(14): p. 13976-83.
7. Wall, M.L., et al., *Novel stable isotope analyses demonstrate significant rates of glucose cycling in mouse pancreatic islets.* Diabetes, 2015. **64**(6): p. 2129-37.
8. Brissova, M., et al., *Assessment of human pancreatic islet architecture and composition by laser scanning confocal microscopy.* J Histochem Cytochem, 2005. **53**(9): p. 1087-97.
9. Pan, C.J., et al., *Transmembrane topology of glucose-6-phosphatase.* J Biol Chem, 1998. **273**(11): p. 6144-8.
10. Williams, R., et al., *IDF Atlas 9th Edition 2019*. 2019.
11. American Diabetes, A., *Standards of Medical Care in Diabetes-2016 Abridged for Primary Care Providers.* Clin Diabetes, 2016. **34**(1): p. 3-21.
12. Atkinson, M.A., G.S. Eisenbarth, and A.W. Michels, *Type 1 diabetes.* Lancet, 2014. **383**(9911): p. 69-82.
13. Zimmerman, C., A. Albanese-O'Neill, and M.J. Haller, *Advances in Type 1 Diabetes Technology Over the Last Decade.* Eur Endocrinol, 2019. **15**(2): p. 70-76.
14. Crofford, O.B., *Diabetes control and complications.* Annu Rev Med, 1995. **46**: p. 267-79.
15. de Boer, I.H., et al., *Long-term renal outcomes of patients with type 1 diabetes mellitus and microalbuminuria: an analysis of the Diabetes Control and Complications Trial/Epidemiology of Diabetes Interventions and Complications cohort.* Arch Intern Med, 2011. **171**(5): p. 412-20.
16. Diabetes, C., et al., *Modern-day clinical course of type 1 diabetes mellitus after 30 years' duration: the diabetes control and complications trial/epidemiology of diabetes interventions and complications and Pittsburgh epidemiology of diabetes complications experience (1983-2005).* Arch Intern Med, 2009. **169**(14): p. 1307-16.
17. Pop-Busui, R., et al., *Effects of prior intensive insulin therapy on cardiac autonomic nervous system function in type 1 diabetes mellitus: the Diabetes Control and Complications Trial/Epidemiology of Diabetes Interventions and Complications study (DCCT/EDIC).* Circulation, 2009. **119**(22): p. 2886-93.
18. Awoniyi, O., R. Rehman, and S. Dagogo-Jack, *Hypoglycemia in patients with type 1 diabetes: epidemiology, pathogenesis, and prevention.* Curr Diab Rep, 2013. **13**(5): p. 669-78.

19. Sprague, J.E. and A.M. Arbelaez, *Glucose counterregulatory responses to hypoglycemia.* Pediatr Endocrinol Rev, 2011. **9**(1): p. 463-73; quiz 474-5.
20. Cryer, P.E., *Hypoglycemia-associated autonomic failure in diabetes.* Am J Physiol Endocrinol Metab, 2001. **281**(6): p. E1115-21.
21. Bolli, G., et al., *Abnormal glucose counterregulation in insulin-dependent diabetes mellitus. Interaction of anti-insulin antibodies and impaired glucagon and epinephrine secretion.* Diabetes, 1983. **32**(2): p. 134-41.
22. Gerich, J.E., et al., *Lack of glucagon response to hypoglycemia in diabetes: evidence for an intrinsic pancreatic alpha cell defect.* Science, 1973. **182**(4108): p. 171-3.
23. Sherr, J., et al., *Evolution of abnormal plasma glucagon responses to mixed-meal feedings in youth with type 1 diabetes during the first 2 years after diagnosis.* Diabetes Care, 2014. **37**(6): p. 1741-4.
24. Brissova, M., et al., *alpha Cell Function and Gene Expression Are Compromised in Type 1 Diabetes.* Cell Rep, 2018. **22**(10): p. 2667-2676.
25. Bluestone, J.A., K. Herold, and G. Eisenbarth, *Genetics, pathogenesis and clinical interventions in type 1 diabetes.* Nature, 2010. **464**(7293): p. 1293-300.
26. Pociot, F. and A. Lernmark, *Genetic risk factors for type 1 diabetes.* Lancet, 2016. **387**(10035): p. 2331-2339.
27. Hutton, J.C. and G.S. Eisenbarth, *A pancreatic beta-cell-specific homolog of glucose-6-phosphatase emerges as a major target of cell-mediated autoimmunity in diabetes.* Proc Natl Acad Sci U S A, 2003. **100**(15): p. 8626-8.
28. Lieberman, S.M., et al., *Identification of the beta cell antigen targeted by a prevalent population of pathogenic CD8+ T cells in autoimmune diabetes.* Proc Natl Acad Sci U S A, 2003. **100**(14): p. 8384-8.
29. Yang, J., et al., *Islet-specific glucose-6-phosphatase catalytic subunit-related protein-reactive CD4+ T cells in human subjects.* J Immunol, 2006. **176**(5): p. 2781-9.
30. Jarchum, I., et al., *Identification of novel IGRP epitopes targeted in type 1 diabetes patients.* Clin Immunol, 2008. **127**(3): p. 359-65.
31. Todd, J.A., *Etiology of type 1 diabetes.* Immunity, 2010. **32**(4): p. 457-67.
32. Herold, K.C., et al., *An Anti-CD3 Antibody, Teplizumab, in Relatives at Risk for Type 1 Diabetes.* N Engl J Med, 2019. **381**(7): p. 603-613.
33. Noble, J.A. and H.A. Erlich, *Genetics of type 1 diabetes.* Cold Spring Harb Perspect Med, 2012. **2**(1): p. a007732.
34. Bakay, M., et al., *The Genetic Contribution to Type 1 Diabetes.* Curr Diab Rep, 2019. **19**(11): p. 116.
35. Pociot, F., et al., *Genetics of type 1 diabetes: what's next?* Diabetes, 2010. **59**(7): p. 1561-71.
36. Watkins, R.A., et al., *Established and emerging biomarkers for the prediction of type 1 diabetes: a systematic review.* Transl Res, 2014. **164**(2): p. 110-21.
37. King, A.J., *The use of animal models in diabetes research.* Br J Pharmacol, 2012. **166**(3): p. 877-94.
38. Nakayama, M., et al., *Prime role for an insulin epitope in the development of type 1 diabetes in NOD mice.* Nature, 2005. **435**(7039): p. 220-3.
39. Takaki, T., et al., *HLA-A*0201-restricted T cells from humanized NOD mice recognize autoantigens of potential clinical relevance to type 1 diabetes.* J Immunol, 2006. **176**(5): p. 3257-65.

40. Serreze, D.V., M.P. Marron, and T.P. Dilorenzo, *"Humanized" HLA transgenic NOD mice to identify pancreatic beta cell autoantigens of potential clinical relevance to type 1 diabetes.* Ann N Y Acad Sci, 2007. **1103**: p. 103-11.
41. Oeser, J.K., et al., *Deletion of the G6pc2 gene encoding the islet-specific glucose-6-phosphatase catalytic subunit-related protein does not affect the progression or incidence of type 1 diabetes in NOD/ShiLtJ mice.* Diabetes, 2011. **60**(11): p. 2922-7.
42. King, A. and J. Bowe, *Animal models for diabetes: Understanding the pathogenesis and finding new treatments.* Biochem Pharmacol, 2016. **99**: p. 1-10.
43. Olokoba, A.B., O.A. Obateru, and L.B. Olokoba, *Type 2 diabetes mellitus: a review of current trends.* Oman Med J, 2012. **27**(4): p. 269-73.
44. Gaulton, K.J., *Mechanisms of Type 2 Diabetes Risk Loci.* Curr Diab Rep, 2017. **17**(9): p. 72.
45. Flannick, J., *The Contribution of Low-Frequency and Rare Coding Variation to Susceptibility to Type 2 Diabetes.* Curr Diab Rep, 2019. **19**(5): p. 25.
46. Misra, S. and K.R. Owen, *Genetics of Monogenic Diabetes: Present Clinical Challenges.* Curr Diab Rep, 2018. **18**(12): p. 141.
47. De Franco, E., et al., *The effect of early, comprehensive genomic testing on clinical care in neonatal diabetes: an international cohort study.* Lancet, 2015. **386**(9997): p. 957-63.
48. Anik, A., et al., *Maturity-onset diabetes of the young (MODY): an update.* J Pediatr Endocrinol Metab, 2015. **28**(3-4): p. 251-63.
49. Flannick, J., S. Johansson, and P.R. Njolstad, *Common and rare forms of diabetes mellitus: towards a continuum of diabetes subtypes.* Nat Rev Endocrinol, 2016. **12**(7): p. 394-406.
50. Billings, L.K. and J.C. Florez, *The genetics of type 2 diabetes: what have we learned from GWAS?* Ann N Y Acad Sci, 2010. **1212**: p. 59-77.
51. Bonnefond, A. and P. Froguel, *Rare and common genetic events in type 2 diabetes: what should biologists know?* Cell Metab, 2015. **21**(3): p. 357-68.
52. Dolensek, J., M.S. Rupnik, and A. Stozer, *Structural similarities and differences between the human and the mouse pancreas.* Islets, 2015. **7**(1): p. e1024405.
53. Steiner, D.J., et al., *Pancreatic islet plasticity: interspecies comparison of islet architecture and composition.* Islets, 2010. **2**(3): p. 135-45.
54. Cabrera, O., et al., *The unique cytoarchitecture of human pancreatic islets has implications for islet cell function.* Proc Natl Acad Sci U S A, 2006. **103**(7): p. 2334-9.
55. Skelin Klemen, M., et al., *The triggering pathway to insulin secretion: Functional similarities and differences between the human and the mouse beta cells and their translational relevance.* Islets, 2017. **9**(6): p. 109-139.
56. Meglasson, M.D. and F.M. Matschinsky, *Pancreatic islet glucose metabolism and regulation of insulin secretion.* Diabetes Metab Rev, 1986. **2**(3-4): p. 163-214.
57. Ashcroft, F.M., *ATP-sensitive potassium channelopathies: focus on insulin secretion.* J Clin Invest, 2005. **115**(8): p. 2047-58.
58. Henquin, J.C., *Triggering and amplifying pathways of regulation of insulin secretion by glucose.* Diabetes, 2000. **49**(11): p. 1751-60.
59. Komatsu, M., et al., *Glucose-stimulated insulin secretion: A newer perspective.* J Diabetes Investig, 2013. **4**(6): p. 511-6.
60. Grimberg, A., et al., *Dysregulation of insulin secretion in children with congenital hyperinsulinism due to sulfonylurea receptor mutations.* Diabetes, 2001. **50**(2): p. 322-8.

61. Seghers, V., et al., *Sur1 knockout mice. A model for K(ATP) channel-independent regulation of insulin secretion.* J Biol Chem, 2000. **275**(13): p. 9270-7.
62. Kalwat, M.A. and M.H. Cobb, *Mechanisms of the amplifying pathway of insulin secretion in the beta cell.* Pharmacol Ther, 2017. **179**: p. 17-30.
63. Henquin, J.C., *The dual control of insulin secretion by glucose involves triggering and amplifying pathways in beta-cells.* Diabetes Res Clin Pract, 2011. **93 Suppl 1**: p. S27-31.
64. Duckworth, W.C., R.G. Bennett, and F.G. Hamel, *Insulin degradation: progress and potential.* Endocr Rev, 1998. **19**(5): p. 608-24.
65. Petersen, M.C. and G.I. Shulman, *Mechanisms of Insulin Action and Insulin Resistance.* Physiol Rev, 2018. **98**(4): p. 2133-2223.
66. Nolan, C.J. and M. Prentki, *Insulin resistance and insulin hypersecretion in the metabolic syndrome and type 2 diabetes: Time for a conceptual framework shift.* Diab Vasc Dis Res, 2019. **16**(2): p. 118-127.
67. Muoio, D.M. and C.B. Newgard, *Mechanisms of disease:Molecular and metabolic mechanisms of insulin resistance and beta-cell failure in type 2 diabetes.* Nat Rev Mol Cell Biol, 2008. **9**(3): p. 193-205.
68. Fabbrini, E., et al., *Intrahepatic fat, not visceral fat, is linked with metabolic complications of obesity.* Proc Natl Acad Sci U S A, 2009. **106**(36): p. 15430-5.
69. Fabbrini, E., et al., *Surgical removal of omental fat does not improve insulin sensitivity and cardiovascular risk factors in obese adults.* Gastroenterology, 2010. **139**(2): p. 448-55.
70. Laybutt, D.R., et al., *Muscle lipid accumulation and protein kinase C activation in the insulin-resistant chronically glucose-infused rat.* Am J Physiol, 1999. **277**(6): p. E1070-6.
71. Perreault, L., et al., *Intracellular localization of diacylglycerols and sphingolipids influences insulin sensitivity and mitochondrial function in human skeletal muscle.* JCI Insight, 2018. **3**(3).
72. Kumashiro, N., et al., *Cellular mechanism of insulin resistance in nonalcoholic fatty liver disease.* Proc Natl Acad Sci U S A, 2011. **108**(39): p. 16381-5.
73. Samuel, V.T., et al., *Mechanism of hepatic insulin resistance in non-alcoholic fatty liver disease.* J Biol Chem, 2004. **279**(31): p. 32345-53.
74. Samuel, V.T., et al., *Inhibition of protein kinase Cepsilon prevents hepatic insulin resistance in nonalcoholic fatty liver disease.* J Clin Invest, 2007. **117**(3): p. 739-45.
75. Koves, T.R., et al., *Mitochondrial overload and incomplete fatty acid oxidation contribute to skeletal muscle insulin resistance.* Cell Metab, 2008. **7**(1): p. 45-56.
76. Lin, J.H., P. Walter, and T.S. Yen, *Endoplasmic reticulum stress in disease pathogenesis.* Annu Rev Pathol, 2008. **3**: p. 399-425.
77. Fu, S., S.M. Watkins, and G.S. Hotamisligil, *The role of endoplasmic reticulum in hepatic lipid homeostasis and stress signaling.* Cell Metab, 2012. **15**(5): p. 623-34.
78. Fonseca, S.G., J. Gromada, and F. Urano, *Endoplasmic reticulum stress and pancreatic beta-cell death.* Trends Endocrinol Metab, 2011. **22**(7): p. 266-74.
79. Ozcan, U., et al., *Endoplasmic reticulum stress links obesity, insulin action, and type 2 diabetes.* Science, 2004. **306**(5695): p. 457-61.
80. Gregor, M.F., et al., *Endoplasmic reticulum stress is reduced in tissues of obese subjects after weight loss.* Diabetes, 2009. **58**(3): p. 693-700.

81. Ozcan, U., et al., *Chemical chaperones reduce ER stress and restore glucose homeostasis in a mouse model of type 2 diabetes.* Science, 2006. **313**(5790): p. 1137-40.
82. Trujillo, M.E. and P.E. Scherer, *Adipose tissue-derived factors: impact on health and disease.* Endocr Rev, 2006. **27**(7): p. 762-78.
83. Felig, P., E. Marliss, and G.F. Cahill, Jr., *Plasma amino acid levels and insulin secretion in obesity.* N Engl J Med, 1969. **281**(15): p. 811-6.
84. Um, S.H., D. D'Alessio, and G. Thomas, *Nutrient overload, insulin resistance, and ribosomal protein S6 kinase 1, S6K1.* Cell Metab, 2006. **3**(6): p. 393-402.
85. Yuan, M., et al., *Reversal of obesity- and diet-induced insulin resistance with salicylates or targeted disruption of Ikkbeta.* Science, 2001. **293**(5535): p. 1673-7.
86. Hill, A.A., et al., *Activation of NF-kappaB drives the enhanced survival of adipose tissue macrophages in an obesogenic environment.* Mol Metab, 2015. **4**(10): p. 665-77.
87. Weisberg, S.P., et al., *Obesity is associated with macrophage accumulation in adipose tissue.* J Clin Invest, 2003. **112**(12): p. 1796-808.
88. Xu, H., et al., *Chronic inflammation in fat plays a crucial role in the development of obesity-related insulin resistance.* J Clin Invest, 2003. **112**(12): p. 1821-30.
89. Olefsky, J.M. and C.K. Glass, *Macrophages, inflammation, and insulin resistance.* Annu Rev Physiol, 2010. **72**: p. 219-46.
90. Hill, A.A., W. Reid Bolus, and A.H. Hasty, *A decade of progress in adipose tissue macrophage biology.* Immunol Rev, 2014. **262**(1): p. 134-52.
91. Ackermann, A.M. and M. Gannon, *Molecular regulation of pancreatic beta-cell mass development, maintenance, and expansion.* J Mol Endocrinol, 2007. **38**(1-2): p. 193-206.
92. Christensen, A.A. and M. Gannon, *The Beta Cell in Type 2 Diabetes.* Curr Diab Rep, 2019. **19**(9): p. 81.
93. Hudish, L.I., J.E. Reusch, and L. Sussel, *beta Cell dysfunction during progression of metabolic syndrome to type 2 diabetes.* J Clin Invest, 2019. **129**(10): p. 4001-4008.
94. Abdul-Ghani, M.A., D. Tripathy, and R.A. DeFronzo, *Contributions of beta-cell dysfunction and insulin resistance to the pathogenesis of impaired glucose tolerance and impaired fasting glucose.* Diabetes Care, 2006. **29**(5): p. 1130-9.
95. Rovira-Llopis, S., et al., *Mitochondrial dynamics in type 2 diabetes: Pathophysiological implications.* Redox Biol, 2017. **11**: p. 637-645.
96. Wang, J., et al., *A mutation in the insulin 2 gene induces diabetes with severe pancreatic beta-cell dysfunction in the Mody mouse.* J Clin Invest, 1999. **103**(1): p. 27-37.
97. Park, S.Y., et al., *Mutant proinsulin proteins associated with neonatal diabetes are retained in the endoplasmic reticulum and not efficiently secreted.* Biochem Biophys Res Commun, 2010. **391**(3): p. 1449-54.
98. Fonseca, S.G., et al., *WFS1 is a novel component of the unfolded protein response and maintains homeostasis of the endoplasmic reticulum in pancreatic beta-cells.* J Biol Chem, 2005. **280**(47): p. 39609-15.
99. Viollet, B., et al., *Cellular and molecular mechanisms of metformin: an overview.* Clin Sci (Lond), 2012. **122**(6): p. 253-70.
100. Maida, A., et al., *Metformin regulates the incretin receptor axis via a pathway dependent on peroxisome proliferator-activated receptor-alpha in mice.* Diabetologia, 2011. **54**(2): p. 339-49.
101. Abbasi, F., et al., *Further evidence for a central role of adipose tissue in the antihyperglycemic effect of metformin.* Diabetes Care, 1998. **21**(8): p. 1301-5.

102. Kim, S.H. and F. Abbasi, *Myths about Insulin Resistance: Tribute to Gerald Reaven.* Endocrinol Metab (Seoul), 2019. **34**(1): p. 47-52.
103. Brown, J.B., C. Conner, and G.A. Nichols, *Secondary failure of metformin monotherapy in clinical practice.* Diabetes Care, 2010. **33**(3): p. 501-6.
104. Sola, D., et al., *Sulfonylureas and their use in clinical practice.* Arch Med Sci, 2015. **11**(4): p. 840-8.
105. Blumenthal, S.A., *Potentiation of the hepatic action of insulin by chlorpropamide.* Diabetes, 1977. **26**(5): p. 485-9.
106. Olefsky, J.M. and G.M. Reaven, *Effects of sulfonylurea therapy on insulin binding to mononuclear leukocytes of diabetic patients.* Am J Med, 1976. **60**(1): p. 89-95.
107. Matthews, D.R., et al., *UKPDS 26: Sulphonylurea failure in non-insulin-dependent diabetic patients over six years. UK Prospective Diabetes Study (UKPDS) Group.* Diabet Med, 1998. **15**(4): p. 297-303.
108. Hauner, H., *The mode of action of thiazolidinediones.* Diabetes Metab Res Rev, 2002. **18 Suppl 2**: p. S10-5.
109. Campbell, I.W. and S. Mariz, *Beta-cell preservation with thiazolidinediones.* Diabetes Res Clin Pract, 2007. **76**(2): p. 163-76.
110. Consoli, A. and G. Formoso, *Do thiazolidinediones still have a role in treatment of type 2 diabetes mellitus?* Diabetes Obes Metab, 2013. **15**(11): p. 967-77.
111. Gallo, L.A., E.M. Wright, and V. Vallon, *Probing SGLT2 as a therapeutic target for diabetes: basic physiology and consequences.* Diab Vasc Dis Res, 2015. **12**(2): p. 78-89.
112. Beitelshees, A.L., B.R. Leslie, and S.I. Taylor, *Sodium-Glucose Cotransporter 2 Inhibitors: A Case Study in Translational Research.* Diabetes, 2019. **68**(6): p. 1109-1120.
113. Hinnen, D., *Glucagon-Like Peptide 1 Receptor Agonists for Type 2 Diabetes.* Diabetes Spectr, 2017. **30**(3): p. 202-210.
114. Kim, W. and J.M. Egan, *The role of incretins in glucose homeostasis and diabetes treatment.* Pharmacol Rev, 2008. **60**(4): p. 470-512.
115. Tasyurek, H.M., et al., *Incretins: their physiology and application in the treatment of diabetes mellitus.* Diabetes Metab Res Rev, 2014. **30**(5): p. 354-71.
116. Smith, E.P., et al., *The role of beta cell glucagon-like peptide-1 signaling in glucose regulation and response to diabetes drugs.* Cell Metab, 2014. **19**(6): p. 1050-7.
117. Burmeister, M.A., et al., *Acute activation of central GLP-1 receptors enhances hepatic insulin action and insulin secretion in high-fat-fed, insulin resistant mice.* Am J Physiol Endocrinol Metab, 2012. **302**(3): p. E334-43.
118. Burmeister, M.A., et al., *The Hypothalamic Glucagon-Like Peptide 1 Receptor Is Sufficient but Not Necessary for the Regulation of Energy Balance and Glucose Homeostasis in Mice.* Diabetes, 2017. **66**(2): p. 372-384.
119. Saisho, Y., *Incretin-based therapy and pancreatitis: accumulating evidence and unresolved questions.* Ann Transl Med, 2018. **6**(7): p. 131.
120. Hutton, J.C. and R.M. O'Brien, *Glucose-6-phosphatase catalytic subunit gene family.* J Biol Chem, 2009. **284**(43): p. 29241-5.
121. Cori, G.T., C.F. Cori, and G. Schmidt, *THE RÔLE OF GLUCOSE-1-PHOSPHATE IN THE FORMATION OF BLOOD SUGAR AND SYNTHESIS OF GLYCOGEN IN THE LIVER.* Journal of Biological Chemistry, 1939. **129**(2): p. 629-639.
122. Shelly, L.L., et al., *Isolation of the gene for murine glucose-6-phosphatase, the enzyme deficient in glycogen storage disease type 1A.* J Biol Chem, 1993. **268**(29): p. 21482-5.

123. Gluecksohn-Waelsch, S., *Genetic control of morphogenetic and biochemical differentiation: lethal albino deletions in the mouse.* Cell, 1979. **16**(2): p. 225-37.
124. Lei, K.J., et al., *Mutations in the glucose-6-phosphatase gene that cause glycogen storage disease type 1a.* Science, 1993. **262**(5133): p. 580-3.
125. Chatelain, F., et al., *Development and regulation of glucose-6-phosphatase gene expression in rat liver, intestine, and kidney: in vivo and in vitro studies in cultured fetal hepatocytes.* Diabetes, 1998. **47**(6): p. 882-9.
126. Shieh, J.J., et al., *The molecular basis of glycogen storage disease type 1a: structure and function analysis of mutations in glucose-6-phosphatase.* J Biol Chem, 2002. **277**(7): p. 5047-53.
127. Chou, J.Y. and B.C. Mansfield, *Mutations in the glucose-6-phosphatase-alpha (G6PC) gene that cause type Ia glycogen storage disease.* Hum Mutat, 2008. **29**(7): p. 921-30.
128. Chou, J.Y., H.S. Jun, and B.C. Mansfield, *Type I glycogen storage diseases: disorders of the glucose-6-phosphatase/glucose-6-phosphate transporter complexes.* J Inherit Metab Dis, 2015. **38**(3): p. 511-9.
129. Mithieux, G., et al., *Glucose-6-phosphatase mRNA and activity are increased to the same extent in kidney and liver of diabetic rats.* Diabetes, 1996. **45**(7): p. 891-6.
130. Ashmore, J., A.B. Hastings, and F.B. Nesbett, *The Effect of Diabetes and Fasting on Liver Glucose-6-Phosphatase.* Proc Natl Acad Sci U S A, 1954. **40**(8): p. 673-8.
131. Vander Kooi, B.T., et al., *The three insulin response sequences in the glucose-6-phosphatase catalytic subunit gene promoter are functionally distinct.* J Biol Chem, 2003. **278**(14): p. 11782-93.
132. Martin, C.C., et al., *Identification and characterization of a human cDNA and gene encoding a ubiquitously expressed glucose-6-phosphatase catalytic subunit-related protein.* J Mol Endocrinol, 2002. **29**(2): p. 205-22.
133. Lin, S.R., et al., *Functional analysis of mutations in a severe congenital neutropenia syndrome caused by glucose-6-phosphatase-beta deficiency.* Mol Genet Metab, 2015. **114**(1): p. 41-5.
134. Wang, Y., et al., *Deletion of the gene encoding the ubiquitously expressed glucose-6-phosphatase catalytic subunit-related protein (UGRP)/glucose-6-phosphatase catalytic subunit-beta results in lowered plasma cholesterol and elevated glucagon.* J Biol Chem, 2006. **281**(52): p. 39982-9.
135. Cheung, Y.Y., et al., *Impaired neutrophil activity and increased susceptibility to bacterial infection in mice lacking glucose-6-phosphatase-beta.* J Clin Invest, 2007. **117**(3): p. 784-93.
136. Jun, H.S., et al., *Glucose-6-phosphatase-beta, implicated in a congenital neutropenia syndrome, is essential for macrophage energy homeostasis and functionality.* Blood, 2012. **119**(17): p. 4047-55.
137. Boztug, K., et al., *A syndrome with congenital neutropenia and mutations in G6PC3.* N Engl J Med, 2009. **360**(1): p. 32-43.
138. Banka, S., et al., *Mutations in the G6PC3 gene cause Dursun syndrome.* Am J Med Genet A, 2010. **152A**(10): p. 2609-11.
139. Banka, S. and W.G. Newman, *A clinical and molecular review of ubiquitous glucose-6-phosphatase deficiency caused by G6PC3 mutations.* Orphanet J Rare Dis, 2013. **8**: p. 84.
140. Hayee, B., et al., *G6PC3 mutations are associated with a major defect of glycosylation: a novel mechanism for neutrophil dysfunction.* Glycobiology, 2011. **21**(7): p. 914-24.

141. Veiga-da-Cunha, M., et al., *Failure to eliminate a phosphorylated glucose analog leads to neutropenia in patients with G6PT and G6PC3 deficiency.* Proc Natl Acad Sci U S A, 2019. **116**(4): p. 1241-1250.
142. Borregaard, N. and T. Herlin, *Energy metabolism of human neutrophils during phagocytosis.* J Clin Invest, 1982. **70**(3): p. 550-7.
143. Arden, S.D., et al., *Molecular cloning of a pancreatic islet-specific glucose-6-phosphatase catalytic subunit-related protein.* Diabetes, 1999. **48**(3): p. 531-42.
144. Shieh, J.J., et al., *The islet-specific glucose-6-phosphatase-related protein, implicated in diabetes, is a glycoprotein embedded in the endoplasmic reticulum membrane.* FEBS Lett, 2004. **562**(1-3): p. 160-4.
145. Ebert, D.H., et al., *Structure and promoter activity of an islet-specific glucose-6-phosphatase catalytic subunit-related gene.* Diabetes, 1999. **48**(3): p. 543-51.
146. Martin, C.C., et al., *Cloning and characterization of the human and rat islet-specific glucose-6-phosphatase catalytic subunit-related protein (IGRP) genes.* J Biol Chem, 2001. **276**(27): p. 25197-207.
147. Wang, Y., et al., *Deletion of the gene encoding the islet-specific glucose-6-phosphatase catalytic subunit-related protein autoantigen results in a mild metabolic phenotype.* Diabetologia, 2007. **50**(4): p. 774-8.
148. Foster, J.D., B.A. Pederson, and R.C. Nordlie, *Glucose-6-phosphatase structure, regulation, and function: an update.* Proc Soc Exp Biol Med, 1997. **215**(4): p. 314-32.
149. Waddell, I.D. and A. Burchell, *The microsomal glucose-6-phosphatase enzyme of pancreatic islets.* Biochem J, 1988. **255**(2): p. 471-6.
150. Sweet, I.R., et al., *Measurement and modeling of glucose-6-phosphatase in pancreatic islets.* Am J Physiol, 1997. **272**(4 Pt 1): p. E696-711.
151. Khan, A., et al., *Glucose cycling is markedly enhanced in pancreatic islets of obese hyperglycemic mice.* Endocrinology, 1990. **126**(5): p. 2413-6.
152. Khan, A., et al., *Glucose cycling in islets from healthy and diabetic rats.* Diabetes, 1990. **39**(4): p. 456-9.
153. Tokuyama, Y., et al., *Evolution of beta-cell dysfunction in the male Zucker diabetic fatty rat.* Diabetes, 1995. **44**(12): p. 1447-57.
154. Argaud, D., et al., *Stimulation of glucose-6-phosphatase gene expression by glucose and fructose-2,6-bisphosphate.* J Biol Chem, 1997. **272**(19): p. 12854-61.
155. Massillon, D., et al., *Carbon flux via the pentose phosphate pathway regulates the hepatic expression of the glucose-6-phosphatase and phosphoenolpyruvate carboxykinase genes in conscious rats.* J Biol Chem, 1998. **273**(1): p. 228-34.
156. Wajngot, A., et al., *Testing of the assumptions made in estimating the extent of futile cycling.* Am J Physiol, 1989. **256**(5 Pt 1): p. E668-75.
157. Coutinho, M., et al., *The relationship between glucose and incident cardiovascular events. A metaregression analysis of published data from 20 studies of 95,783 individuals followed for 12.4 years.* Diabetes Care, 1999. **22**(2): p. 233-40.
158. Lawes, C.M., et al., *Blood glucose and risk of cardiovascular disease in the Asia Pacific region.* Diabetes Care, 2004. **27**(12): p. 2836-42.
159. Gerstein, H.C., et al., *Annual incidence and relative risk of diabetes in people with various categories of dysglycemia: a systematic overview and meta-analysis of prospective studies.* Diabetes Res Clin Pract, 2007. **78**(3): p. 305-12.

160. Bouatia-Naji, N., et al., *A variant near MTNR1B is associated with increased fasting plasma glucose levels and type 2 diabetes risk.* Nat Genet, 2009. **41**(1): p. 89-94.
161. Prokopenko, I., et al., *Variants in MTNR1B influence fasting glucose levels.* Nat Genet, 2009. **41**(1): p. 77-81.
162. Lyssenko, V., et al., *Common variant in MTNR1B associated with increased risk of type 2 diabetes and impaired early insulin secretion.* Nat Genet, 2009. **41**(1): p. 82-8.
163. Weedon, M.N., et al., *A common haplotype of the glucokinase gene alters fasting glucose and birth weight: association in six studies and population-genetics analyses.* Am J Hum Genet, 2006. **79**(6): p. 991-1001.
164. Iynedjian, P.B., *Molecular physiology of mammalian glucokinase.* Cell Mol Life Sci, 2009. **66**(1): p. 27-42.
165. Matschinsky, F.M. and D.F. Wilson, *The Central Role of Glucokinase in Glucose Homeostasis: A Perspective 50 Years After Demonstrating the Presence of the Enzyme in Islets of Langerhans.* Front Physiol, 2019. **10**: p. 148.
166. Weedon, M.N., et al., *Genetic regulation of birth weight and fasting glucose by a common polymorphism in the islet cell promoter of the glucokinase gene.* Diabetes, 2005. **54**(2): p. 576-81.
167. Chen, W.M., et al., *Variations in the G6PC2/ABCB11 genomic region are associated with fasting glucose levels.* J Clin Invest, 2008. **118**(7): p. 2620-8.
168. Bouatia-Naji, N., et al., *A polymorphism within the G6PC2 gene is associated with fasting plasma glucose levels.* Science, 2008. **320**(5879): p. 1085-8.
169. Dupuis, J., et al., *New genetic loci implicated in fasting glucose homeostasis and their impact on type 2 diabetes risk.* Nat Genet, 2010. **42**(2): p. 105-16.
170. Manning, A.K., et al., *A genome-wide approach accounting for body mass index identifies genetic variants influencing fasting glycemic traits and insulin resistance.* Nat Genet, 2012. **44**(6): p. 659-69.
171. Baerenwald, D.A., et al., *Multiple functional polymorphisms in the G6PC2 gene contribute to the association with higher fasting plasma glucose levels.* Diabetologia, 2013. **56**(6): p. 1306-16.
172. Reiling, E., et al., *Combined effects of single-nucleotide polymorphisms in GCK, GCKR, G6PC2 and MTNR1B on fasting plasma glucose and type 2 diabetes risk.* Diabetologia, 2009. **52**(9): p. 1866-70.
173. Soranzo, N., et al., *Common variants at 10 genomic loci influence hemoglobin A(1)(C) levels via glycemic and nonglycemic pathways.* Diabetes, 2010. **59**(12): p. 3229-39.
174. Boortz, K.A., et al., *G6PC2 Modulates Fasting Blood Glucose In Male Mice in Response to Stress.* Endocrinology, 2016. **157**(8): p. 3002-8.
175. Boortz, K.A., et al., *G6PC2 Modulates the Effects of Dexamethasone on Fasting Blood Glucose and Glucose Tolerance.* Endocrinology, 2016. **157**(11): p. 4133-4145.
176. Charmandari, E., C. Tsigos, and G. Chrousos, *Endocrinology of the stress response.* Annu Rev Physiol, 2005. **67**: p. 259-84.
177. Boortz, K.A., et al., *Effects of G6pc2 deletion on body weight and cholesterol in mice.* J Mol Endocrinol, 2017. **58**(3): p. 127-139.
178. Thorens, B., et al., *Ins1(Cre) knock-in mice for beta cell-specific gene recombination.* Diabetologia, 2015. **58**(3): p. 558-65.
179. Maniatis, T., E.F. Fritsch, and J. Sambrook, *Molecular cloning : a laboratory manual*. 1982, Cold Spring Harbor, N.Y.: Cold Spring Harbor Laboratory. x, 545 p.

180. Morgan, C.R. and A.L. Lazarow, *Immunoassay of insulin: two antibody system: plasma insulin of normal, subdiabetic, and diabetic rats.* Am J Med Sci, 1963. **257**: p. 415-19.
181. Syring, K.E., et al., *Combined Deletion of Slc30a7 and Slc30a8 Unmasks a Critical Role for ZnT8 in Glucose-Stimulated Insulin Secretion.* Endocrinology, 2016. **157**(12): p. 4534-4541.
182. Livak, K.J. and T.D. Schmittgen, *Analysis of relative gene expression data using real-time quantitative PCR and the 2(-Delta Delta C(T)) Method.* Methods, 2001. **25**(4): p. 402-8.
183. Pulley, J., et al., *Principles of human subjects protections applied in an opt-out, de-identified biobank.* Clin Transl Sci, 2010. **3**(1): p. 42-8.
184. Roden, D.M., et al., *Development of a large-scale de-identified DNA biobank to enable personalized medicine.* Clin Pharmacol Ther, 2008. **84**(3): p. 362-9.
185. Denny, J.C., et al., *PheWAS: demonstrating the feasibility of a phenome-wide scan to discover gene-disease associations.* Bioinformatics, 2010. **26**(9): p. 1205-10.
186. Denny, J.C., et al., *Systematic comparison of phenome-wide association study of electronic medical record data and genome-wide association study data.* Nat Biotechnol, 2013. **31**(12): p. 1102-10.
187. Ashcroft, S.J., et al., *The pentose cycle and insulin release in mouse pancreatic islets.* Biochem J, 1972. **126**(3): p. 525-32.
188. Tamarit-Rodriguez, J., et al., *Lactate production in pancreatic islets.* Diabetes, 1998. **47**(8): p. 1219-23.
189. Wang, H. and P.B. Iynedjian, *Modulation of glucose responsiveness of insulinoma beta-cells by graded overexpression of glucokinase.* Proc Natl Acad Sci U S A, 1997. **94**(9): p. 4372-7.
190. Chan, T.M. and J.H. Exton, *A rapid method for the determination of glycogen content and radioactivity in small quantities of tissue or isolated hepatocytes.* Anal Biochem, 1976. **71**(1): p. 96-105.
191. Boustead, J.N., et al., *Identification and characterization of a cDNA and the gene encoding the mouse ubiquitously expressed glucose-6-phosphatase catalytic subunit-related protein.* J Mol Endocrinol, 2004. **32**(1): p. 33-53.
192. Streeper, R.S., et al., *Hepatocyte nuclear factor-1 acts as an accessory factor to enhance the inhibitory action of insulin on mouse glucose-6-phosphatase gene transcription.* Proc Natl Acad Sci U S A, 1998. **95**(16): p. 9208-13.
193. Bischof, L.J., et al., *Characterization of the mouse islet-specific glucose-6-phosphatase catalytic subunit-related protein gene promoter by in situ footprinting: correlation with fusion gene expression in the islet-derived betaTC-3 and hamster insulinoma tumor cell lines.* Diabetes, 2001. **50**(3): p. 502-14.
194. Wang, Y., et al., *Activation of ATF6 and an ATF6 DNA binding site by the endoplasmic reticulum stress response.* J Biol Chem, 2000. **275**(35): p. 27013-20.
195. Pan, C.J., et al., *SLC37A1 and SLC37A2 are phosphate-linked, glucose-6-phosphate antiporters.* PLoS One, 2011. **6**(9): p. e23157.
196. Gerin, I., et al., *Sequence of a putative glucose 6-phosphate translocase, mutated in glycogen storage disease type Ib.* FEBS Lett, 1997. **419**(2-3): p. 235-8.
197. Ku, G.M., et al., *Research resource: RNA-Seq reveals unique features of the pancreatic beta-cell transcriptome.* Mol Endocrinol, 2012. **26**(10): p. 1783-92.

198. Stolovich-Rain, M., et al., *Weaning triggers a maturation step of pancreatic beta cells.* Dev Cell, 2015. **32**(5): p. 535-45.
199. Denny, J.C., et al., *Variants near FOXE1 are associated with hypothyroidism and other thyroid conditions: using electronic medical records for genome- and phenome-wide studies.* Am J Hum Genet, 2011. **89**(4): p. 529-42.
200. Ritchie, M.D., et al., *Genome- and phenome-wide analyses of cardiac conduction identifies markers of arrhythmia risk.* Circulation, 2013. **127**(13): p. 1377-85.
201. Shameer, K., et al., *A genome- and phenome-wide association study to identify genetic variants influencing platelet count and volume and their pleiotropic effects.* Hum Genet, 2014. **133**(1): p. 95-109.
202. Yaghootkar, H. and T.M. Frayling, *Recent progress in the use of genetics to understand links between type 2 diabetes and related metabolic traits.* Genome Biol, 2013. **14**(3): p. 203.
203. Rooyackers, O.E. and K.S. Nair, *Hormonal regulation of human muscle protein metabolism.* Annu Rev Nutr, 1997. **17**: p. 457-85.
204. Conrad, E., et al., *The MAFB transcription factor impacts islet alpha-cell function in rodents and represents a unique signature of primate islet beta-cells.* Am J Physiol Endocrinol Metab, 2016. **310**(1): p. E91-E102.
205. Xin, Y., et al., *RNA Sequencing of Single Human Islet Cells Reveals Type 2 Diabetes Genes.* Cell Metab, 2016. **24**(4): p. 608-615.
206. American Diabetes, A., *2. Classification and Diagnosis of Diabetes: Standards of Medical Care in Diabetes-2019.* Diabetes Care, 2019. **42**(Suppl 1): p. S13-S28.
207. Boulling, A., et al., *Discovery and Functional Annotation of PRSS1 Promoter Variants in Chronic Pancreatitis.* Hum Mutat, 2016. **37**(11): p. 1149-1152.
208. Le Marechal, C., et al., *Hereditary pancreatitis caused by triplication of the trypsinogen locus.* Nat Genet, 2006. **38**(12): p. 1372-4.
209. Shi, Y., et al., *Meta-analyses of the association of G6PC2 allele variants with elevated fasting glucose and type 2 diabetes.* PLoS One, 2017. **12**(7): p. e0181232.
210. Brunzell, J.D., et al., *Relationships between fasting plasma glucose levels and insulin secretion during intravenous glucose tolerance tests.* J Clin Endocrinol Metab, 1976. **42**(2): p. 222-9.
211. Brereton, M.F., et al., *Reversible changes in pancreatic islet structure and function produced by elevated blood glucose.* Nat Commun, 2014. **5**: p. 4639.
212. Wang, Z., et al., *Pancreatic beta cell dedifferentiation in diabetes and redifferentiation following insulin therapy.* Cell Metab, 2014. **19**(5): p. 872-82.
213. Halban, P.A., et al., *beta-cell failure in type 2 diabetes: postulated mechanisms and prospects for prevention and treatment.* Diabetes Care, 2014. **37**(6): p. 1751-8.
214. Weir, G.C. and S. Bonner-Weir, *Five stages of evolving beta-cell dysfunction during progression to diabetes.* Diabetes, 2004. **53 Suppl 3**: p. S16-21.
215. Decode Study Group, E.D.E.G., *Is the current definition for diabetes relevant to mortality risk from all causes and cardiovascular and noncardiovascular diseases?* Diabetes Care, 2003. **26**(3): p. 688-96.
216. Khaw, K.T., et al., *Glycated haemoglobin, diabetes, and mortality in men in Norfolk cohort of european prospective investigation of cancer and nutrition (EPIC-Norfolk).* BMJ, 2001. **322**(7277): p. 15-8.

217. Fardet, L. and B. Feve, *Systemic glucocorticoid therapy: a review of its metabolic and cardiovascular adverse events.* Drugs, 2014. **74**(15): p. 1731-45.
218. Rafacho, A., et al., *Glucocorticoid treatment and endocrine pancreas function: implications for glucose homeostasis, insulin resistance and diabetes.* J Endocrinol, 2014. **223**(3): p. R49-62.
219. van Raalte, D.H. and M. Diamant, *Steroid diabetes: from mechanism to treatment?* Neth J Med, 2014. **72**(2): p. 62-72.
220. Lacroix, A., et al., *Cushing's syndrome.* Lancet, 2015. **386**(9996): p. 913-27.
221. Gonder, J.C. and K. Laber, *A renewed look at laboratory rodent housing and management.* ILAR J, 2007. **48**(1): p. 29-36.
222. Abdul-Ghani, M.A. and R.A. DeFronzo, *Plasma glucose concentration and prediction of future risk of type 2 diabetes.* Diabetes Care, 2009. **32 Suppl 2**: p. S194-8.
223. Edelman, D., et al., *Utility of hemoglobin A1c in predicting diabetes risk.* J Gen Intern Med, 2004. **19**(12): p. 1175-80.
224. Gibson, G., *Rare and common variants: twenty arguments.* Nat Rev Genet, 2012. **13**(2): p. 135-45.
225. Bouatia-Naji, N., et al., *Genetic and functional assessment of the role of the rs13431652-A and rs573225-A alleles in the G6PC2 promoter that are strongly associated with elevated fasting glucose levels.* Diabetes, 2010. **59**(10): p. 2662-71.
226. Manolio, T.A., et al., *Finding the missing heritability of complex diseases.* Nature, 2009. **461**(7265): p. 747-53.
227. Grupe, A., et al., *Transgenic knockouts reveal a critical requirement for pancreatic beta cell glucokinase in maintaining glucose homeostasis.* Cell, 1995. **83**(1): p. 69-78.
228. Mahajan, A., et al., *Identification and functional characterization of G6PC2 coding variants influencing glycemic traits define an effector transcript at the G6PC2-ABCB11 locus.* PLoS Genet, 2015. **11**(1): p. e1004876.
229. Ng, N., et al., *Tissue-Specific Alteration of Metabolic Pathways Influences Glycemic Regulation.* 2019.
230. Doherty, J.K., et al., *The HER-2/neu receptor tyrosine kinase gene encodes a secreted autoinhibitor.* Proc Natl Acad Sci U S A, 1999. **96**(19): p. 10869-74.
231. Ghosh, A., et al., *The catalytic center of glucose-6-phosphatase. HIS176 is the nucleophile forming the phosphohistidine-enzyme intermediate during catalysis.* J Biol Chem, 2002. **277**(36): p. 32837-42.
232. Vaser, R., et al., *SIFT missense predictions for genomes.* Nat Protoc, 2016. **11**(1): p. 1-9.
233. Shameli, A., et al., *Endoplasmic reticulum stress caused by overexpression of islet-specific glucose-6-phosphatase catalytic subunit-related protein in pancreatic Beta-cells.* Rev Diabet Stud, 2007. **4**(1): p. 25-32.
234. Pan, C.J., K.J. Lei, and J.Y. Chou, *Asparagine-linked oligosaccharides are localized to a luminal hydrophilic loop in human glucose-6-phosphatase.* J Biol Chem, 1998. **273**(34): p. 21658-62.
235. Hiraiwa, H., et al., *Inactivation of the glucose 6-phosphate transporter causes glycogen storage disease type 1b.* J Biol Chem, 1999. **274**(9): p. 5532-6.
236. Wessel, J., et al., *Low-frequency and rare exome chip variants associate with fasting glucose and type 2 diabetes susceptibility.* Nat Commun, 2015. **6**: p. 5897.
237. Hu, C., et al., *A genetic variant of G6PC2 is associated with type 2 diabetes and fasting plasma glucose level in the Chinese population.* Diabetologia, 2009. **52**(3): p. 451-6.

238. Hu, C., et al., *Effects of GCK, GCKR, G6PC2 and MTNR1B variants on glucose metabolism and insulin secretion.* PLoS One, 2010. **5**(7): p. e11761.
239. Wang, H., et al., *Large scale meta-analyses of fasting plasma glucose raising variants in GCK, GCKR, MTNR1B and G6PC2 and their impacts on type 2 diabetes mellitus risk.* PLoS One, 2013. **8**(6): p. e67665.
240. Newsholme, P., et al., *Oxidative stress pathways in pancreatic beta-cells and insulin-sensitive cells and tissues: importance to cell metabolism, function, and dysfunction.* Am J Physiol Cell Physiol, 2019. **317**(3): p. C420-C433.
241. Nunemaker, C.S., et al., *Insulin secretion in the conscious mouse is biphasic and pulsatile.* Am J Physiol Endocrinol Metab, 2006. **290**(3): p. E523-9.
242. Uruno, A., Y. Yagishita, and M. Yamamoto, *The Keap1-Nrf2 system and diabetes mellitus.* Arch Biochem Biophys, 2015. **566**: p. 76-84.
243. Yagishita, Y., et al., *Nrf2 protects pancreatic beta-cells from oxidative and nitrosative stress in diabetic model mice.* Diabetes, 2014. **63**(2): p. 605-18.
244. Hirotsu, Y., et al., *Nrf2-MafG heterodimers contribute globally to antioxidant and metabolic networks.* Nucleic Acids Res, 2012. **40**(20): p. 10228-39.
245. Mitsuishi, Y., et al., *Nrf2 redirects glucose and glutamine into anabolic pathways in metabolic reprogramming.* Cancer Cell, 2012. **22**(1): p. 66-79.
246. Zhan, X., et al., *Elevated intracellular trypsin exacerbates acute pancreatitis and chronic pancreatitis in mice.* Am J Physiol Gastrointest Liver Physiol, 2019. **316**(6): p. G816-G825.
247. Sahin-Toth, M. and M. Toth, *Gain-of-function mutations associated with hereditary pancreatitis enhance autoactivation of human cationic trypsinogen.* Biochem Biophys Res Commun, 2000. **278**(2): p. 286-9.
248. Chen, J.M., et al., *Copy number variations in chronic pancreatitis.* Cytogenet Genome Res, 2008. **123**(1-4): p. 102-7.
249. Masson, E., et al., *Trypsinogen copy number mutations in patients with idiopathic chronic pancreatitis.* Clin Gastroenterol Hepatol, 2008. **6**(1): p. 82-8.
250. Whitcomb, D.C., et al., *Common genetic variants in the CLDN2 and PRSS1-PRSS2 loci alter risk for alcohol-related and sporadic pancreatitis.* Nat Genet, 2012. **44**(12): p. 1349-54.
251. Weiss, F.U., et al., *Common variants in the CLDN2-MORC4 and PRSS1-PRSS2 loci confer susceptibility to acute pancreatitis.* Pancreatology, 2018.
252. Chen, J.M., et al., *"Loss of function" mutations in the cationic trypsinogen gene (PRSS1) may act as a protective factor against pancreatitis.* Mol Genet Metab, 2003. **79**(1): p. 67-70.
253. Iwabe, C., et al., *Role of endogenous insulin in pancreatic secretion in rats.* Pancreatology, 2001. **1**(4): p. 300-5.
254. Barreto, S.G., et al., *The islet-acinar axis of the pancreas: more than just insulin.* Am J Physiol Gastrointest Liver Physiol, 2010. **299**(1): p. G10-22.
255. Okabayashi, Y., et al., *Insulin and other stimulants have nonparallel translational effects on protein synthesis.* Diabetes, 1987. **36**(9): p. 1054-60.
256. Sans, M.D. and J.A. Williams, *Translational control of protein synthesis in pancreatic acinar cells.* Int J Gastrointest Cancer, 2002. **31**(1-3): p. 107-15.

257. Renaud, W., et al., *Regulation of concentrations of mRNA for amylase, trypsinogen I and chymotrypsinogen B in rat pancreas by secretagogues.* Biochem J, 1986. **235**(1): p. 305-8.
258. Stratowa, C. and W.J. Rutter, *Selective regulation of trypsin gene expression by calcium and by glucose starvation in a rat exocrine pancreas cell line.* Proc Natl Acad Sci U S A, 1986. **83**(12): p. 4292-6.
259. Tian, J., et al., *Effects of postprandial starvation on mRNA expression of endocrine-, amino acid and peptide transporter-, and metabolic enzyme-related genes in zebrafish (Danio rerio).* Fish Physiol Biochem, 2015. **41**(3): p. 773-87.
260. Matthews, D.R., et al., *Pulsatile insulin has greater hypoglycemic effect than continuous delivery.* Diabetes, 1983. **32**(7): p. 617-21.
261. Paolisso, G., et al., *Pulsatile insulin delivery has greater metabolic effects than continuous hormone administration in man: importance of pulse frequency.* J Clin Endocrinol Metab, 1991. **72**(3): p. 607-15.
262. Hunter, S.J., et al., *Association between insulin secretory pulse frequency and peripheral insulin action in NIDDM and normal subjects.* Diabetes, 1996. **45**(5): p. 683-6.
263. Meier, J.J., et al., *Hyperglycaemia is associated with impaired pulsatile insulin secretion: effect of basal insulin therapy.* Diabetes Obes Metab, 2013. **15**(3): p. 258-63.
264. Bertram, R., L.S. Satin, and A.S. Sherman, *Closing in on the Mechanisms of Pulsatile Insulin Secretion.* Diabetes, 2018. **67**(3): p. 351-359.
265. Li, X., et al., *Additive effects of genetic variation in GCK and G6PC2 on insulin secretion and fasting glucose.* Diabetes, 2009. **58**(12): p. 2946-53.
266. Rose, C.S., et al., *A variant in the G6PC2/ABCB11 locus is associated with increased fasting plasma glucose, increased basal hepatic glucose production and increased insulin release after oral and intravenous glucose loads.* Diabetologia, 2009. **52**(10): p. 2122-9.
267. Ingelsson, E., et al., *Detailed physiologic characterization reveals diverse mechanisms for novel genetic Loci regulating glucose and insulin metabolism in humans.* Diabetes, 2010. **59**(5): p. 1266-75.
268. Ayala, J.E., et al., *Standard operating procedures for describing and performing metabolic tests of glucose homeostasis in mice.* Dis Model Mech, 2010. **3**(9-10): p. 525-34.